1973

An experimental investigation of the heat transfer characteristics of a heated cylinder placed in a cross flow of air.

Meyer, John Ferrandello

Monterey, California. Naval Postgraduate School

AN EXPERIMENTAL INVESTIGATION OF THE HEAT TRANSFER CHARACTERISTICS OF A HEATED CYLINDER PLACED IN A CROSS FLOW OF AIR

John Ferrandello Meyer

NAVAL POSTGRADUATE SCHOOL
Monterey, California

THESIS

An Experimental Investigation of the Heat Transfer Characteristics of a Heated Cylinder Placed in a Cross Flow of Air

by

John Ferrandello Meyer

Thesis Advisor: Thomas E. Cooper

June 1973

Approved for public release; distribution unlimited.

An Experimental Investigation of the Heat Transfer Characteristics of a Heated Cylinder Placed in a Cross Flow of Air

by

John Ferrandello Meyer
Lieutenant Commander, United States Navy
B.S., United States Naval Academy, 1964

Submitted in partial fulfillment of the
requirements for the degrees of

MASTER OF SCIENCE IN MECHANICAL ENGINEERING
and
MECHANICAL ENGINEER

from the

NAVAL POSTGRADUATE SCHOOL
June 1973

ABSTRACT

Local heat transfer and pressure coefficients around a right circular cylinder were experimentally determined at Reynolds numbers ranging from 57,000 to 495,000. The turbulence intensity of the free stream was approximately 0.5%. The cylinder was heated externally with a constant heat flux and simultaneously cooled in a cross flow of air. A uniform heat source was provided by energizing Nichrome ribbon with a constant, measured current. The steady state surface temperature increase above the air temperature was indicated by thermocouple information. Employing Newton's law of cooling, heat transfer coefficients were determined as a function of the angular location from the forward stagnation line. The free stream dynamic pressure and surface pressure distribution around the cylinder were obtained using static pressure pickups and their associated manometers. A comparison is made between the heat transfer and pressure data collected. Experimental results compared within about six per cent of the theoretical solution of Schuh.

TABLE OF CONTENTS

LIST OF ILLUSTRATIONS

NOMENCLATURE

English Letter Symbols

A_1	Cross-sectional area of wind tunnel in settling chamber	ft^2
A_2	Cross-sectional area of wind tunnel at entrance to test section	ft^2
A_n	Cross-sectional area of Nichrome ribbon	ft^2
A_s	External surface area of an element of Nichrome ribbon	ft^2
C_p	Pressure coefficient as a function of angular location on cylinder surface	
D	Diameter of cylinder	ft
e	Root mean square voltage of hot wire anemometer	volts
f	subscript; Quantity evaluated at film temperature	
F	Froessling number, $F = Nu/\sqrt{Re}$	
h	Convective heat transfer coefficient	$\frac{BTU}{hr\text{-}ft^2\text{-}^\circ F}$
h_θ	Local convective heat transfer coefficient as a function of angular location	$\frac{BTU}{hr\text{-}ft^2\text{-}^\circ F}$
I	Current	amps
k	Thermal conductivity of air evaluated at film temperature	$\frac{BTU}{hr\text{-}ft\text{-}^\circ F}$
k_n	Thermal conductivity of Nichrome	$\frac{BTU}{hr\text{-}ft\text{-}^\circ F}$
Nu	Nusselt number, $Nu = hD/k$	
P_1	Static pressure of air in settling chamber	lbf/ft^2

English Letter Symbols

P_2	Static pressure of air at entrance to test section	lbf/ft^2
P_3	Static pressure of air in test section	lbf/ft^2
P_θ	Surface pressure on cylinder as a function of angular location	in of water
Pr	Prandtl number	
ΔP_{1-2}	Static pressure drop between settling chamber and entrance to test section	cm of water
$\Delta P_{cylinder}$	Pressure difference between surface pressure on cylinder and static pressure at entrance to test section, $\Delta P_{cylinder} = P_\theta - P_2$	cm of water
q	Heat flux	$BTU/hr\text{-}ft^2$
q_θ	Local heat flux from an element at some angular location	$BTU/hr\text{-}ft^2$
q_i	Dynamic pressure at any location, i	lbf/ft^2
q_{ideal}	Ideal dynamic pressure in test section	lbf/ft^2
q_{actual}	Actual dynamic pressure in test section	lbf/ft^2
Q	Heat transfer rate	BTU/hr
Q_k	Heat transfer rate through Nichrome element by conduction	BTU/hr
Q_i'	Heat generation rate within any Nichrome element, i	BTU/hr
Q_h	Heat transfer rate by convection from external surface of Nichrome element	BTU/hr
Q_{rad}	Heat transfer rate by radiation from external surface of Nichrome element	BTU/hr
Re	Reynolds number, $Re = UD/\nu$	

English Letter Symbols

R	Resistance of main heating circuit	ohms
T	Surface temperature of cylinder	°F
T_θ	Local surface temperature of cylinder at some angular location, θ	°F
T_∞	Temperature of ambient air in wind tunnel	°F
T_i	Surface Temperature at any element of Nichrome ribbon, i	°F
ΔT	Local temperature difference between cylinder surface and the ambient air, $\Delta T = T_\theta - T_\infty$	°F
Tu	Turbulence intensity level	
U	Free stream velocity	ft/sec
U_1	Free stream velocity in settling chamber	ft/sec
U_2	Free stream velocity at entrance to test section	ft/sec
U_3	Free stream velocity in test section	ft/sec
$\overline{U}$	Mean free stream velocity	ft/sec
$\sqrt{\overline{U'^2}}$	Mean fluctuation in free stream velocity	ft/sec
V	Voltage in heating circuits	volts
V_0	Initial probe voltage of hot wire anemometer at zero free stream velocity	volts
Δx	Arc length of an element of Nichrome ribbon	ft
X	Tunnel Correction Factor	

Greek Letter Symbols

ε	Thermal emissivity of Nichrome	
ε_{sb}	Wind tunnel boundary correction for solid blockage	
ε_{wb}	Wind tunnel boundary correction for wake blockage	
ε_t	Total wind tunnel boundary correction, $\varepsilon_t = \varepsilon_{sb} + \varepsilon_{wb}$	
ρ_1	Density of air in settling chamber	lbm/ft^3
ρ_2	Density of air at entrance to test section	lbm/ft^3
ρ_3	Density of air in test section	lbm/ft^3
ω_i	Uncertainty interval of quantity i	
ν	Kinematic viscosity of air evaluated at film temperature	ft^2/hr

ACKNOWLEDGEMENT

I wish to express my sincere appreciation to Mr. George F. Bixler and Mr. Thomas Christian for their invaluable assistance of constructing and participating in the design of the test cylinder.

I am also very grateful to my advisor, Professor Thomas E. Cooper, for his able professional guidance and sincere encouragement. These were a major source of motivation for me.

My deepest appreciation is extended to my wife, Martina, for her many personal sacrifices and endless patience during this thesis work.

Finally, I wish to thank God for answering the prayers of so many people, and for giving me a degree of academic success that I could have never achieved alone.

I. INTRODUCTION

Local heat transfer and pressure coefficients around a cylinder were experimentally determined at ten different Reynolds numbers that ranged from 57,000 to 495,000. The turbulence intensity level of the free stream was determined with a hot wire anemometer and found to be approximately 0.5 per cent.

The cylinder was heated externally with a constant heat flux, and simultaneously cooled in a crossflow of air by forced convection heat transfer.

A uniform surface heat flux was provided by helically winding Nichrome ribbon into shallow surface grooves that extended around the circumference of the cylinder. Approximately half of the thirty-two inch length of the cylinder was wrapped with the main heating circuit. Two smaller guard heater circuits were similarly installed on each end of the main circuit. Thermal energy dissipated by Joulean heating, as described by Wood in Ref. 1, was then applied to the surface by energizing the electrically resistant ribbon with a constant, measured current. The guard heater circuits were separately controlled.

The 4.5 inch diameter cylinder spanned the entire height of the wind tunnel test section, permitting a two dimensional study. To prevent any internal free convection, the cylinder was filled with foam rubber insulation.

After the thermal capacity of the cylinder was saturated, a steady state condition was achieved. Then all of the heat added was removed by convection, less any losses due to thermal radiation to the tunnel walls or circumferential conduction through the Nichrome ribbon. The guard heaters barred heat from being conducted out the ends. The local surface temperature increase above the ambient air temperature, delta T, was indicated by copper-constantan thermocouples welded to the inner surface of the Nichrome ribbon. The test section, which was located at the axial midpoint of the cylinder, was instrumented with four of these thermocouples welded to the center wrap of the Nichrome ribbon at ninety degree intervals. Since the cylinder was mounted on a turntable, delta T could be measured at any desired angular position. Employing Newton's law of cooling, local heat transfer coefficients were then determined as a function of angular location from the forward stagnation line.

Two static pressure taps were also installed on the cylinder, ninety degrees apart. These were connected to U-tube manometers which were referenced against the static pressure. Local surface pressure variations around the circumference of the cylinder could then be measured directly. The free stream dynamic pressure was measured by two static pressure pickups installed in the wind tunnel, and indicated on the "air speed" manometer. The measurement system, described in detail in Section III, provided

sufficient information to evaluate the pressure coefficient at any desired angular position.

Local experimentally determined heat transfer coefficients were compared with the measured pressure coefficients in order to correlate heat transfer trends with the various flow regimes which developed around the circumference of the cylinder. The location of the laminar, transitional and turbulent boundary layers as well as separation and its attendant wake were found, as expected, to produce definite trends in the heat transfer data.

The Froessling number, $Nu/\sqrt{Re}$, was determined at various angular locations and was compared with the experimental and theoretical results of other researchers. The low free stream turbulence intensity maintained throughout the present investigation led to experimental results that were significantly lower than those previously reported. Experimental results were found to agree within about six per cent of the theoretical model developed by Schuh for predicting local heat transfer coefficients on the forward portion of a constant heat flux cylinder.

II. BACKGROUND

Almost immediately after beginning a study of heat transfer from a cylinder, two absolute facts become apparent. First comes a total realization that the heat transfer mechanism is closely interrelated with the associated fluid mechanics. An adequate treatment of the former, whether it be analytical or experimental in nature, requires a basic understanding of the movement, pressure, and general behaviour of the fluid particles which conduct and convect thermal energy.

Secondly, it is certainly true that a vast amount of research has been devoted to each aspect of the thermal-hydrodynamic interface around a heated cylinder placed in a uniform stream. A mere listing of all that has been published would be voluminous. Instead the approach has been taken to review the better known, standard works and some that are unique. The details of the many factors involved are discussed within the framework of this review.

A. FLUID FLOW AROUND A HEATED CYLINDER

A brief description of this flow model is summarized in this section based on discussions contained in Refs. 2-5.

The potential flow of an inviscid, ideal fluid around the surface of a cylinder consists of an acceleration from zero velocity at a forward stagnation point, to a maximum

velocity at ninety degrees on both sides, and finally a deceleration to zero velocity at the rear stagnation point. The corresponding surface pressure distribution around the cylinder for ideal flow is simply an inversion of the velocity distribution. The pressure maxima are located at the stagnation points and the pressure minima are located at ninety degrees.

The flow of a real fluid around a cylinder is best analyzed in terms of changes that occur within the boundary layer that forms near the surface. This thin film of fluid which grows from a minimum thickness near the forward stagnation line is a result of the adherence of a viscous fluid to the surface, where a no-slip condition of zero velocity exists. As long as this layer is attached to a heated surface it is the medium into which thermal energy is first conducted. The fluid motion in the boundary layer then convects this heated fluid away from the surface. The velocity profile through the boundary layer varies as a function of the angular location from the forward stagnation line. Hence, the heat transfer rate from the cylinder surface becomes a function of the angular location. As this angular position increases, the boundary layer grows thicker, the fluid velocity is increasingly retarded and less heat is removed from the surface.

A boundary layer may be classified as either laminar or turbulent. Flow within a laminar boundary layer is characterized by fluid particles moving in a smooth, orderly

fashion and in layers. A turbulent boundary layer is characterized by individual fluid "packets" flowing in irregular patterns within the bounds of a composite motion in the direction of flow. A turbulent boundary layer is conducive to a higher heat transfer rate.

As the kinetic energy of the free stream attenuates within the slower moving boundary layer, the pressure near the surface becomes less favorable to the established flow direction. Finally, when the remaining kinetic energy of the fluid near the surface cannot overcome the adverse pressure rise, the boundary layer separates, as a reverse flow is initiated near the surface. Eddies of turbulence result wherein packets of fluid "scrub" the heated surface, significantly increasing the heat transfer rate. The resultant wake behind a cylinder is characterized by low pressure relative to the pressure on the forward half of a cylinder. At Reynolds numbers ranging from about 60 to 5000 [5], a regular pattern of shed vortices persists in the wake; it is known as the Karman vortex-street, named after the scientist Theodore von Karman. At the higher Reynolds numbers pertaining to this study the wake is characterized by irregular turbulent flow.

Form or pressure drag is a direct result of this low pressure region in the wake caused by boundary layer separation. For the range of flow velocities considered in the present investigation ($50{,}000<Re<500{,}000$) the form drag is large in comparison to skin friction drag. At higher

velocities transition to turbulence occurs prior to separation. The separation point moves farther back around the cylinder and form drag decreases.

The characteristics of the boundary layer, the location of the separation point, and the characteristics of the wake and resultant pressure distribution are dependent upon the Reynolds number,

$$Re = \frac{UD}{\nu} , \qquad (1)$$

where U is the free stream velocity, D is the diameter of the cylinder, and ν is the kinematic viscosity of the fluid. The location of the separation point also depends upon the magnitude of the free stream turbulence and surface roughness.

Instability first occurs at the rear stagnation point at a Reynolds number of about ten, and half of the total drag is then form drag.

The Karman vortex-street first occurs at Reynolds numbers of about 100. Form drag is then predominant.

At Reynolds numbers between 1,000 and 100,000 a laminar boundary layer separates from the surface at an angular location of 80-85 deg from the forward stagnation line. Skin friction drag is negligible in this range.

Above a Reynolds number of 100,000 the fluid in the boundary layer may contain sufficient kinetic energy to remain attached for a greater distance and not separate until reaching an angle of 130 deg with the flow direction. This

was shown experimentally by Fage and Falkner [Refs. 6 and 7] to occur, if the boundary layer had become turbulent. The critical point of transition from a laminar to a turbulent boundary layer moves farther back from the front of a cylinder as the Reynolds number is increased. It generally lies in the vicinity of 80-95 deg. Boundary layer transition prior to separation is given as a cause of the rapid decrease of the drag coefficient at a Reynolds number between 200,000 and 500,000.

At Reynolds numbers above 50,000 the heat transfer downstream of separation is larger than on the front half. This difference continues to increase with increasing Reynolds numbers.

Schlichting [5] reviews some previous experimental work as follows: Hiemenz measured pressure distribution around a cylinder in 1911, determining a separation angle of 81 deg. His boundary layer calculations provided a comparable separation angle of 82 deg. Extensive experimental data on the pressure distribution were later collected by Flachsbart. His data exhibited a strong dependency on Reynolds number. For subcritical Reynolds numbers he recorded a pressure minimum at an angle of about 70 deg and a fairly constant pressure over the downstream portion. At Reynolds numbers above the critical value he reported a pressure minimum at 90 deg and generally a closer agreement with potential flow theory. Thom investigated the laminar boundary layer on a circular cylinder in 1928 at a Reynolds number of 28,000.

Fage's study [6] of the boundary layer in the region of separation from a cylinder included Reynolds numbers from 100,000 to 350,000. Fage concluded that a critical point on a cylinder exists where the boundary layer begins a transition to a turbulent state, and that separation occurs just beyond the critical point. The critical point was shown to be the inflection point in the normal pressure distribution curve that immediately follows the point of maximum negative pressure. The latter point was also shown to move farther around the cylinder with higher Reynolds numbers.

In Ref. 8, Roshko combined free-streamline theory with Karman's theory of the vortex-street, and developed a solution for drag that is dependent on one experimental input, the shedding frequency. In the process, he defined a universal wake Strouhal number which is a function only of wake Reynolds number.

Roshko's study of flow past a cylinder at very high Reynolds numbers is described in Ref. 9. He observed that a second transition" range occurs as the drag coefficient "increases in the range, $10^6<Re<3.5\times10^6$, from a value of about 0.3 to 0.7, and then levels off at the latter value." He also observed that vortex shedding occurs at $Re>3.5\times10^6$.

Achenbach [10] describes measurements of local pressure and skin friction around a cylinder over a range of Reynolds numbers from 60,000 to 5,000,000. He determined the locations of separation points and transition regions

(separation bubbles), and analyzed the data in relation to the flow regions involved.

In Ref. 11, Coder organized and compiled previous experimental and theoretical determinations of the boundary layer separation point. He also compared this information with his own data collected using hot films. His summary included separation points at all Reynolds numbers from "creeping" flow to "transcritical" flow. His measurements were made in the "transition" (or "supercritical") flow regime.

B. THE EVALUATION OF HEAT TRANSFER FROM A CYLINDER

In the past twenty years it appears that the emphasis has shifted from experimental to analytical studies. Reference 12 leads one to conclude that about three approximate solution methods for heat transfer in the forward half prior to boundary layer separation have been proposed every two years. This trend has evolved a crucial need for accurate experimental data to verify the theories. It is this motivation which led the author to pursue and refine an experimental technique.

A study of forced convection heat transfer from a cylinder may employ one of two separate approaches. These are related to either a constant wall temperature cylinder or a constant heat flux cylinder. In the former model, delta T is held constant and a measured heat flux is increased or decreased as necessary to maintain a constant temperature

wall. In the latter model, the heat flux is held constant and the resulting delta T is measured as a function of a angular location.

Both approaches culminate with an application of Newton's law of cooling

$$q_\theta = \left(\frac{Q}{A_s}\right)_\theta = h_\theta(\Delta T)_\theta \qquad (2)$$

where for a specified surface h_θ is the local heat transfer coefficient at angular location θ, Q is the heat transfer rate, A_s is the surface area of interest, q_θ is the local heat flux and $(\Delta T)_\theta$ is the local surface temperature increase above the ambient air temperature. Generally, h_θ is presented in the dimensionless form of the local Nusselt number

$$Nu = \frac{h_\theta D}{k} \qquad (3)$$

where D is the diameter of the cylinder and k is the thermal conductivity of the fluid.

Experimental and analytical results are often presented in the form of the Froessling number, named after N. Froessling, which is defined by

$$F = \frac{Nu}{\sqrt{Re}} \qquad (4)$$

1. Some Previous Experimental Work

a. Ernst Schmidt and Karl Wenner

Schmidt and Wenner present in Ref. 13 their well known results for heat transfer over the circumference of a heated cylinder. A constant surface temperature cylinder was used in their experiment. Specifically, a hollow brass cylinder was maintained at one hundred degrees Centigrade by passing steam vapor through it. A londitudinal strip was insulated from the vapor. In fact, the strip was physically removed and replaced with a copper element that contained an internal electrical heating element. By controlling the electrical power into the heating element and making use of comparative thermocouple information, the strip was maintained at the same temperature as the cylinder wall. Hence, the heat flux was varied to maintain a constant wall temperature. A pressure pickup was also installed on the cylinder wall. By rotating the entire cylinder "about a graduated disk," both heat transfer and pressure data were collected at various angles with the air flow. It was stated that their data were generally only taken on half of the cylinder, but symmetry was checked with no "substantial difference" between both halves.

Schmidt and Wenner published the following results over a range of Reynolds numbers from 5000 to 426,000: "At Reynolds numbers up to around 100,000 high maxima of the heat transfer occurred in the forward stagnation point at 0 deg and on the rear side at 180 deg, while at around

80 deg the heat-transfer coefficient on both sides of the cylinder behind the forward stagnation point manifested distinct minimums. Two other maximums occurred at around 115 deg behind the forward stagnation point between 170,000 and 426,000. At 426,000, the heat transfer at the location of these maximums was almost twice as great as in the forward stagnation point, and the rear half of the cylinder diffused about 60% of the entire heat.... On the rear of the cylinder at ϕ = 180 deg the heat-transfer coefficients for Reynolds numbers of from 25,000 to 426,000 are greater than in the forward stagnation point." Heat transfer around a cylinder was stated to be a strong function of the Reynolds number and the angle from the forward stagnation line. Additionally, their results for heat transfer at the forward stagnation point were said to agree with Squire's solution, described in Ref. 14.

Although Schmidt and Wenner did not directly refer to a turbulence factor, Giedt, in Ref. 15, stated that there was a minimum of turbulence and that their data were taken in a "relatively narrow jet of air with a nearly uniform velocity distribution."

b. R.M. Fand

In Ref. 16, Fand describes his work which involved a constant wall temperature cylinder immersed in a uniform stream of water. The Reynolds numbers studied were between 11,000 and 64,000. His cylinder was composed of a copper core with a surface covering of chromium.

Thermocouples and electrical heaters were encapsulated in hypodermic containers and embedded longitudinally into drilled holes in the test cylinder. The high thermal conductivity of the copper core enabled a uniform surface temperature to be maintained when the heaters were energized. A major design limitation was identified as the low power capability of the heaters which provided a temperature increase of only 4 to 10 °F. Guard heater sections similar in design to the test cylinder, were controlled separately to prevent any heat flow out the ends.

Fand's results were shown to be in close agreement with the McAdams correlation, which had been based upon Reynolds numbers from 0.1 to 200. Fand then concluded that this correlation which is used to calculate the average Nusselt number,

$$(Nu)_f = [0.35 + 0.56(Re)_f^{0.52}](Pr)_f^{0.30} \qquad (5)$$

could be extended to a Reynolds number of 100,000. Fand built a strong argument for a second preferred form of correlation formula originated by Douglas and Churchill in Ref. 17,

$$(Nu)_f = a(Re)_f^{0.50} + b(Re)_f \ . \qquad (6)$$

In this form the first term was said to represent the heat transfer through the laminar boundary layer on the front portion of the cylinder. The second component, according to Fand, represented the heat transfer in the separated region in the rear half.

Fand mentioned that in Ref. 18, Van der Hegge Zijnen proposed a similar form, and that Richardson in Ref. 19 stated that the term representing heat transfer in the separated region is a "function of $(Re)_f^{0.67}$." Fand summarized these developments and arrived at the following correlation formula,

$$(Nu)_f = a(Re)_f^{0.50} + b(Re)_f^{0.67} . \qquad (7)$$

He stated that Perkins and Leppert [20] correlated their data for water and ethylene glycol with formula (7). However, Fand correlated his data successfully with the following formula, similar in form to (7),

$$(Nu)_f = [0.35 + 0.34(Re)_f^{0.50} + 0.15(Re)_f^{0.58}](Pr)_f^{0.30} \qquad (8)$$

where the term $0.15(Re)_f^{0.58}$ represents the heat transferred to the separated region. Fand opined that this formula was more "related to the physical processes involved" than McAdams' formula, and did, in fact, represent his data equally well. Fand further stipulated that equation (8) was only valid over the range of Reynolds numbers between 200 and 100,000.

c. W.H. Giedt

Giedt [15] experimented with a constant heat flux cylinder. The relatively large cylinder (4 inch O.D.) that he used permitted the investigation of Reynolds numbers from 70,800 to 219,000. The turbulence factor of the wind tunnel used by Giedt was given as 2.25%. The

constant heat flux surface boundary was generated by electrically heating a thin Nichrome ribbon that was wrapped helically around the cylinder. The temperature rise of the cylinder surface above the free stream air temperature was measured with thermocouples that were welded to the inner surface of the Nichrome. The heating circuit was composed of five turns of ribbon, the center turn being the test section and the two on either side functioning as guard heaters. By maintaining constant power, and measuring the temperature increase, Giedt determined the heat transfer coefficient from equation (2)

$$h = \frac{\frac{Q}{A_s}}{\Delta T} \tag{9}$$

The center of the hollow cylinder was filled with glass wool to reduce conduction losses, which were determined to be a maximum of two percent. A static-pressure tap was also installed on the cylinder. Then, by rotating the cylinder, both heat transfer and pressure information were collected at any desired angle to the flow direction. It was stated that in general, data were taken on one half of the cylinder circumference but that several measurements were made around the entire cylinder circumference with no substantial differences noted.

Giedt performed a heat balance on a differential element of Nichrome ribbon and thereby accounted for heat loss by circumferential conduction through the Nichrome ribbon.

As Schmidt and Wenner [13] had found previously, Giedt again noted that heat transfer is a function of Reynolds number and "location along the cylinder circumference." The other major conclusions of Giedt are reiterated here for subsequent reference, as follows:

1. Maximum values of h_θ occur approximately ten degrees further back along the cylinder circumference than the minimum static-pressure values.
2. Both minimum h_θ values and pressures move back along the cylinder with increasing values of Re.
3. For values of Re up to around 100,000, maximum h_θ values occur at the 0 degree and 180 degree points.
4. At values of Re = 140,000 and up, h_θ at the rear stagnation point is greater than at the forward stagnation point.
5. At values of Re from 140,000 to 219,000, distinct maximum h_θ values occur between 110 and 115 degrees.
6. For this same range of Re, two distinct minimum h_θ values occur. The lower of the two is between 80 and 93 degrees on the front half of the cylinder. The second is between 140 and 150 degrees on the back half.
7. Also for this same range of Re, inflection points occur in the pressure distribution curves at the same locations as the minimum h_θ values just noted.

It is noted that conclusion 3 above agrees identically with Schmidt and Wenner [13].

Giedt made a significant comparison of his heat transfer results with the skin-friction and static-pressure distributions given by Fage and Falkner [6,7]. In his discussion for the runs with Re = 140,000 and 219,000 he stated that "the first minimum of the Nusselt number curves coincide in location with the first inflection points of the corresponding pressure curves. These inflection points, according to Fage and Falkner, mark the location of the minimum of the skin friction. The fact that the point unit heat transfer coefficients drop to a minimum and then abruptly rise near these inflection points also substantiates their conclusion that transition from laminar to turbulent flow in the boundary layer occurred at this same location." Giedt also concluded that "the second inflection points which occur between 140 and 150 degrees in the pressure-distribution curves for these same values of Re, coincide with the locations of the second minimum h_θ values." Giedt stated that based upon Fage and Falkners' work "these second inflection points would also indicate the locations of second minimums or zero values of the skin friction." Giedt finally expressed a parallel between the location of the peak h_θ value in the vicinity of 110 degrees to the peak in the skin friction curve that rises after the first minimum.

d. H.C. Perkins, Jr. and G. Leppert

Perkins and Leppert experimented with two different techniques using a constant heat flux cylinder. The

cylinders in both instances were small stainless steel tubes that were mounted in a test channel, heated uniformly by their electrical resistance to an applied, direct current, and cooled in a cross flow of fluid.

Their first technique was especially intriguing as it employed a constant heat flux cylinder to determine the average heat transfer coefficient. As described in Ref. 20, a single thermocouple was located along the center-line of the cylinder, and the measured center-line temperature was mathematically shown to equal the mean temperature of the inside surface of the tube. This temperature was used to calculate the temperature drop through the tube wall and thus to determine the surface mean temperature of the external surface of the tube. The average heat transfer coefficient was calculated from the latter surface mean temperature. The cooling fluid was water and ethylene glycol.

Perkins and Leppert correlated the data from this first approach at Reynolds numbers from 40 to 100,000 and Prandtl numbers from 1 to 300 using several methods of correlation. They were most satisfied with results obtained using the methods of Sieder and Tate for pipe flow and Vliet and Leppert for flow around spheres. The variation in viscosity across the boundary layer was taken into account by means of a viscosity ratio factor. Other fluid properties were evaluated at the bulk temperature.

The other formulas used to correlate this data were of two forms, the one proposed by Richardson [19], equation (7), and the one proposed by Douglas and Churchill [17], equation (6). Perkins and Leppert reported that both formulas, after being modified to include the Prandtl number and the viscosity ratio, correlated their data well. It was stated that equation (6) as modified might be limited to Reynolds numbers not greater than 100,000.

Perkins and Leppert also illustrated that the latter formulas after modification correlate the data of some others for a Reynolds number greater than 10. Fand [16], however, reported that equation (7) in its modified form predicts average Nusselt numbers that are 54-76% higher than the experimental results that he obtained. Fand suggested that the "free stream turbulence, secondary-flows and boundary-layer effects associated with the rectangular duct in the apparatus of Perkins and Leppert are the cause of this discrepancy."

In the second experimental technique, described in Ref. 21, Perkins and Leppert measured local heat transfer coefficients. The surface temperature measurement method and cooling fluid were different. This time a thermocouple was attached to the inside wall of the tube and utilized to measure temperature as a function of angle. The cooling fluid, water, had Prandtl numbers from 1 to 7. A pressure pickup was also built into the cylinder to provide a pressure measurement capability. Local heat

transfer coefficients were determined at Reynolds numbers from 2000 to 120,000.

Both references reflect the significant effort made by the two experimenters with regard to blockage effects. Potential flow theory was utilized extensively for this analysis.

An analysis was carried out [21] for predicting the heat transfer that occurs prior to separation using "integral methods with the Pohlhausen velocity profile in the momentum boundary layer and a third order temperature profile in the thermal boundary layer."

Perkins and Leppert found [21] that "on the rear part of the tube, in the separated region, the temperature underwent rapid and large fluctuations." An oscillograph was used to record "not only the temperature-time dependence at each angle in the separated region but also provided an accurate way to determine the time averaged temperature on that part of the tube." The local heat transfer coefficients were calculated using the temperature rise above the ambient air temperature, the measured, constant heat flux, and the application of Newton's law of cooling. The viscosity ratio correction was employed to develop local Nusselt number correlations.

The turbulence level was reported to be about 2.9 per cent. It was demonstrated, however, that the data collected using both techniques "appears more in line with a 1 per cent turbulence level."

e. Jerome R. Jarcy

Jarcy conducted an experimental study of heat transfer from constant heat flux cylinders at relatively high temperatures. Reference 22 describes his study of flow field, drag and heat transfer characteristics of a mica cylinder. The cylinder was heated electrically using Nichrome ribbon wound around the cylinder. The average surface temperatures were from 250°F to 1100°F above the ambient air temperature. Jarcy reported that the flow for his experiment was subcritical and that separation was laminar. He determined this from the pressure distribution around the cylinder. Velocities involved were between 40 and 160 feet per second.

Jarcy's conclusions stated that "When a cylinder is heated, the value of the dynamic and total pressures in the wake of the cylinder decreases as compared to a zero heating rate."

f. P.D. Richardson

Richardson considered [19] the separated flow region in the rear of a bluff body immersed in a transverse stream. He was particularly concerned with turbulent flows at high Reynolds numbers that do not reattach after separation. Richardson concluded that heat transfer at the rear stagnation point "is proportional to the two-thirds power of Reynolds number." He also pointed out that it is known from the photographic record of Fage and observations of

Roshko that in the separated flow region variation occurs in the direction of the axis of the cylinder.

Richardson described an approximate method for calculating the convective heat transfer in the separated flow region of a bluff body and applied this method to a cylinder. This method accounts for the separate physical mechanisms of heat transfer that exist in the laminar boundary layer and separated regions. His method represents heat transfer in the separated region as being proportional to the two-thirds power of Reynolds number. He mentioned previous observations "that separated flow develops first at the rear stagnation point and then spreads forward round the cylinder at a decreasing rate with increase of Reynolds number until a position about 80 deg from the forward stagnation point is reached." He reported that the initial development apparently occurs at a Reynolds number of 10. In Ref. 23 he stated that blockage effects are felt within the separated region. Richardson compared his results with the experimental data of others and reported good agreement.

g. H.H. Sogin and V.S. Subramanian

Reference 24 describes an experimental study of mass transfer from naphthalene cylinders in a cross flow of air by Sogin and Subramanian. They credited this technique to Froessling's work in 1938 and 1940, which made use of the analogy between constant-property incompressible heat transfer and low concentration incompressible mass transfer. The specific technique used in their investigation was said

to be the same as that of Christian who measured local rates of mass transfer from hollow napthalene cylinders in axisymmetric flow. Their measurements spanned a range of Reynolds numbers from 122,000 to 342,000. Their results before boundary layer separation were compared with the approximate analytical solutions of H. Schuh and H.J. Merk as well as other experimental works.

2. Some Available Theoretical Work

Because of the complexity of the flow pattern once the laminar boundary layer separates or becomes turbulent, analytical solutions have not been found that predict local heat transfer over the entire cylinder. They generally are limited to approximate methods for calculating heat transfer in the front region of the cylinder extending from the forward stagnation line back to about eighty degrees. In Ref. 12, Spalding and Pun have compiled a summary, classification, and comparison of fifteen theoretical analyses of heat transfer in this region for a constant temperature cylinder. Included are the analyses of Froessling, Seban, Squire, Eckert, Schuh and Lighthill. Spalding and Pun emphasized the need for experimental data collected at a low free stream turbulence level, to act as a standard of comparison and assist in the verification and evaluation of the proposed solutions.

Seban and Chan present in Ref. 25 various methods for predicting heat transfer to laminar and turbulent boundary layers. The variable wall temperature case is

considered and, in particular, the constant heat flux case. Lighthill's method for laminar boundary layers with almost constant properties is also included in the report and "recommended for general application, although in certain instances, the error in the predicted heat transfer may attain twenty per cent."

Reference 26 contains Schuh's method for calculating laminar heat transfer on cylinders having either a constant wall temperature or a constant heat flux surface. Schuh compares the former with the data of Schmidt and Wenner [13] and the latter with the data of Giedt [15]. Good agreement was shown at Reynolds numbers below 100,000 with deviations otherwise. Schuh reports that these deviations were pronounced at and near the forward stagnation point, with the experimental values up to 20% higher.

In Ref. 27, Squire's exact solution for forced convection heat transfer at the forward stagnation point of a cylinder is contained as an unpublished inclusion. His resulting value of Nusselt number is given as

$$Nu = \alpha_3 \left[\frac{\beta_1 D^2}{\nu}\right]^{\frac{1}{2}} , \qquad (10)$$

where α_3 is a function of the Prandtl number (a table of values of α_3 is provided), and β_1 is defined by

$$\beta_1 = \frac{u_1}{x} . \qquad (11)$$

The velocity outside the boundary layer is given as

$$u_1 = \frac{4Ux}{D} , \tag{12}$$

where x is the distance from the forward stagnation point and U is the velocity of the uniform stream. Then,

$$\beta_1 = \frac{u_1}{x} = \frac{4U}{D} , \tag{13}$$

and taking for example, an average Prandtl number for air as 0.71, one obtains the result

$$Nu = 0.995 \left[\frac{UD}{\nu}\right]^{\frac{1}{2}} . \tag{14}$$

3. The Effects of Free Stream Turbulence on Heat Transfer Rate

It has long been recognized that free stream turbulence has a significant effect on the heat transfer from a heated bluff body in cross flow. Some of the major efforts to resolve and account for these effects have been that of J. Kestin (Refs. 28, 29, 30, 31), P.F. Maeder [29], R.T. Wood [31], R.A. Seban (Refs. 32, 33) and W.H. Giedt (Ref. 34). Kestin [28] describes a dual effect, one a broad change in the heat transfer rate resulting from the change in flow pattern, and the other a possible local effect at a given angle. Some of his other conclusions are:

a. The magnitude of the heat transfer variation due to the presence of free stream turbulence intensity seems to be larger at lower Reynolds numbers.

b. The turbulence intensity local effect seems to be an increase in the heat transfer rate.

c. The primary local effect occurs in the heat transfer "across a laminar boundary layer developed under the influence of a favorable pressure gradient" and is "of the order of 10 per cent." For a laminar boundary layer near the forward stagnation line of a cylinder, the local effect is more pronounced and is "of the order of 70-80 per cent for an intensity of turbulence of 2.5-3.0 per cent."

d. The local effect on the heat transfer rate is non-existent across a turbulent boundary layer or for separated flow.

Kestin mentions [30] that all laminar boundary layers "carry stochastic oscillations whose amplitude and frequency spectrum is related to the turbulence intensity in the free stream," and that if these disturbances do not amplify, the Tollmien-Schlichting theory of stability classifies the boundary layer as laminar.

Giedt [34] also found an increase of local heat transfer rates due to free stream turbulence, including a maximum 33.3 per cent increase over the calculated value at the forward stagnation point, when a rope net was placed about two feet upstream of the leading edge of the cylinder.

Seban [32] summarized the effect of free stream turbulence as an over-all heat transfer increase due to

effects such as a lower Reynolds number for transition to turbulent flow which permits higher heat transfer rates, an increase of heat transfer rate to the laminar layer, and an alteration of the character of the flow in the separated region which may ultimately cause a movement of the separation point. He also reported that for flow with a laminar boundary layer the local recovery factor doesn't vary due to free stream turbulence alterations.

Regarding the nature of turbulence, Seban measured a longitudinal component intensity and spectral distribution. Near the stagnation point he included a previous suggestion that a Goertler type instability might occur.

More recently Kestin and Wood [31] found that the instability near the stagnation line of a blunt body is different from Goertler's. As a result of this instability, Kestin and Wood reported that "the flow field acquires a system of evenly distributed, concentrated vortices arrayed in the axial direction and wrapped around the upstream portion of the body; their spacing is inversely proportional to the square root of the Reynolds number. The factor multiplying $Re^{-\frac{1}{2}}$ depends on the turbulence intensity, Tu, of the free stream and has a nonvanishing value even for Tu=0, decreasing with an increase in Tu." Therefore these authors conclude that "the flow field in the laminar boundary layer outside a stagnation line is not two dimensional.... Thus the effect of free stream turbulence on heat and mass-transfer rates from the forward portion of blunt bodies is

indirect. First, a system of vortices is formed under all conditions, and this enhances the transfer rates. The latter are further enhanced when the intensity of turbulence is increased because the spacing is decreased thereby."

4. Correlation Formulae For Forced Convection Heat Transfer

Although there does not exist a complete analytical solution for heat transfer around a cylinder due to the complexity of the flow in the region where the boundary layer is turbulent or has separated, design requirements for this information must be satisfied. The answers are generally provided by means of empirically determined correlation formulae. All correlations are for average Nusselt numbers and not local Nusselt numbers. Although the present work is concerned with the latter, this discussion of correlations is included for the sake of completeness. The contributions in this branch of the study have been numerous and tailored for almost every conceivable combination of flow conditions. Perhaps the best known, and one of the earliest, was the work of Hilpert [35] in 1933 whose data included Reynolds numbers from about 500 to 200,000. Unfortunately, the turbulence intensity of his wind tunnel is unknown.

Richardson in Ref. 36 concluded that Hilpert's measurements "do not correspond well with present-day understanding of the heat transfer distribution around a circular

cylinder." As mentioned before, Richardson subscribed to a correlation formula with a separate term to represent heat transfer in the separated region, that is proportional to Reynolds number to the two-thirds power.

In Ref. 37 McAdams has put together a compilation of much of the work in this area.

After a review of previous work, Van der Hegge Zijnen presented [18] a new correlation formula for combined free and forced convection heat transfer from cylinders to air.

III. THEORY

The overall objective of this study was to experimentally determine local, convective heat transfer coefficients around a right circular cylinder placed in a cross flow of air exhibiting a low turbulence intensity (~0.5%). To accomplish this objective, an experiment was designed that embodied several basic theoretical concepts. These concepts include the governing equations for the flow of air around a two-dimensional cylinder mounted vertically in a closed, low-speed wind tunnel. Also involved are the relations that govern the heat generation technique employed and the modes of heat transfer to the environment.

A. DESCRIPTION OF THE FLUID MOTION

Figure 1 is a schematic diagram of the system considered. Location one is upstream, location two is the

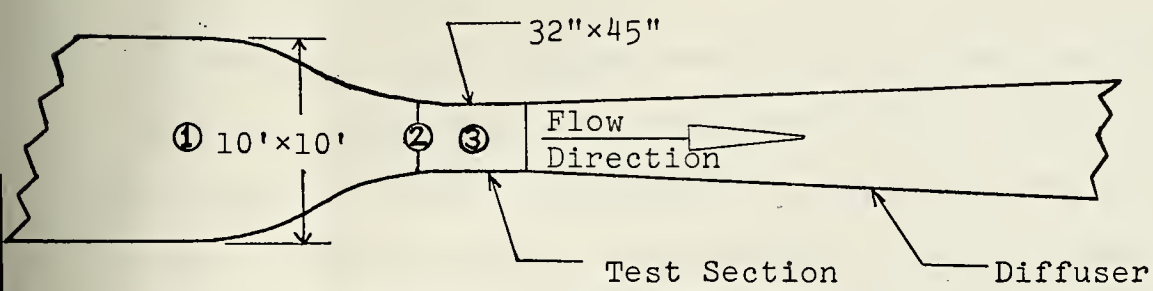

Figure 1. Schematic Diagram of the Air Flow System

entrance to the test section, and location three is the center of the test section. All pressure pickups that were mounted either in the wind tunnel or on the cylinder were within this system. The applicable equations for calculating the velocity in the test section (section 3) are (see nomenclature for definitions of terms):

1. Continuity Equation (clear tunnel, without cylinder)

$$\rho_1 A_1 U_1 = \rho_2 A_2 U_2 \tag{15}$$

2. Bernoulli's Equation (clear tunnel, without cylinder)

$$P_1 + \frac{1}{2} \rho_1 U_1^2 = P_2 + \frac{1}{2} \rho_2 U_2^2 \tag{16}$$

3. Dynamic Pressure at Any Location, i

$$q_i = \frac{1}{2} \rho_i U_i^2 \tag{17}$$

4. Pressure Coefficient at Any Angular Location on the Cylinder, θ

$$C_p = \frac{P_\theta - P_3}{\frac{1}{2}\rho_3 U_3^2} \tag{18}$$

It was assumed that the density of air was constant throughout the system at any instant of time. This assumptin implies that the flow was incompressible, and since density is a function of temperature, it also implies that any temperature rise through the system was uniform. Specifically,

$$\rho_1 = \rho_2 = \rho_3 = \rho \tag{19}$$

Combining equations (15), (16) and (19) and noting that the Aerolab tunnel had a contraction ratio of $A_2/A_1 = 0.1$, it is found that

$$(P_1 - P_2) = \Delta P_{1-2} = 0.99 \left(\frac{\rho U_2^2}{2} \right) . \qquad (20)$$

Ideal test section behaviour may be described as the state existing if the static pressure and velocity at location three are identical to those at location two. The static pressure variation across the test section was negligible for the purposes of the experiment. Therefore the static pressure at location two, P_2, was assumed to be identical to P_3.

The dynamic pressure at location three is given as

$$q_3 = \tfrac{1}{2}\rho U_3^2 . \qquad (21)$$

Ideally, $U_3 = U_2$, and the ideal dynamic pressure at location three may be written as

$$q_{ideal} = \tfrac{1}{2}\rho U_2^2 . \qquad (22)$$

Combining equations (20) and (22)

$$\tfrac{1}{2}\rho U_2^2 = \frac{\Delta P_{1-2}}{0.99} = q_{ideal} \qquad (23)$$

is written as a second result. The numerator can be measured directly.

It is now convenient to manipulate equation (18) into a more suitable form. Since the static pressure was

assumed to be constant, the numerator may be rearranged as follows

$$P_\theta - P_3 = P_\theta - P_2 \quad . \tag{24}$$

This latter form can be measured directly and may be designated as

$$P_\theta - P_2 = \Delta P_{cylinder} \quad . \tag{25}$$

The denominator of equation (18) is sometimes described as

$$q_{actual} = \tfrac{1}{2}\rho U_3^2 \quad . \tag{26}$$

The ratio of q actual to q ideal is termed the tunnel correction factor, X, and is a function of the particular wind tunnel. For the wind tunnel used,

$$X = \frac{q_{actual}}{q_{ideal}} = 0.99 \quad . \tag{27}$$

Now, combining equations (18), (24), (25), (26) and (27) the pressure coefficient is found to equal

$$C_p = \frac{\Delta P_{cylinder}}{\Delta P_{1-2}} \quad . \tag{28}$$

The free stream velocity is found by combining equations (23), (26) and (27). The final result is

$$U_3 = \sqrt{\frac{2 \cdot \Delta P_{1-2}}{\rho}} \quad . \tag{29}$$

The Reynolds number may then be calculated directly,

$$Re = \frac{U_3 D}{\nu} \quad . \tag{30}$$

Since the above results were derived from equations one and two for a clear tunnel, blockage effects due to the presence of a bluff body in a constrained channel have not yet been included. Blockage corrections to the free stream velocity and Reynolds number are computed in Appendix A.

B. THERMAL ENERGY GENERATION AND TRANSFER

Thermal energy was generated by energizing thin Nichrome ribbon with a direct current, I. By means of the uniform electrical resistance of the Nichrome, R, electrical energy was transformed uniformly into thermal energy. This technique was described by Wood [1] as a Joulean heating rate, where

$$Q = I^2R. \tag{31}$$

Once generated, the thermal energy was dispersed by all three modes of heat transfer. Convection was the primary mode, and forced convection in particular was the mode of interest. References 38-40 support the assumption made that external free convection could be neglected.

Convection internal to the cylinder was considered to be negligible, as the cylinder was filled with foam rubber which prevented any major circulation of air.

It is helpful to consider an intuitive account of the external forced convection involved in the cooling of a heated cylinder immersed in a cross flow of air. At the forward stagnation point the cylinder receives the full strength of the wind and, as one would expect, is

relatively cooler. Proceeding back along the sides of the cylinder one would expect a continued decrease of the cooling effect of the wind and a gradual increase in the wall temperature of the cylinder. Once the boundary layer separates or becomes turbulent it seems logical that the cylinder wall would rapidly begin to be cooled again, by the turbulent packets of fluid "scrubbing" the surface and transporting thermal energy from the cylinder surface.

The concept employed for quantitatively evaluating the external forced convection was the same as that used by Giedt [15]. It consists of applying Newton's law of cooling,

$$\frac{Q}{A_s} = q_\theta = h_\theta (T_\theta - T_\infty) \tag{32}$$

to the previously discussed expression,

$$Q = I^2 R \ .$$

(See nomenclature for definitions of terms.) Then the basic expression for the local heat transfer coefficient can be written as

$$h_\theta = \frac{I^2 R}{A_s (T_\theta - T_\infty)} \ . \tag{33}$$

Conduction of thermal energy out the ends of the cylinder was prevented by the installation of guard heaters. Since data were collected at steady state conditions, radial conduction of heat energy into the interior of the cylinder was neglected. Circumferential conduction of thermal

energy through the Nichrome was considered. This transfer should vary with position since the temperature gradient is a variable of position. Near the forward stagnation point, plus or minus about 20 deg, the temperature gradient should be small and circumferential conduction should have a minimal effect. However, one would expect that farther around the cylinder the trend would eventually be a flow of heat into a relatively cool region. A net flow of heat into an element in this region augments the heat generated within the element, causing the wall temperature to be higher than it would be otherwise. In the vicinity of the separation point the temperature gradient should be steep and the effect of circumferential conduction would be maximized. A net flow of heat out of an element in this region of relatively high temperature would tend to indicate a higher heat transfer rate than an ideal case without circumferential conduction.

Radiation of electromagnetic thermal energy from the cylinder to the tunnel walls was taken into account and treated as a loss. Radiation losses were relatively small because of the small temperature differences involved, but were not considered to be negligible.

An elemental heat balance has been developed for an element of Nichrome ribbon to derive the detailed expression required for calculating the local heat transfer coefficient, h_θ. The resulting expression contains all applicable modes of heat transfer. The components of this

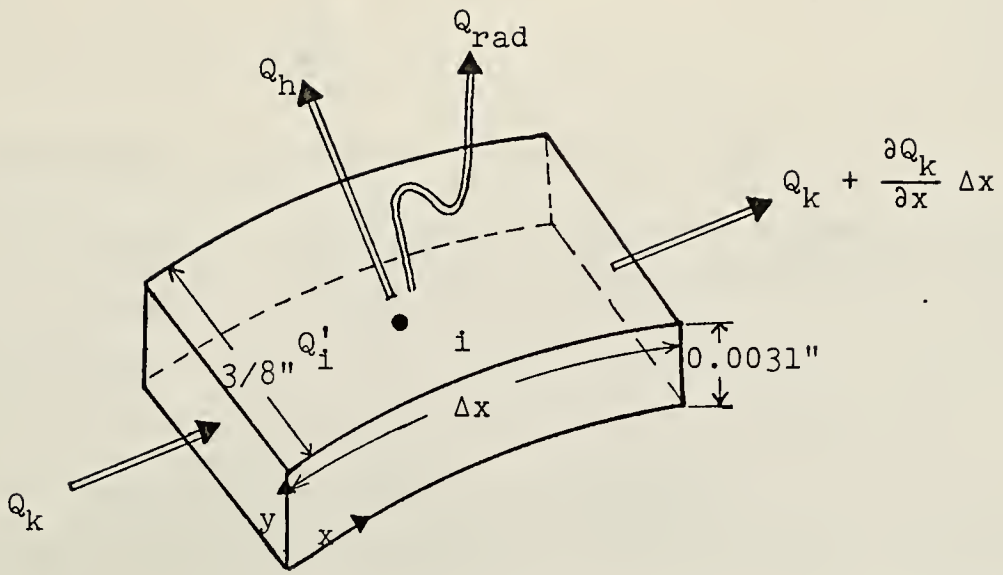

Figure 2. Heat Transfer for an Element of Nichrome Ribbon

expression are depicted in Figure 2. (See nomenclature for definitions of terms.) The heat balance is first written

$$Q_k + Q_i' - Q_h - Q_{rad} - Q_k - \frac{\partial Q_k}{\partial x} \Delta x = 0. \tag{34}$$

It is noted that

$$Q_k = -k_n A_n \frac{\partial T}{\partial x} , \tag{35}$$

$$\frac{\partial Q_k}{\partial x} \Delta x = -k_n A_n \frac{\partial^2 T}{\partial x^2} \Delta x , \tag{36}$$

$$Q_h = h_\theta A_s (T_\theta - T_\infty) , \tag{37}$$

$$Q_{rad} = \sigma \varepsilon (T_\theta^4 - T_\infty^4) A_s , \tag{38}$$

and

$$Q_i' = (I^2R)_i = \left(\frac{V^2}{R}\right)_i . \tag{39}$$

Substituting into the heat balance one has

$$k_n A_n \frac{\partial^2 T}{\partial x^2} \Delta x + \left(\frac{V^2}{R}\right)_i - h_\theta A_s (T_\theta - T_\infty) - \sigma \varepsilon A_s (T_\theta^4 - T_\infty^4) = 0. \tag{40}$$

Rearranging

$$h_\theta = \frac{k_n A_n \frac{\partial^2 T}{\partial x^2} \Delta x + \left(\frac{V^2}{R}\right)_i - \sigma \varepsilon A_s (T_\theta^4 - T_\infty^4)}{A_s (T_\theta - T_\infty)} . \tag{41}$$

Rewriting in a finite difference formulation

$$h_\theta = \frac{\frac{k_n A_n}{\Delta x} (T_{i-1} + T_{i+1} - 2T_i) + \left(\frac{V^2}{R}\right)_i - \sigma \varepsilon A_s (T_i^4 - T_\infty^4)}{A_s (T_i - T_\infty)} \tag{42}$$

This formula is the core of the computer program in Appendix B that was written for data reduction.

The above expression doesn't account for aerodynamic heating of the cylinder, and for the continuous rapid heating of the ambient air by the wind tunnel boundaries and impeller at velocities above 125 feet per second. Because the former effect tended to raise the unheated cylinder above its initial temperature and the latter caused the slower responding cylinder to lag the ambient air temperature, the two effects labored in opposition. Their combined, resultant effect was calibrated out of the data as shown in Appendix C.

IV. EXPERIMENTAL APPARATUS

A. LOW SPEED WIND TUNNEL

The experimental study was carried out in the low speed Aerolab wind tunnel, located in the Aeronautics Laboratory in Halligan Hall, U.S. Navy Postgraduate School. A schematic diagram of the wind tunnel is provided in Figure 3.

The turbulence intensity level of the wind tunnel was measured using a hot wire anemometer and its associated electronic equipment. The turbulence level ranged from 0.67 for the low speed run to 0.43 for the high speed runs. The details of these measurements and the equipment used are described in Appendix D.

The wind tunnel is powered by a 100 hp electric motor, and has a four speed transmission. All experimental runs conducted at a Reynolds number less than 350,000 were in third gear and the high speed runs were conducted in fourth gear. The tunnel was capable of achieving a maximum speed of 200 mph with a clear test section. However, with the cylinder in place, the peak speed was only about 172 mph.

Air speed information was determined by observing the pressure drop between two static pressure manifolds which indicated static pressure in the settling chamber (Figure 1, location one) and near the entrance to the test section (Figure 1, location two). This static pressure difference, ΔP_{1-2}, was read on the water-filled air speed manometer.

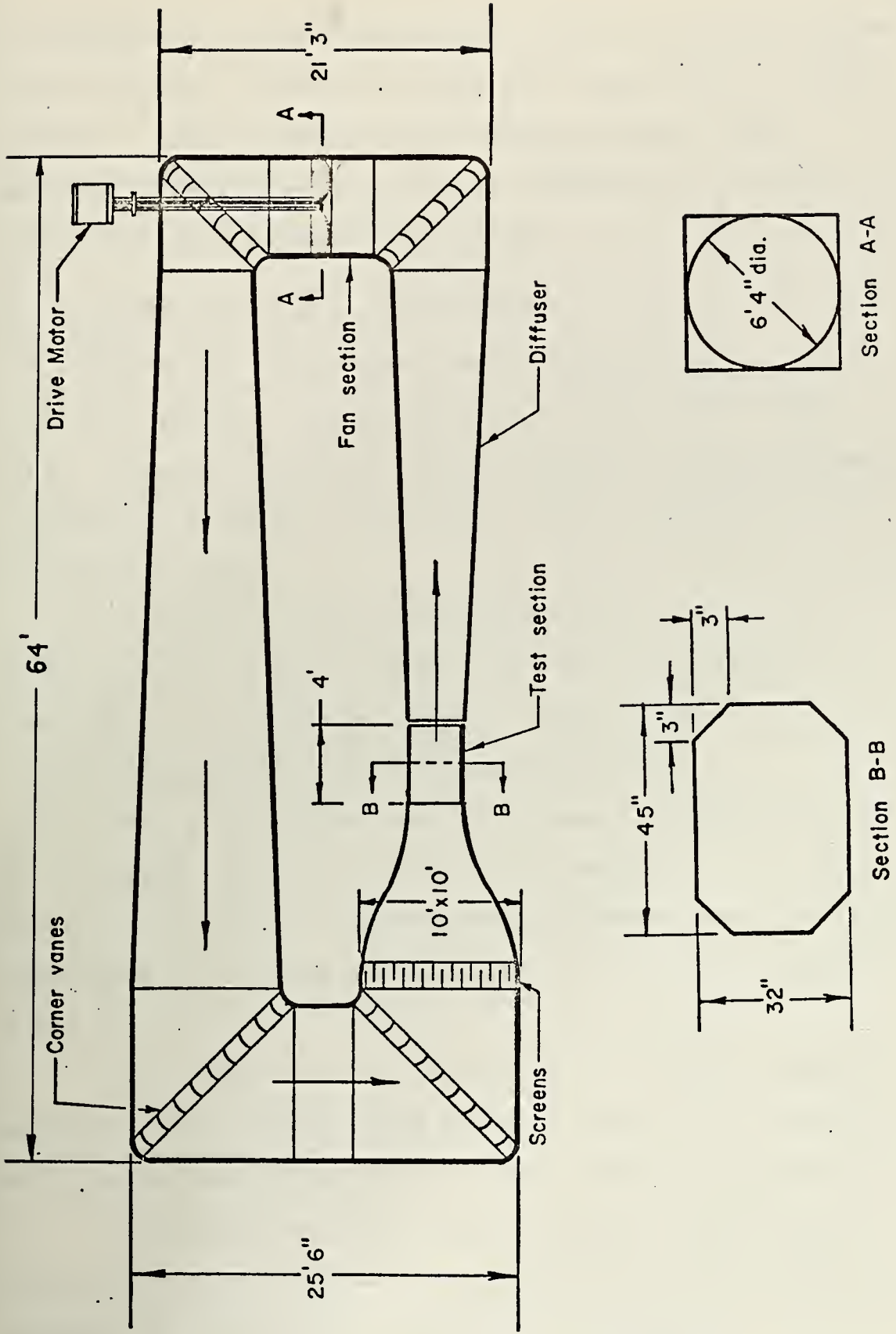

Figure 3. Schematic Diagram of the Wind Tunnel

The manifold for each location was connected to four static pressure pickups installed in the wind tunnel walls at that location. Setting the zero and reading the air speed manometer required a great deal of consistent, meticulous effort to obtain acceptable accuracy.

B. CYLINDER DESIGN AND CONSTRUCTION

All data for this project were collected with a 4.47 in (o.d.) cylinder constructed from a cast acrylic resin tube. A second cylinder made from phenolic tubing has been designed and partially constructed, and is expected to be an improved model.

As is apparent in the descriptions which follow, the design concept of both cylinders was the same as that of Giedt [15] with only some physical alterations.

1. The Cylinder Made From Acrylic Tubing

The test cylinder was 32 in long and spanned the entire height of the wind tunnel test section. Its 4.47 in (o.d.) diameter and 0.30 in wall thickness were the final dimensions after being machined into round from an original 4.625 in (o.d.).

The choice of a relatively large cylinder diameter permitted sufficiently large Reynolds numbers for examining all flow regimes in spite of a fairly limited air speed.

A circuit for generating a constant heat flux on the surface of the cylinder was installed by helically wrapping Nichrome ribbon around the circumference of the

cylinder. The Nichrome ribbon was 0.375 in wide and 0.0031 in thick, and had a resistance of 0.456 ohms per foot of length. This particular size was selected primarily on the basis of availability. It also possessed a sufficient total resistance to accommodate enough current to drive the surface temperature well above the ambient air temperature, even for high speed flows.

To facilitate the wrapping process and to promote a smooth surface, the cylinder was grooved 2.5 threads per in, 0.375 in wide, and 0.005 in deep. This left a separation of only about 0.025 in between individual wraps, giving a close approximation to a uniform heat flux. The ends of the ribbon were led through slots from, and back into, the interior of the cylinder where they were connected to power leads. The ribbon was bonded to the cylinder with RTV-108, silicone rubber adhesive.

The main circuit consisted of 39 wraps and had a total resistance of 20.527 ohms as measured on a Rosemount commutating bridge, model 920A. Variations in the resistance due to an increase in temperature were considered negligible over the temperature range involved. This circuit was located approximately in the center of the tube, beginning 9.125 in from the base and extending up 15.125 in of the tube's length.

Two smaller guard heater circuits were similarly installed above and below the main circuit. These consisted of three wraps of Nichrome ribbon whose ends were led

through separate slots. Each pair of guard leads were then connected to a separate pair of power leads. This arrangement allowed the guard heater circuits to be controlled individually. As shown in Figure 4, the guard heater circuits were laid down in the same continuous groove as the main circuit and adjacent circuit slots were separated by only 0.5 in. The smaller circuits each had a resistance of about two ohms.

While the guard heater circuits were the primary means of precluding heat conduction losses out the ends of the tube, the wall thickness at each end was also shaved to 0.0625 in to minimize conduction losses.

Temperature information was measured using premium grade copper-constantan bead thermocouples made from 0.005 in wire. One thermocouple was shielded and located on a screen in the settling chamber, where the velocity was a tenth of the test section velocity. It therefore provided a true measure of the ambient air temperature. It was referenced against an ice junction, and acted as a reference for the remaining eight thermocouples which were installed on the cylinder surface in the following manner. They were led through drilled holes in the cylinder wall and were spot welded to the inner surface of the ribbon just prior to the sealing of the ribbon to the surface. These thermocouples directly indicated the temperature difference between the cylinder surface and the ambient air. Their location on the cylinder is pictured in Figure 4.

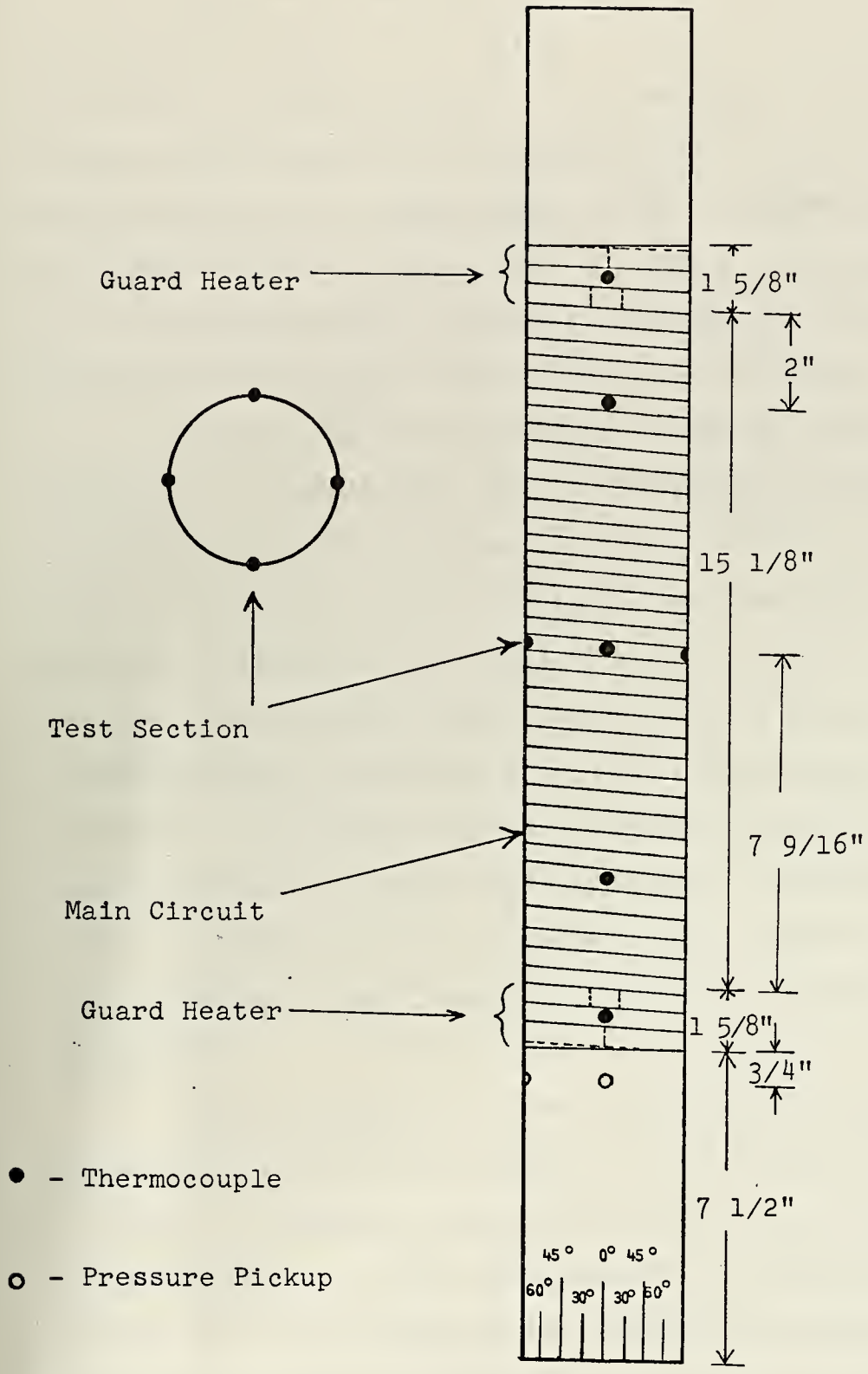

Figure 4. Test Cylinder

The test section was designated as the center wrap of the main circuit. It consisted of four thermocouples attached at 90 deg intervals. The remaining four thermocouples were used solely for guard heater control. Two were located on the center wrap of the two guard circuits. The other two were located near the edges of the main circuit and provided the comparative temperature information required for the guard heater system to function.

To avoid any contamination or damage to the test cylinder, the actual test thermocouples were not calibrated. Instead, an identical thermocouple was welded to a small strip of Nichrome. This representative test thermocouple was then calibrated in the Rosemount constant temperature bath system which had a platinum resistance thermometer connected across the Rosemount commutating bridge as a standard. An ice bath was used for the reference junction. Since the results showed close agreement with the published table for copper-constantan thermocouples over the applicable temperature range, the table was used for data reduction.

An additional check was performed on a similar representative test thermocouple to insure that no extraneous EMF, as described by Davenport and others in Ref. 41, was generated due to its attachment to a direct-current heater. The test consisted of pulsing the small strip of Nichrome with direct current and observing the response of the attached thermocouple on a Honeywell chart recorder.

Only an exponential rise and fall of thermally induced EMF were observed. No step changes, which would be indicative of an extraneous electrical EMF, were observed. This conclusion was in agreement with Davenport [41] for a bead thermocouple making point contact with an electrically heated substrate.

Another simple experiment was performed to gain insight into the relatively larger thermal expansion of the acrylic tube in comparison to the Nichrome ribbon. The objective was also to determine an upper limit for surface temperature, based upon the endurance of the acrylic to resist a combination of continuous high temperatures and potentially deforming hoop stress which was applied by the cinching action of the ribbon. A third objective of the experiment was to determine the ability of the R.T.V. sealant to resist high temperatures. The details of the experiment are given in Appendix E. The results are briefly summarized as follows. Deformation is probable in still air at temperatures above 130°F, and the R.T.V. held solidly at temperatures up to 180°F.

As the R.T.V. cured after the Nichrome ribbon was bonded to the final test cylinder, a contraction of the sealant occurred, resulting in various peaks and recesses in the ribbon and therefore a somewhat lumpy surface rather than the desired smooth one. The effects of these flaws are discussed later in the thesis.

Two static pressure pickups were installed in the cylinder wall 0.75 in. below the lower guard heater and at 90 deg intervals. These were made of 0.040 in (o.d.) stainless steel tubing, and had an orifice of 0.032 in (i.d.). In this way, surface pressure was measured and input to one side of a U-tube water-filled manometer. The manometer was referenced against the static pressure at the entrance to the test section, P_2.

After the thermocouples and pressure taps were in place, the cylinder was filled with Silastic, S-5370, RTV foam, a low density resilient silicone rubber. The foam rubber was easily poured into the cylinder and quickly expanded, uniformly filling every crevice. It provided support for the fine thermocouple wires. Internal free convection was practically eliminated, and the foam was an excellent insulator, exhibiting a thermal conductivity of 0.026 BTU/hr-ft-°F. Unfortunately, a serious disadvantage of the foam was its large thermal capacity which considerably increased the delay before reaching steady state conditions. Long experimental runs were the outcome of this objectionable feature.

The cylinder was mounted on a turntable base that could be rotated from outside the wind tunnel. A disk, that was marked every five degrees, rotated with the cylinder base. Therefore, temperature difference and surface pressure could be determined at any desired angular location.

Figures 5 and 6 show the cylinder mounted in the test section.

2. A Proposed Phenolic Test Cylinder

A second cylinder made from 4 in (o.d.) phenolic tubing has been designed and partially constructed. It is based upon the same experimental concept as the first cylinder, but has several different and potentially better features.

The coefficient of thermal expansion is not as large as the acrylic tube, but is closer to that of the Nichrome. Therefore, it is possible that a sealant would not be required over the entire length of the ribbon, if required at all. This would preclude the development of surface irregularities.

The phenolic tubing can withstand much higher temperatures for long periods of time without experiencing deformation.

A space for four additional thermocouples has been provided on one side of the cylinder in the test section region, resulting in thermocouples spaced every 30 deg. This feature will expedite data collection.

At the time of this writing, the phenolic tubing has been machined and grooved to accept the three circuits. The rotating base has been modified to accept the smaller diameter tube, and electrical design requirements have been completed.

Figure 5. Test Cylinder Mounted in the Wind Tunnel Test Section

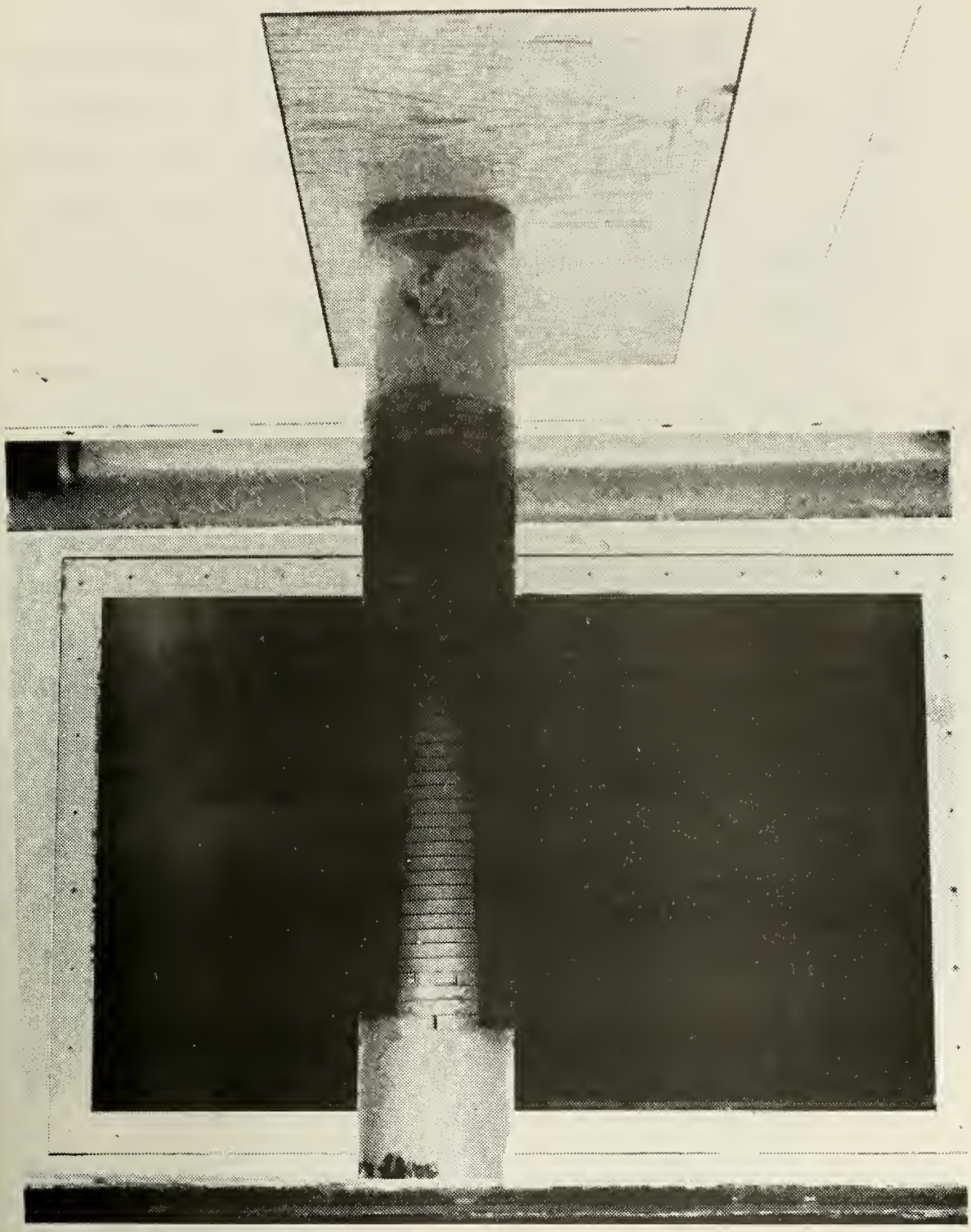

Figure 6. Closeup View of Test Cylinder

C. ELECTRICAL CIRCUITRY AND EQUIPMENT

All power leads and thermocouple wires were led down the interior of the cylinder and out of the wind tunnel through a hole in the cylinder base. Each pair of power leads for the three circuits was connected to individual Lambda model LK 345A FM 60-volt regulated power supplies. A Non-Linear Systems Inc., Model 481 digital voltmeter was used to monitor the power settings for any of the three circuits to the nearest millivolt.

The thermocouple wires were connected to a ten position rotary switch: eight positions for the thermocouples on the cylinder, one position for the thermocouple in the settling chamber and the tenth position was used to include the ice junction. The output leads from the switch were connected to either a Honeywell chart recorder during the transient, warming up period, or to a Leeds and Northrup millivolt potentiometer for the accurate data collection at steady state conditions.

Figures 7 and 8 illustrate the arrangement of the equipment.

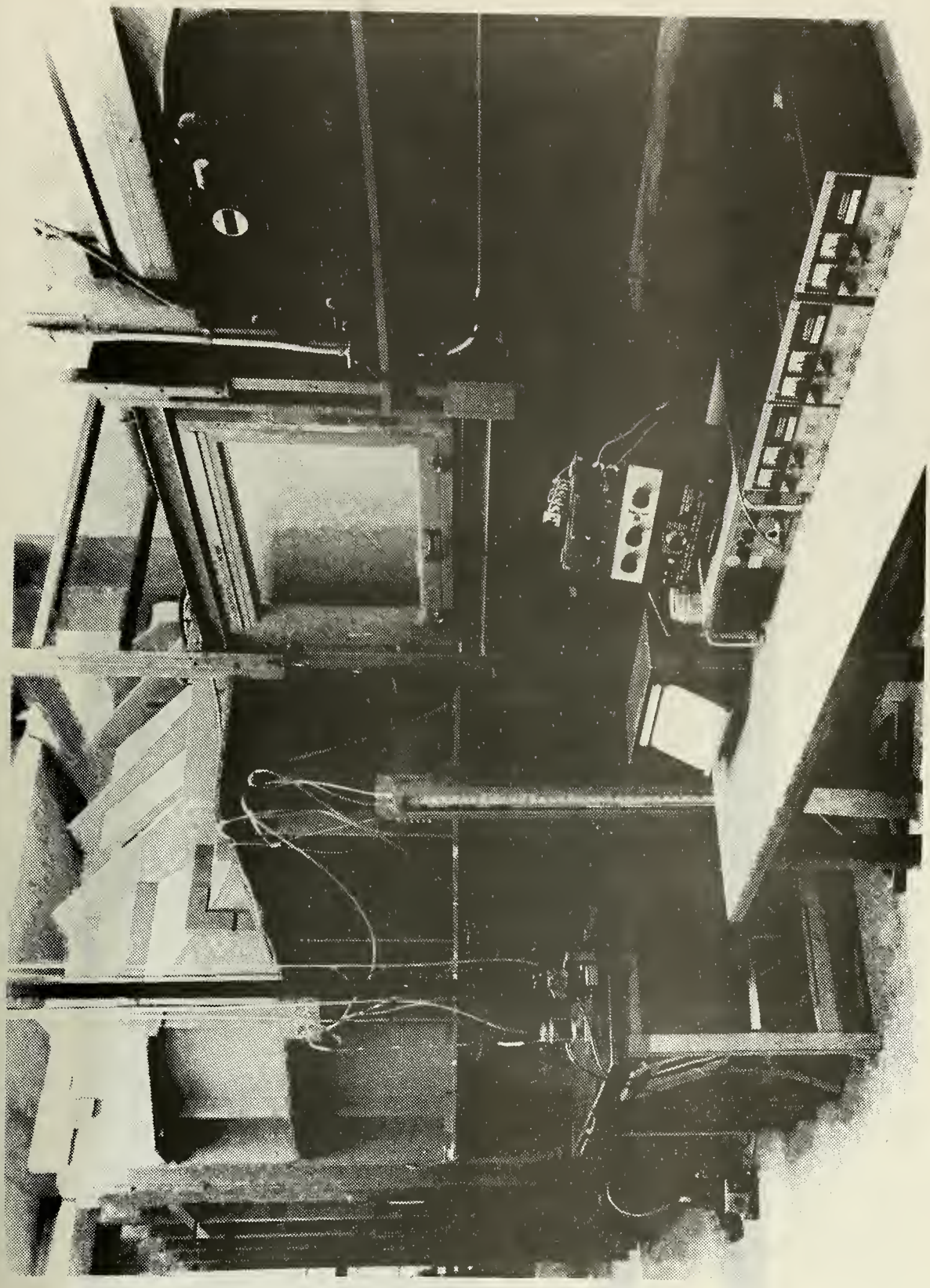

Figure 7. Arrangement of the Experimental Apparatus

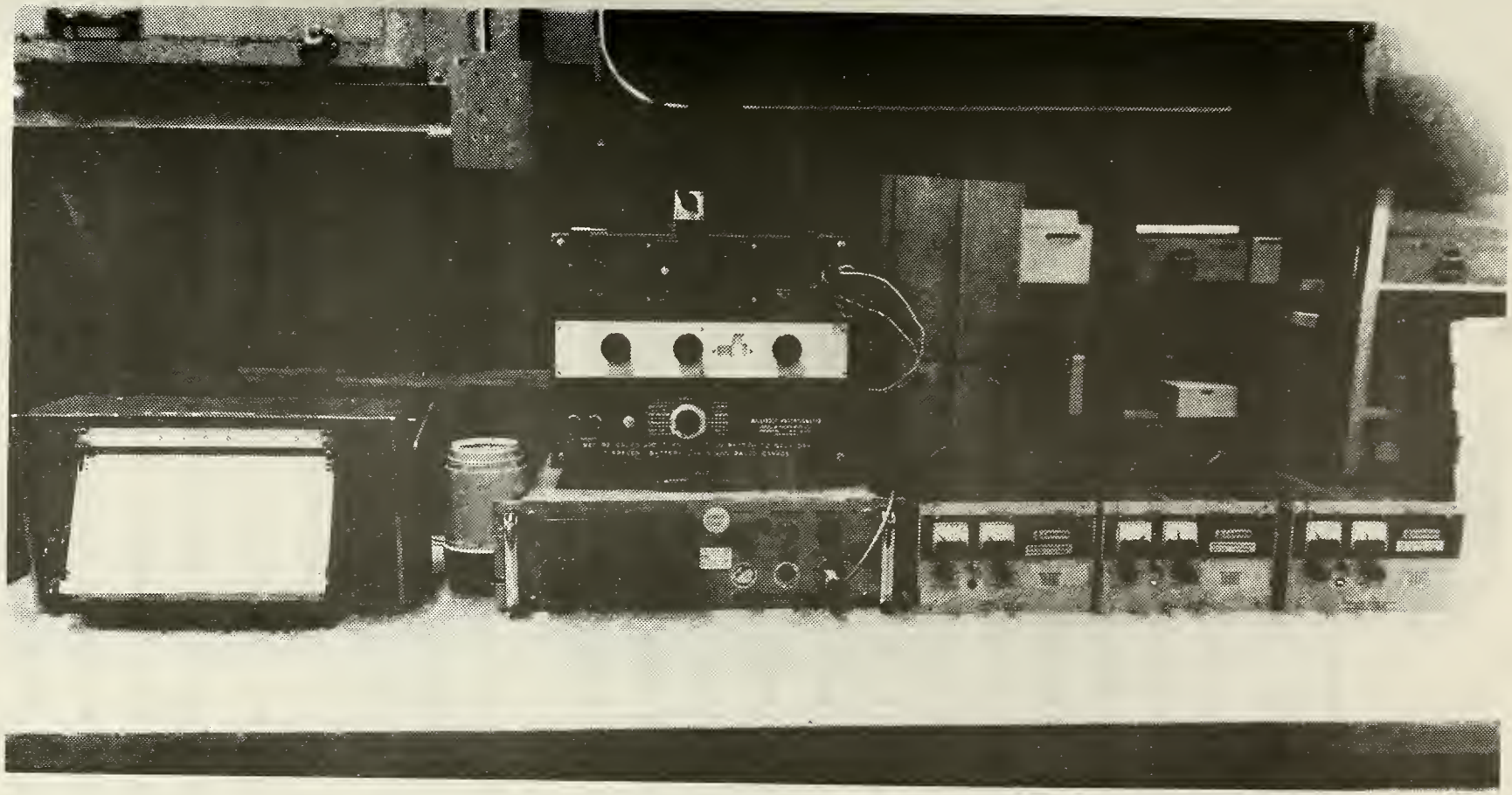

Figure 8. Close Up View of the Electrical Equipment

V. EXPERIMENTAL PROCEDURE

In the development of a precise experimental technique for the test cylinder constructed for this study and others that might follow, there were three distinct phases of experimentation, each spanning several months of research.

Initially, the heat transfer characteristics of the cylinder were investigated at a single Reynolds number of 153,000. During this time a large amount of preliminary data were recorded to determine if the temperature distribution over one side of the cylinder was the same as on the opposite side so that data could be collected from one side only; to ascertain which side of the cylinder was preferable and would provide the smoother data, particularly in view of the surface irregularities mentioned previously; and to resolve a preferable pattern of rotation in conjunction with the preferred side.

The second phase of experimenting consisted of an investigation of eight different Reynolds numbers, and was originally intended to provide the final results. This would, in fact, have been the case had the author been more experienced in the art of wind-tunnel testing. However, at various times in the process of collecting this data, flaws in the experimental technique were discovered which detracted from the credibility of the results. For this reason, the author elected to perform an additional

series of runs which incorporated a detailed experimental procedure. The following tasks, which compose this procedure, are discussed in their approximate order of accomplishment.

The air speed and U-tube manometers were carefully set to zero, and all pressure line connections were checked for tightness.

The Nichrome ribbon wrappings on the test cylinder were cleaned before each run with acetone to remove any film of dust, oil or oxidation. The cylinder was oriented into its initial position and the accesses to the test section were secured.

All electronic equipment was turned on to begin warming up. The initial voltmeter reading was recorded for the main circuit with no current flowing. This reading was invariably -0.065 volts.

The wind tunnel was put in the proper gear, turned on and the air speed increased to only about ten mph. This circulated and brought the air to a uniform temperature.

The zero was set on the millivolt potentiometer and the initial readings for all thermocouples were recorded including the initial air temperature. Just prior to recording these and all subsequent temperature data, a check was made to insure that a proper water-ice interface existed at the ice junction.

The air speed was increased to provide the Reynolds number desired for the run. Choosing the correct air speed

for this purpose was not obvious. The air temperature in the tunnel generally increased with time to some level, at which the time rate of temperature rise was a minimum. For higher velocities the air temperature increased to higher levels. Since the viscosity and density of the air are dependent upon the air temperature, prior knowledge of the resultant level of air temperature was required for setting the air speed of the run.

The output leads from the thermocouple rotary switch were removed from the potentiometer and connected to the chart recorder. The voltage to the main circuit was then increased gradually to the desired power level for the run. This level was chosen to be the amount of power that would maximize the temperature increase of the cylinder surface above the ambient air temperature without surpassing the high temperature endurance limit of the acrylic tube. Maximizing delta T enhanced the degree of accuracy of the heat transfer data and tended to alleviate many of the surface irregularities by driving more thermal energy into the sealant, thereby expanding some of the recesses.

Power was increased to each guard heater circuit until an approximately equivalent amount of current was flowing as in the main circuit; the voltage was about an order of magnitude less than the main circuit voltage. As the main circuit settled to the desired level of power, fine adjustments were made to the guard heaters. Their surface temperature should be maintained equal to the surface temperature

at the edges of the main circuit by comparing the guard heater thermocouple readings to those on the edges of the main circuit.

After the thermal capacity of the acrylic tube and its foam rubber filler were saturated, a steady state condition existed. Then, all of the heat added was removed by convection, less any losses due to thermal radiation to the tunnel walls or circumferential conduction through the Nichrome ribbon. The progress of the surface temperatures toward their steady state values was observed and tracked on the chart recorder. It generally required about two hours to reach steady state, depending on the velocity of the air. The higher speed runs required up to three hours and the lower speed runs were sometimes steady after 1.5 hours.

The experiment was modeled on TRUMP, a computer program developed at Lawrence Radiation Laboratory, Livermore, Calif., for solving transient and steady-state temperature distributions in multidimensional systems. Reference 43 is the manual for applying TRUMP. The time required to reach steady state was predicted reasonably well using the TRUMP model.

After the cylinder was in a steady state condition, the thermocouple rotary switch output leads were again connected to the potentiometer. The potentiometer was again mechanically and electrically set to zero, as it was just prior to any recording of temperature data, and the steady

state values of the surface temperature increases above the ambient air were recorded for the initial position of the cylinder. The ambient air temperature was also recorded. The cylinder surface pressure was measured by the U-tube manometers and recorded.

The cylinder was then rotated five degrees to a new position. The time required to reach steady state at the new position was generally 15 to 30 minutes. This was more than adequate time to check the ice junction, collect the pressure data at this new position and zero the potentiometer. Once steady state was reached at the new position, the temperature data were recorded as before, and the cylinder again rotated five degrees.

In this way, temperature and pressure data could be obtained at any desired angular location. All data were collected on one side of the cylinder only. The experimental runs required 8-10 hours each due to the large thermal capacity of the cylinder, and the small number of test thermocouples installed.

VI. PRESENTATION OF RESULTS

Raw data, including temperature information in millivolts and pressure information in cm or in of water, were read directly into the computer program in Appendix B. The density, thermal conductivity and kinematic viscosity of air were evaluated at the film temperature, T_f, which was computed by

$$(T_f)_{run} = (T_{amb})_{avg} + 0.5(\Delta T)_{avg} \tag{43}$$

for each run, where $(T_{amb})_{avg}$ is the average ambient temperature and $(\Delta T)_{avg}$ is the average local surface temperature increase at steady state.

A. TABULAR RESULTS

The computer program provided detailed results for all thirteen experimental runs. These are presented in tabular form on pages 72-84. The pressure coefficient, heat transfer coefficient, Nusselt number and Froessling number are provided at five deg intervals from the forward to the rear stagnation points for all runs except three runs which omitted the pressure information. Two of these runs are duplicates of others which include pressure information. Therefore, a complete set of results is presented at ten different Reynolds numbers.

"DELTAX" is the arc length, "ASURF" is the surface area, and "QGEN" is the heat generation rate of a 5 deg element

FORCED CONVECTION HEAT TRANSFER FROM A UNIFORMLY

HEATED CYLINDER IN A CROSSFLOW OF AIR

FREE STREAM DYN. HEAD EQUALS 0.35 CM OF WATER
FREE STREAM VELOCITY EQUALS 25.1 FT.PER SEC.(UNCORRECTED)
FREE STREAM VELOCITY EQUALS 26.1 FT.PER SEC.(CORRECTED)
THE REYNOLDS NUMBER EQUALS 54785. (UNCORRECTED)
THE REYNOLDS NUMBER EQUALS 56878. (CORRECTED)
DELTAX EQUALS 0.01625 FEET
ASURF EQUALS 0.000508 SQUARE FEET
QGEN EQUALS 0.12008 BTU PER HOUR
TU EQUALS 0.67 PER CENT

THETA (DEG)	DELTA-P (CM)	CP	DELTA-T (DEG F)	DELTA-T CORRECTION	DELTA-T CORRECTED	QCOND (BTU/HR)	QRAD (BTU/HR)	HT TRANS COEFF	NUSSELT NR	FROESSLING NR
0.0	0.28	0.80	26.58	0.0	26.58	0.00168	0.01012	8.27	202.02	0.8471
5.0	0.25	0.73	26.58	0.0	26.58	0.00084	0.01013	8.21	200.50	0.8407
10.0	0.23	0.65	26.80	0.0	26.80	-0.00050	0.01022	8.04	196.23	0.8228
15.0	0.20	0.58	26.89	0.0	26.89	-0.00017	0.01026	8.03	196.11	0.8223
20.0	0.16	0.46	26.94	0.0	26.94	0.00134	0.01029	8.13	198.43	0.8320
25.0	0.10	0.29	27.34	0.0	27.34	-0.00034	0.01047	7.87	192.21	0.8059
30.0	0.0	0.0	27.66	0.0	27.66	0.00034	0.01060	7.82	190.96	0.8007
35.0	-0.08	-0.22	28.06	0.0	28.06	0.00000	0.01078	7.67	187.33	0.7855
40.0	-0.18	-0.51	28.47	0.0	28.47	0.00017	0.01095	7.56	184.65	0.7743
45.0	-0.25	-0.73	28.92	0.0	28.92	0.00084	0.01113	7.48	182.60	0.7656
50.0	-0.30	-0.87	29.59	0.0	29.59	0.00218	0.01141	7.38	180.15	0.7554
55.0	-0.36	-1.02	30.85	0.0	30.85	0.00302	0.01190	7.10	173.34	0.7268
60.0	-0.38	-1.09	32.92	0.0	32.92	0.00084	0.01274	6.47	158.03	0.6626
65.0	-0.39	-1.12	35.22	0.0	35.22	0.00050	0.01371	5.98	145.94	0.6119
70.0	-0.39	-1.12	37.65	0.0	37.65	0.00135	0.01478	5.58	136.23	0.5712
75.0	-0.38	-1.09	40.44	0.0	40.44	0.01545	0.01601	5.82	142.14	0.5960
80.0	-0.36	-1.02	47.38	0.0	47.38	-0.00445	0.01911	4.01	97.98	0.4108
85.0	-0.33	-0.94	53.12	0.0	53.12	-0.02323	0.02179	2.78	67.95	0.2849
90.0	-0.36	-1.02	52.63	0.0	52.63	-0.00066	0.02157	3.66	89.41	0.3749
95.0	-0.37	-1.07	51.97	0.0	51.97	-0.00099	0.02127	3.71	90.53	0.3796
100.0	-0.38	-1.09	51.04	0.0	51.04	-0.00379	0.02084	3.68	89.94	0.3771
105.0	-0.38	-1.09	49.10	0.0	49.10	-0.00231	0.01994	3.92	95.83	0.4018
110.0	-0.38	-1.09	46.54	0.0	46.54	-0.00577	0.01878	4.04	98.73	0.4140
115.0	-0.38	-1.09	42.43	0.0	42.43	0.01483	0.01695	5.48	133.70	0.5606
120.0	-0.38	-1.09	42.30	0.0	42.30	-0.00346	0.01690	4.64	113.39	0.4754
125.0	-0.38	-1.09	41.24	0.0	41.24	-0.00809	0.01644	4.56	111.44	0.4673
130.0	-0.38	-1.09	38.01	0.0	38.01	0.00583	0.01502	5.75	140.30	0.5883
135.0	-0.38	-1.09	36.34	0.0	36.34	-0.00386	0.01429	5.52	134.88	0.5656
140.0	-0.38	-1.09	33.64	0.0	33.64	0.00403	0.01312	6.50	158.65	0.6652
145.0	-0.37	-1.05	32.02	0.0	32.02	0.00034	0.01240	6.64	162.23	0.6802
150.0	-0.36	-1.02	30.49	0.0	30.49	0.00168	0.01172	7.11	173.56	0.7277
155.0	-0.36	-1.04	29.41	0.0	29.41	-0.00151	0.01126	7.19	175.46	0.7357
160.0	-0.37	-1.05	27.93	0.0	27.93	0.00252	0.01066	7.89	192.77	0.8083
165.0	-0.38	-1.09	27.12	0.0	27.12	0.00017	0.01034	7.98	194.94	0.8174
170.0	-0.37	-1.05	26.35	0.0	26.35	0.00571	0.01002	8.65	211.29	0.8860
175.0	-0.36	-1.02	27.12	0.0	27.12	-0.00454	0.01034	7.64	186.59	0.7824
180.0	-0.36	-1.02	26.67	0.0	26.67	0.00336	0.01016	8.37	204.30	0.8566

FORCED CONVECTION HEAT TRANSFER FROM A UNIFORMLY

HEATED CYLINDER IN A CROSSFLOW OF AIR

FREE STREAM DYN. HEAD EQUALS 0.72 CM OF WATER
FREE STREAM VELOCITY EQUALS 35.9 FT.PER SEC.(UNCORRECTED)
FREE STREAM VELOCITY EQUALS 37.3 FT.PER SEC.(CORRECTED)
THE REYNOLDS NUMBER EQUALS 79296. (UNCORRECTED)
THE REYNOLDS NUMBER EQUALS 82326. (CORRECTED)
DELTAX EQUALS 0.01625 FEET
ASURF EQUALS 0.000508 SQUARE FEET
QGEN EQUALS 0.09492 BTU PER HOUR
TU EQUALS 0.63 PER CENT

THETA (DEG)	DELTA-P (CM)	CP	DELTA-T (DEG F)	DELTA-T CORRECTION	DELTA-T CORRECTED	QCOND (BTU/HR)	QRAD (BTU/HR)	HT TRANS COEFF	NUSSELT NR	FROESSLING NR
0.0	0.66	0.92	16.86	0.0	16.86	-0.00017	0.00639	10.32	253.57	0.8837
5.0	0.63	0.88	16.63	0.0	16.63	0.00085	0.00628	10.60	260.35	0.9074
10.0	0.56	0.78	16.63	0.0	16.63	0.00051	0.00624	10.56	259.48	0.9044
15.0	0.51	0.71	16.77	0.0	16.77	0.00034	0.00631	10.45	256.67	0.8946
20.0	0.41	0.56	17.00	0.0	17.00	0.00051	0.00641	10.31	253.40	0.8832
25.0	0.23	0.32	17.37	0.0	17.37	-0.00119	0.00656	9.88	242.88	0.8465
30.0	0.13	0.18	17.41	0.0	17.41	0.00085	0.00658	10.09	247.88	0.8639
35.0	-0.05	-0.07	17.69	0.0	17.69	0.00119	0.00670	9.96	244.64	0.8526
40.0	-0.25	-0.35	18.01	0.0	18.01	0.00000	0.00683	9.63	236.74	0.8251
45.0	-0.41	-0.56	18.60	0.0	18.60	-0.00119	0.00709	9.17	225.39	0.7855
50.0	-0.53	-0.74	18.88	0.0	18.88	0.00119	0.00718	9.28	228.01	0.7947
55.0	-0.63	-0.88	19.47	0.0	19.47	0.00034	0.00742	8.89	218.33	0.7609
60.0	-0.76	-1.06	20.16	0.0	20.16	0.00307	0.00771	8.82	216.74	0.7554
65.0	-0.76	-1.06	21.67	0.0	21.67	0.00205	0.00833	8.06	197.98	0.6900
70.0	-0.71	-0.99	23.73	0.0	23.73	0.00278	0.00917	7.35	180.58	0.6294
75.0	-0.69	-0.95	26.53	0.0	26.53	0.00532	0.01034	6.67	163.99	0.5715
80.0	-0.61	-0.85	30.76	0.0	30.76	-0.02284	0.01212	3.84	94.32	0.3287
85.0	-0.66	-0.92	28.87	0.0	28.87	0.00302	0.01132	5.91	145.19	0.5060
90.0	-0.66	-0.92	27.79	0.0	27.79	-0.00067	0.01086	5.91	145.20	0.5061
95.0	-0.63	-0.88	26.53	0.0	26.53	0.00470	0.01031	6.63	162.92	0.5678
100.0	-0.63	-0.88	26.53	0.0	26.53	0.00168	0.01023	6.41	157.54	0.5490
105.0	-0.63	-0.88	26.98	0.0	26.98	-0.01008	0.01044	5.43	133.44	0.4651
110.0	-0.63	-0.88	24.73	0.0	24.73	0.01142	0.00953	7.71	189.44	0.6602
115.0	-0.63	-0.88	25.54	0.0	25.54	-0.01184	0.00988	5.64	138.69	0.4834
120.0	-0.66	-0.92	23.18	0.0	23.18	0.00660	0.00891	7.87	193.37	0.6739
125.0	-0.63	-0.88	22.58	0.0	22.58	-0.00000	0.00868	7.52	184.82	0.6441
130.0	-0.63	-0.88	21.99	0.0	21.99	0.00017	0.00843	7.76	190.73	0.6647
135.0	-0.63	-0.88	21.44	0.0	21.44	0.00034	0.00823	7.99	196.45	0.6847
140.0	-0.63	-0.88	20.98	0.0	20.98	-0.00034	0.00803	8.12	199.64	0.6958
145.0	-0.63	-0.88	20.43	0.0	20.43	0.00034	0.00780	8.43	207.15	0.7219
150.0	-0.63	-0.88	19.97	0.0	19.97	-0.00307	0.00764	8.30	204.02	0.7110
155.0	-0.63	-0.88	18.69	0.0	18.69	0.00615	0.00712	9.90	243.20	0.8476
160.0	-0.66	-0.92	19.06	0.0	19.06	-0.00751	0.00727	8.28	203.48	0.7092
165.0	-0.66	-0.92	17.41	0.0	17.41	0.00376	0.00661	10.41	255.87	0.8918
170.0	-0.66	-0.92	16.77	0.0	16.77	0.00137	0.00635	10.56	259.49	0.9044
175.0	-0.64	-0.88	16.50	0.0	16.50	0.00085	0.00625	10.69	262.62	0.9153
180.0	-0.63	-0.88	16.45	0.0	16.45	0.01195	0.00623	12.05	296.05	1.0318

FORCED CONVECTION HEAT TRANSFER FROM A UNIFORMLY HEATED CYLINDER IN A CROSSFLOW OF AIR

FREE STREAM DYN. HEAD EQUALS 1.13 CM OF WATER
FREE STREAM VELOCITY EQUALS 45.3 FT.PER SEC.(UNCORRECTED)
FREE STREAM VELOCITY EQUALS 47.1 FT.PER SEC.(CORRECTED)
THE REYNOLDS NUMBER EQUALS 97522. (UNCORRECTED)
THE REYNOLDS NUMBER EQUALS 101249. (CORRECTED)
DELTAX EQUALS 0.01625 FEET
ASURF EQUALS 0.000508 SQUARE FEET
QGEN EQUALS 0.17929 BTU PER HOUR
TU EQUALS 0.60 PER CENT

THETA (DEG)	DELTA-P (CM)	CP	DELTA-T (DEG F)	DELTA-T CORRECTION	DELTA-T CORRECTED	QCOND (BTU/HR)	QRAD (BTU/HR)	HT TRANS COEFF	NUSSELT NR	FRCESSLING NR
0.0	1.09	0.97	28.65	0.0	28.65	-0.00218	0.01130	11.40	276.53	0.8691
5.0	1.02	0.90	28.11	0.0	28.11	0.00084	0.01108	11.85	287.36	0.9031
10.0	0.97	0.85	27.79	0.0	27.79	0.00269	0.01094	12.12	294.04	0.9241
15.0	0.84	0.74	28.20	0.0	28.20	-0.00101	0.01111	11.68	283.26	0.8902
20.0	0.86	0.58	28.33	0.0	28.33	0.00050	0.01117	11.72	284.36	0.8937
25.0	0.46	0.40	28.60	0.0	28.60	0.00084	0.01129	11.63	282.05	0.8864
30.0	0.20	0.18	29.10	0.0	29.10	-0.00084	0.01150	11.30	274.14	0.8616
35.0	-0.05	-0.04	29.37	0.0	29.37	0.00017	0.01161	11.26	273.08	0.8582
40.0	-0.38	-0.34	29.68	0.0	29.68	0.00101	0.01174	11.18	271.31	0.8527
45.0	-0.61	-0.54	30.27	0.0	30.27	-0.00050	0.01195	10.85	263.29	0.8274
50.0	-0.84	-0.74	30.72	0.0	30.72	-0.00050	0.01215	10.68	259.13	0.8144
55.0	-1.04	-0.92	31.03	0.0	31.03	0.00017	0.01233	10.61	257.31	0.8086
60.0	-1.14	-1.01	31.39	0.0	31.39	0.00588	0.01249	10.83	262.81	0.8259
65.0	-1.22	-1.08	33.33	0.0	33.33	0.00991	0.01334	10.39	252.10	0.7923
70.0	-1.14	-1.01	37.92	0.0	37.92	-0.01898	0.01537	7.53	182.61	0.5739
75.0	-1.02	-0.90	37.42	0.0	37.42	0.01245	0.01516	9.29	225.42	0.7084
80.0	-0.99	-0.88	40.26	0.0	40.26	-0.00104	0.01644	7.91	191.99	0.6034
85.0	-0.97	-0.85	42.85	0.0	42.85	-0.03962	0.01760	5.61	136.18	0.4280
90.0	-0.97	-0.85	34.77	0.0	34.77	0.02436	0.01396	10.74	260.66	0.8192
95.0	-0.99	-0.86	33.24	0.0	33.24	0.02356	0.01329	11.55	280.24	0.8807
100.0	-1.04	-0.92	39.47	0.0	39.47	-0.02474	0.01605	6.91	167.65	0.5269
105.0	-1.02	-0.90	39.07	0.0	39.07	-0.02264	0.01587	7.10	172.14	0.5410
110.0	-0.97	-0.85	32.61	0.0	32.61	0.00279	0.01301	10.21	247.72	0.7785
115.0	-0.97	-0.85	26.89	0.0	26.89	0.04569	0.01056	15.70	380.96	1.1972
120.0	-0.99	-0.88	33.42	0.0	33.42	-0.03023	0.01336	8.00	194.00	0.6097
125.0	-1.02	-0.90	31.84	0.0	31.84	0.01176	0.01267	11.03	267.64	0.8411
130.0	-1.02	-0.90	33.42	0.0	33.42	-0.00941	0.01336	9.22	223.78	0.7033
135.0	-0.94	-0.83	32.47	0.0	32.47	-0.01142	0.01295	9.40	227.94	0.7163
140.0	-0.94	-0.83	28.47	0.0	28.47	0.04518	0.01122	14.75	357.91	1.1248
145.0	-0.99	-0.88	36.57	0.0	36.57	-0.02605	0.01476	7.35	178.31	0.5604
150.0	-0.97	-0.85	37.15	0.0	37.15	-0.01125	0.01502	8.11	196.76	0.6184
155.0	-0.99	-0.88	34.72	0.0	34.72	0.0	0.01396	9.38	227.49	0.7149
160.0	-0.99	-0.88	32.29	0.0	32.29	0.01092	0.01289	10.81	262.35	0.8245
165.0	-0.99	-0.88	32.79	0.0	32.79	-0.00487	0.01311	9.69	235.05	0.7387
170.0	-0.97	-0.85	31.98	0.0	31.98	-0.02100	0.01276	8.96	217.44	0.6834
175.0	-0.97	-0.85	25.54	0.0	25.54	0.02318	0.01000	14.84	360.05	1.1315
180.0	-0.99	-0.88	25.32	0.0	25.32	0.00504	0.00990	13.57	329.21	1.0346

FORCED CONVECTION HEAT TRANSFER FROM A UNIFORMLY

HEATED CYLINDER IN A CROSSFLOW OF AIR

FREE STREAM DYN. HEAD EQUALS 2.56 CM OF WATER
FREE STREAM VELOCITY EQUALS 68.1 FT.PER SEC.(UNCORRECTED)
FREE STREAM VELOCITY EQUALS 70.7 FT.PER SEC.(CORRECTED)
THE REYNOLDS NUMBER EQUALS 147675. (UNCORRECTED)
THE REYNOLDS NUMBER EQUALS 153319. (CORRECTED)
DELTAX EQUALS 0.01625 FEET
ASURF EQUALS 0.000508 SQUARE FEET
QGEN EQUALS 0.17929 BTU PER HOUR
TU EQUALS 0.55 PER CENT

THETA (DEG)	DELTA-P (CM)	CP	DELTA-T (DEG F)	DELTA-T CORRECTION	DELTA-T CORRECTED	QCOND (BTU/HR)	QRAD (BTU/HR)	HT TRANS COEFF	NUSSELT NR	FROESSLING NR
0.0	2.51	0.98	22.44	0.0	22.44	0.0	0.00878	14.96	364.62	0.9312
5.0	2.44	0.95	22.44	0.0	22.44	0.00017	0.00879	14.98	364.98	0.9321
10.0	2.26	0.88	22.49	0.0	22.49	0.00119	0.00881	15.03	366.37	0.9357
15.0	1.93	0.75	22.86	0.0	22.86	-0.00119	0.00897	14.57	355.15	0.9070
20.0	1.60	0.63	22.90	0.0	22.90	0.00034	0.00897	14.68	357.65	0.9134
25.0	1.09	0.43	23.04	0.0	23.04	0.00068	0.00904	14.61	356.10	0.9095
30.0	0.56	0.22	23.36	0.0	23.36	-0.00102	0.00917	14.26	347.43	0.8873
35.0	-0.08	-0.03	23.41	0.0	23.41	0.00017	0.00920	14.33	349.14	0.8917
40.0	-0.76	-0.30	23.50	0.0	23.50	-0.00017	0.00924	14.24	347.01	0.8862
45.0	-1.37	-0.54	23.54	0.0	23.54	0.00017	0.00926	14.24	347.00	0.8862
50.0	-1.90	-0.74	23.63	0.0	23.63	0.00085	0.00930	14.24	346.96	0.8861
55.0	-2.31	-0.90	23.95	0.0	23.95	0.00052	0.00939	14.01	341.46	0.8721
60.0	-2.62	-1.02	24.41	0.0	24.41	-0.00004	0.00949	13.69	333.73	0.8523
65.0	-2.69	-1.05	24.86	0.0	24.86	0.00017	0.00969	13.45	327.69	0.8369
70.0	-2.29	-0.89	25.36	0.0	25.36	0.00067	0.00991	13.21	321.83	0.8219
75.0	-2.08	-0.81	26.04	0.0	26.04	-0.00084	0.01023	12.72	310.11	0.7920
80.0	-2.03	-0.79	26.49	0.0	26.49	-0.00034	0.01044	12.53	305.38	0.7799
82.5	-2.06	-0.80	27.03	0.0	27.03	-0.00537	0.00534	11.50	280.36	0.7160
85.0	-2.08	-0.81	26.85	0.0	26.85	-0.00252	0.01060	12.19	297.09	0.7587
90.0	-2.06	-0.80	26.53	0.0	26.53	-0.01527	0.01050	11.40	277.74	0.7093
95.0	-2.08	-0.81	22.12	0.0	22.12	0.00705	0.00865	15.82	385.48	0.9845
100.0	-2.11	-0.82	19.61	0.0	19.61	0.00854	0.00762	18.10	441.11	1.1265
105.0	-2.11	-0.82	19.38	0.0	19.38	0.00222	0.00753	17.68	430.89	1.1004
110.0	-2.11	-0.82	19.75	0.0	19.75	0.01110	0.00767	18.22	444.15	1.1343
115.0	-2.11	-0.82	23.08	0.0	23.08	-0.00280	0.00905	14.28	348.12	0.8891
120.0	-2.11	-0.82	25.68	0.0	25.68	-0.00681	0.01015	12.45	303.46	0.7750
125.0	-2.16	-0.84	26.44	0.0	26.44	-0.00705	0.01048	12.05	293.62	0.7499
130.0	-2.01	-0.78	25.32	0.0	25.32	0.01797	0.01000	14.57	355.03	0.9067
135.0	-2.08	-0.81	29.01	0.0	29.01	-0.00420	0.01158	11.10	270.56	0.6910
140.0	-2.11	-0.82	31.57	0.0	31.57	-0.01226	0.01270	9.63	234.62	0.5992
145.0	-2.08	-0.81	30.85	0.0	30.85	-0.00151	0.01233	10.56	257.38	0.6573
150.0	-2.08	-0.81	29.73	0.0	29.73	0.0	0.01173	11.10	270.54	0.6909
155.0	-2.08	-0.81	28.60	0.0	28.60	0.00202	0.01127	11.71	285.34	0.7287
160.0	-2.08	-0.81	28.02	0.0	28.02	0.00302	0.01103	12.04	293.43	0.7494
165.0	-2.08	-0.81	28.24	0.0	28.24	-0.00537	0.01117	11.35	276.59	0.7064
170.0	-2.06	-0.80	27.03	0.0	27.03	0.00487	0.01066	12.64	308.12	0.7869
175.0	-2.06	-0.80	27.12	0.0	27.12	-0.00067	0.01072	12.19	297.20	0.7590
180.0	-2.03	-0.79	27.03	0.0	27.03	-0.00470	0.01071	11.94	291.04	0.7433

FORCED CONVECTION HEAT TRANSFER FROM A UNIFORMLY

HEATED CYLINDER IN A CROSSFLOW OF AIR

FREE STREAM DYN. HEAD EQUALS 3.23 CM OF WATER
FREE STREAM VELOCITY EQUALS 76.4 FT.PER SEC.(UNCORRECTED)
FREE STREAM VELOCITY EQUALS 79.3 FT.PER SEC.(CORRECTED)
THE REYNOLDS NUMBER EQUALS 166381. (UNCORRECTED)
THE REYNOLDS NUMBER EQUALS 172739. (CORRECTED)
DELTAX EQUALS 0.01625 FEET
ASURF EQUALS 0.000508 SQUARE FEET
QGEN EQUALS 0.17929 BTU PER HOUR
TU EQUALS 0.54 PER CENT

THETA (DEG)	DELTA-P (CM)	CP	DELTA-T (DEG F)	DELTA-T CORRECTION	DELTA-T CORRECTED	QCOND (BTU/HR)	QRAD (BTU/HR)	HT TRANS COEFF	NUSSELT NR	FROESSLING NR
0.0	3.28	1.01	21.21	0.0	21.21	0.00085	0.00818	15.97	389.91	0.9381
5.0	3.23	1.00	21.25	0.0	21.25	0.00034	0.00822	15.88	387.82	0.9331
10.0	2.92	0.90	21.39	0.0	21.39	-0.00068	0.00830	15.68	382.86	0.9212
15.0	2.54	0.79	21.35	0.0	21.35	0.00137	0.00829	15.90	388.31	0.9343
20.0	2.11	0.65	21.67	0.0	21.67	0.01074	0.00843	16.51	403.06	0.9698
25.0	1.45	0.45	24.86	0.0	24.86	-0.02301	0.00978	11.60	283.33	0.6817
30.0	0.69	0.21	21.90	0.0	21.90	0.01313	0.00854	16.54	403.86	0.9717
35.0	-0.13	-0.04	22.44	0.0	22.44	-0.00085	0.00874	14.89	363.61	0.8749
40.0	-0.99	-0.31	22.76	0.0	22.76	0.00034	0.00887	14.77	360.74	0.8679
45.0	-1.75	-0.54	23.18	0.0	23.18	-0.00051	0.00908	14.42	352.12	0.8472
50.0	-2.44	-0.75	23.45	0.0	23.45	0.00034	0.00915	14.32	349.59	0.8411
55.0	-3.02	-0.94	23.82	0.0	23.82	0.00036	0.00931	14.09	343.95	0.8276
60.0	-3.48	-1.08	24.28	0.0	24.28	-0.00005	0.00954	13.76	336.13	0.8087
65.0	-3.53	-1.09	24.73	0.0	24.73	0.00017	0.00973	13.52	330.06	0.7941
70.0	-3.05	-0.94	25.23	0.0	25.23	0.00084	0.00994	13.29	324.46	0.7807
75.0	-2.74	-0.85	25.95	0.0	25.95	-0.00101	0.01024	12.75	311.47	0.7494
80.0	-2.69	-0.83	26.40	0.0	26.40	0.00437	0.01025	12.94	315.93	0.7601
85.0	-2.62	-0.81	28.02	0.0	28.02	0.00134	0.01099	11.93	291.21	0.7007
90.0	-2.69	-0.83	30.00	0.0	30.00	-0.00571	0.01186	10.62	259.26	0.6238
92.5	-2.74	-0.85	30.54	0.0	30.54	-0.00470	0.00606	10.17	248.44	0.5978
95.0	-2.74	-0.85	30.45	0.0	30.45	-0.02795	0.01209	9.01	219.94	0.5292
100.0	-2.74	-0.85	23.41	0.0	23.41	0.02252	0.00913	16.21	395.89	0.9525
105.0	-2.72	-0.84	22.40	0.0	22.40	-0.01349	0.00873	13.81	337.25	0.8114
110.0	-2.74	-0.85	17.78	0.0	17.78	0.02270	0.00685	21.62	527.90	1.2701
115.0	-2.74	-0.85	19.24	0.0	19.24	-0.00085	0.00745	17.50	427.34	1.0282
120.0	-2.77	-0.86	20.48	0.0	20.48	0.00478	0.00796	16.94	413.60	0.9952
125.0	-2.87	-0.89	22.99	0.0	22.99	0.00179	0.00896	14.74	359.98	0.8661
130.0	-2.67	-0.83	25.99	0.0	25.99	-0.00413	0.01022	12.50	305.20	0.7343
135.0	-2.72	-0.84	27.88	0.0	27.88	-0.01646	0.01107	10.72	261.77	0.6298
140.0	-2.74	-0.85	25.36	0.0	25.36	0.00588	0.01000	13.60	332.18	0.7992
145.0	-2.74	-0.85	24.41	0.0	24.41	0.00739	0.00960	14.28	348.81	0.8392
150.0	-2.79	-0.87	25.45	0.0	25.45	-0.00924	0.01003	12.38	302.37	0.7275
155.0	-2.79	-0.87	24.01	0.0	24.01	0.00329	0.00943	14.20	346.82	0.8345
160.0	-2.74	-0.85	23.45	0.0	23.45	0.00140	0.00919	14.40	351.69	0.8462
165.0	-2.74	-0.85	23.27	0.0	23.27	-0.00051	0.00912	14.36	350.66	0.8437
170.0	-2.74	-0.85	22.95	0.0	22.95	0.00324	0.00883	14.91	364.03	0.8759
175.0	-2.74	-0.85	23.50	0.0	23.50	-0.00137	0.00910	14.15	345.54	0.8314
180.0	-2.74	-0.85	23.68	0.0	23.68	-0.00256	0.00920	13.93	340.23	0.8186

FORCED CONVECTION HEAT TRANSFER FROM A UNIFORMLY HEATED CYLINDER IN A CROSSFLOW OF AIR

FREE STREAM DYN. HEAD EQUALS 5.58 CM OF WATER
FREE STREAM VELOCITY EQUALS 101.0 FT.PER SEC.(UNCORRECTED)
FREE STREAM VELOCITY EQUALS 104.6 FT.PER SEC.(CORRECTED)
THE REYNOLDS NUMBER EQUALS 215044. (UNCORRECTED)
THE REYNOLDS NUMBER EQUALS 222724. (CORRECTED)
DELTAX EQUALS 0.01625 FEET
ASURF EQUALS 0.000508 SQUARE FEET
QGEN EQUALS 0.20623 BTU PER HOUR
TU EQUALS 0.49 PER CENT

THETA (DEG)	DELTA-P (CM)	CP	DELTA-T (DEG F)	DELTA-T CORRECTION	DELTA-T CORRECTED	QCOND (BTU/HR)	QRAD (BTU/HR)	HT TRANS COEFF	NUSSELT NR	FROESSLING NR
0.0	0.0	0.0	21.44	0.0	21.44	0.0	0.00866	18.15	438.15	0.9284
5.0	0.0	0.0	21.44	0.0	21.44	-0.00017	0.00865	18.14	437.79	0.9276
10.0	0.0	0.0	21.39	0.0	21.39	0.00068	0.00862	18.26	440.70	0.9338
15.0	0.0	0.0	21.53	0.0	21.53	-0.00085	0.00867	18.00	434.38	0.9204
20.0	0.0	0.0	21.44	0.0	21.44	0.00051	0.00863	18.20	439.36	0.9310
25.0	0.0	0.0	21.48	0.0	21.48	-0.00017	0.00863	18.10	436.91	0.9258
30.0	0.0	0.0	21.48	0.0	21.48	0.00068	0.00863	18.18	438.79	0.9298
35.0	0.0	0.0	21.67	0.0	21.67	0.00051	0.00876	18.00	434.43	0.9205
40.0	0.0	0.0	21.99	0.0	21.99	0.00017	0.00889	17.70	427.07	0.9049
45.0	0.0	0.0	22.35	0.0	22.35	0.00222	0.00910	17.57	424.00	0.8984
50.0	0.0	0.0	23.31	0.0	23.31	-0.00099	0.00947	16.54	399.24	0.8460
55.0	0.0	0.0	24.01	0.0	24.01	-0.00125	0.00977	16.02	386.55	0.8191
60.0	0.0	0.0	24.37	0.0	24.37	-0.00000	0.00996	15.87	382.90	0.8113
65.0	0.0	0.0	24.73	0.0	24.73	0.00050	0.01011	15.66	378.01	0.8010
70.0	0.0	0.0	25.23	0.0	25.23	0.00084	0.01032	15.36	370.82	0.7857
75.0	0.0	0.0	25.95	0.0	25.95	-0.00050	0.01063	14.81	357.50	0.7575
80.0	0.0	0.0	26.53	0.0	26.53	0.00286	0.01088	14.72	355.18	0.7526
85.0	0.0	0.0	27.88	0.0	27.88	0.0	0.01148	13.76	332.09	0.7037
90.0	0.0	0.0	29.23	0.0	29.23	0.00118	0.01207	13.16	317.70	0.6732
95.0	0.0	0.0	30.90	0.0	30.90	-0.00521	0.01280	12.00	289.63	0.6137
97.5	0.0	0.0	31.17	0.0	31.17	-0.00202	0.00645	11.97	288.77	0.6119
100.0	0.0	0.0	31.17	0.0	31.17	-0.02385	0.01290	10.71	258.54	0.5478
105.0	0.0	0.0	25.05	0.0	25.05	-0.00786	0.01019	14.80	357.24	0.7570
110.0	0.0	0.0	16.82	0.0	16.82	0.03121	0.00668	27.03	652.35	1.3823
112.5	0.0	0.0	16.82	0.0	16.82	0.00102	0.00334	23.61	569.92	1.2076
115.0	0.0	0.0	16.95	0.0	16.95	0.00597	0.00672	23.87	576.19	1.2209
120.0	0.0	0.0	18.69	0.0	18.69	0.00205	0.00745	21.16	510.77	1.0823
125.0	0.0	0.0	20.98	0.0	20.98	0.00017	0.00846	18.58	448.54	0.9504
130.0	0.0	0.0	23.31	0.0	23.31	-0.00717	0.00947	16.02	386.64	0.8193
135.0	0.0	0.0	23.73	0.0	23.73	0.00893	0.00969	17.06	411.73	0.8724
140.0	0.0	0.0	26.53	0.0	26.53	-0.01802	0.01092	13.16	317.70	0.6732
145.0	0.0	0.0	24.50	0.0	24.50	0.00380	0.00998	16.08	388.11	0.8224
150.0	0.0	0.0	23.50	0.0	23.50	0.00240	0.00958	16.69	402.74	0.8534
155.0	0.0	0.0	23.13	0.0	23.13	-0.00051	0.00941	16.72	403.48	0.8550
160.0	0.0	0.0	22.63	0.0	22.63	-0.00290	0.00919	16.90	407.90	0.8643
165.0	0.0	0.0	21.35	0.0	21.35	0.00273	0.00863	18.49	446.17	0.9454
170.0	0.0	0.0	20.80	0.0	20.80	0.00188	0.00840	18.92	456.54	0.9674
175.0	0.0	0.0	20.75	0.0	20.75	-0.00205	0.00838	18.59	448.60	0.9505
180.0	0.0	0.0	20.16	0.0	20.16	0.00102	0.00811	19.46	469.70	0.9953

FORCED CONVECTION HEAT TRANSFER FROM A UNIFORMLY

HEATED CYLINDER IN A CROSSFLOW OF AIR

FREE STREAM DYN. HEAD EQUALS 5.58 CM OF WATER
FREE STREAM VELOCITY EQUALS 101.0 FT.PER SEC.(UNCORRECTED)
FREE STREAM VELOCITY EQUALS 104.6 FT.PER SEC.(CORRECTED)
THE REYNOLDS NUMBER EQUALS 215185. (UNCORRECTED)
THE REYNOLDS NUMBER EQUALS 222870. (CORRECTED)
DELTAX EQUALS 0.01625 FEET
ASURF EQUALS 0.000508 SQUARE FEET
QGEN EQUALS 0.20628 BTU PER HOUR
TU EQUALS 0.49 PER CENT

THETA (DEG)	DELTA-P (CM)	CP	DELTA-T (DEG F)	DELTA-T CORRECTION	DELTA-T CORRECTED	QCOND (BTU/HR)	QRAD (BTU/HR)	HT TRANS COEFF	NUSSELT NR	FROESSLING NR
0.0	5.38	0.97	21.58	0.0	21.58	-0.00102	0.00869	17.94	433.32	0.9179
5.0	5.31	0.95	21.44	0.0	21.44	0.00051	0.00866	18.20	439.57	0.9311
10.0	4.95	0.89	21.44	0.0	21.44	0.0	0.00866	18.15	438.44	0.9287
15.0	4.29	0.77	21.44	0.0	21.44	0.0	0.00866	18.15	438.44	0.9287
20.0	3.56	0.64	21.44	0.0	21.44	0.00222	0.00866	18.36	443.36	0.9391
25.0	2.41	0.43	22.03	0.0	22.03	-0.00119	0.00891	17.53	423.47	0.8970
30.0	1.22	0.22	22.31	0.0	22.31	-0.00102	0.00903	17.32	418.37	0.8862
35.0	-0.15	-0.03	22.31	0.0	22.31	-0.00051	0.00903	17.37	419.46	0.8885
40.0	-1.57	-0.28	22.17	0.0	22.17	0.00051	0.00897	17.57	424.38	0.8989
45.0	-2.90	-0.52	22.17	0.0	22.17	0.00085	0.00897	17.60	425.12	0.9005
50.0	-4.14	-0.74	22.40	0.0	22.40	0.00017	0.00907	17.35	419.12	0.8878
55.0	-5.18	-0.93	22.67	0.0	22.67	0.00341	0.00919	17.42	420.60	0.8909
60.0	-5.97	-1.07	23.86	0.0	23.86	-0.00410	0.00970	15.89	383.64	0.8126
65.0	-6.15	-1.10	23.95	0.0	23.95	0.00138	0.00974	16.27	392.96	0.8324
70.0	-5.33	-0.96	24.41	0.0	24.41	-0.00121	0.00994	15.74	380.11	0.8052
75.0	-4.75	-0.85	24.55	0.0	24.55	0.00067	0.01000	15.80	381.56	0.8082
80.0	-4.67	-0.84	24.86	0.0	24.86	-0.00017	0.01014	15.52	374.86	0.7940
82.5	-4.67	-0.84	25.05	0.0	25.05	-0.00067	0.00511	15.31	369.78	0.7833
85.0	-4.65	-0.83	25.14	0.0	25.14	-0.00797	0.01026	14.73	355.83	0.7537
87.5	-4.67	-0.84	24.23	0.0	24.23	-0.00050	0.00493	15.88	383.53	0.8124
90.0	-4.75	-0.85	23.27	0.0	23.27	-0.00345	0.00941	16.37	395.36	0.8375
95.0	-4.75	-0.85	20.48	0.0	20.48	0.00205	0.00825	19.24	464.72	0.9844
100.0	-4.72	-0.85	18.24	0.0	18.24	0.00273	0.00730	21.78	526.10	1.1144
105.0	-4.65	-0.83	16.73	0.0	16.73	0.00751	0.00667	24.39	588.99	1.2476
107.5	-4.62	-0.83	16.73	0.0	16.73	0.00376	0.00333	24.39	588.99	1.2476
110.0	-4.60	-0.82	17.23	0.0	17.23	0.01571	0.00688	24.59	593.82	1.2579
115.0	-4.57	-0.82	21.94	0.0	21.94	-0.00785	0.00887	17.01	410.90	0.8704
120.0	-4.67	-0.84	24.55	0.0	24.55	-0.00436	0.01000	15.40	371.81	0.7876
125.0	-4.70	-0.84	25.99	0.0	25.99	-0.00353	0.01063	14.56	351.58	0.7447
130.0	-4.75	-0.85	26.49	0.0	26.49	-0.00353	0.01085	14.27	344.61	0.7300
135.0	-4.75	-0.85	26.04	0.0	26.04	-0.00168	0.01065	14.67	354.31	0.7505
140.0	-4.80	-0.86	25.14	0.0	25.14	-0.00190	0.01026	15.21	367.33	0.7781
145.0	-4.90	-0.88	23.73	0.0	23.73	0.00594	0.00964	16.82	406.10	0.8602
150.0	-4.90	-0.88	23.91	0.0	23.91	-0.00051	0.00972	16.15	389.99	0.8261
155.0	-4.83	-0.86	23.95	0.0	23.95	-0.00154	0.00974	16.03	387.18	0.8201
160.0	-4.83	-0.86	23.59	0.0	23.59	0.00188	0.00958	16.58	400.39	0.8481
165.0	-4.80	-0.86	23.73	0.0	23.73	-0.00222	0.00964	16.14	389.74	0.8256
170.0	-4.83	-0.86	23.27	0.0	23.27	0.00222	0.00945	16.85	406.88	0.8619
175.0	-4.83	-0.86	23.41	0.0	23.41	-0.00051	0.00950	16.51	398.82	0.8448
180.0	-4.80	-0.86	23.41	0.0	23.41	0.0	0.00947	16.56	399.93	0.8471

FORCED CONVECTION HEAT TRANSFER FROM A UNIFORMLY

HEATED CYLINDER IN A CROSSFLOW OF AIR

FREE STREAM DYN. HEAD EQUALS 7.71 CM OF WATER
FREE STREAM VELOCITY EQUALS 119.1 FT.PER SEC.(UNCORRECTED)
FREE STREAM VELOCITY EQUALS 123.2 FT.PER SEC.(CORRECTED)
THE REYNOLDS NUMBER EQUALS 250655. (UNCORRECTED)
THE REYNOLDS NUMBER EQUALS 259294. (CORRECTED)
DELTAX EQUALS 0.01625 FEET
ASURF EQUALS 0.000508 SQUARE FEET
QGEN EQUALS 0.20628 BTU PER HOUR
TU EQUALS 0.47 PER CENT

THETA (DEG)	DELTA-P (CM)	CP	DELTA-T (DEG F)	DELTA-T CORRECTION	DELTA-T CORRECTED	QCOND (BTU/HR)	QRAD (BTU/HR)	HT TRANS COEFF	NUSSELT NR	FROESSLING NR
0.0	0.0	0.0	19.97	0.0	19.97	0.00034	0.00824	19.56	469.34	0.9217
5.0	0.0	0.0	19.97	0.0	19.97	0.0	0.00823	19.53	468.55	0.9201
10.0	0.0	0.0	19.97	0.0	19.97	0.00034	0.00821	19.56	469.40	0.9218
15.0	0.0	0.0	20.07	0.0	20.07	-0.00068	0.00825	19.37	464.77	0.9127
20.0	0.0	0.0	19.97	0.0	19.97	-0.00017	0.00818	19.52	468.27	0.9196
25.0	0.0	0.0	19.84	0.0	19.84	0.00051	0.00806	19.73	473.42	0.9297
30.0	0.0	0.0	19.84	0.0	19.84	0.00154	0.00803	19.84	475.94	0.9347
35.0	0.0	0.0	20.25	0.0	20.25	-0.00068	0.00836	19.18	460.30	0.9040
40.0	0.0	0.0	20.48	0.0	20.48	0.00068	0.00846	19.09	458.08	0.8996
45.0	0.0	0.0	20.89	0.0	20.89	0.00068	0.00872	18.69	448.47	0.8807
50.0	0.0	0.0	21.48	0.0	21.48	-0.00034	0.00890	18.06	433.40	0.8511
55.0	0.0	0.0	21.99	0.0	21.99	0.00034	0.00912	17.69	424.47	0.8336
60.0	0.0	0.0	22.58	0.0	22.58	-0.00137	0.00946	17.05	409.01	0.8032
65.0	0.0	0.0	22.81	0.0	22.81	0.00119	0.00955	17.09	410.02	0.8052
70.0	0.0	0.0	23.36	0.0	23.36	0.00017	0.00979	16.58	397.83	0.7813
75.0	0.0	0.0	23.95	0.0	23.95	0.00118	0.01004	16.23	389.45	0.7648
80.0	0.0	0.0	24.86	0.0	24.86	0.00114	0.01042	15.60	374.38	0.7352
85.0	0.0	0.0	26.08	0.0	26.08	0.00151	0.01096	14.86	356.63	0.7004
90.0	0.0	0.0	27.70	0.0	27.70	-0.00336	0.01167	13.60	326.25	0.6407
92.5	0.0	0.0	28.47	0.0	28.47	-0.00605	0.00602	12.60	302.39	0.5938
95.0	0.0	0.0	28.42	0.0	28.42	-0.00873	0.01199	12.86	308.52	0.6059
100.0	0.0	0.0	26.80	0.0	26.80	-0.02216	0.01123	12.70	304.85	0.5987
105.0	0.0	0.0	19.24	0.0	19.24	0.01438	0.00789	21.78	522.51	1.0261
110.0	0.0	0.0	15.54	0.0	15.54	0.01297	0.00628	27.00	647.78	1.2721
112.5	0.0	0.0	15.44	0.0	15.44	-0.00034	0.00313	25.42	609.92	1.1978
115.0	0.0	0.0	15.31	0.0	15.31	0.00802	0.00614	26.78	642.61	1.2620
120.0	0.0	0.0	17.23	0.0	17.23	0.00051	0.00692	22.85	548.21	1.0766
125.0	0.0	0.0	19.29	0.0	19.29	-0.00205	0.00794	20.04	480.91	0.9444
130.0	0.0	0.0	20.80	0.0	20.80	-0.00188	0.00860	18.54	444.89	0.8737
135.0	0.0	0.0	21.80	0.0	21.80	-0.00341	0.00912	17.50	419.89	0.8246
140.0	0.0	0.0	21.90	0.0	21.90	0.00137	0.00917	17.85	428.36	0.8412
145.0	0.0	0.0	22.35	0.0	22.35	-0.00171	0.00928	17.21	412.85	0.8108
150.0	0.0	0.0	22.35	0.0	22.35	-0.00256	0.00936	17.12	410.89	0.8069
155.0	0.0	0.0	21.67	0.0	21.67	0.00410	0.00904	18.30	439.10	0.8623
160.0	0.0	0.0	22.08	0.0	22.08	-0.00717	0.00922	16.94	406.42	0.7981
165.0	0.0	0.0	20.57	0.0	20.57	0.00119	0.00854	19.05	457.04	0.8975
170.0	0.0	0.0	19.38	0.0	19.38	-0.00068	0.00800	20.08	481.82	0.9462
175.0	0.0	0.0	18.01	0.0	18.01	0.00341	0.00740	22.12	530.88	1.0425
180.0	0.0	0.0	17.55	0.0	17.55	0.00341	0.00719	22.73	545.29	1.0709

FORCED CONVECTION HEAT TRANSFER FROM A UNIFORMLY

HEATED CYLINDER IN A CROSSFLOW OF AIR

FREE STREAM DYN. HEAD EQUALS 7.71 CM OF WATER
FREE STREAM VELOCITY EQUALS 118.9 FT.PER SEC.(UNCORRECTED)
FREE STREAM VELOCITY EQUALS 123.0 FT.PER SEC.(CORRECTED)
THE REYNOLDS NUMBER EQUALS 251928. (UNCORRECTED)
THE REYNOLDS NUMBER EQUALS 260611. (CORRECTED)
DELTAX EQUALS 0.01625 FEET
ASURF EQUALS 0.000508 SQUARE FEET
QGEN EQUALS 0.20628 BTU PER HOUR
TU EQUALS 0.47 PER CENT

THETA (DEG)	DELTA-P (CM)	CP	DELTA-T (DEG F)	DELTA-T CORRECTION	DELTA-T CORRECTED	QCOND (BTU/HR)	QRAD (BTU/HR)	HT TRANS COEFF	NUSSELT NR	FROESSLING NR
0.0	7.52	0.98	19.97	0.0	19.97	0.00017	0.00814	19.55	470.69	0.9220
5.0	7.34	0.95	19.97	0.0	19.97	0.0	0.00815	19.54	470.26	0.9212
10.0	6.83	0.89	19.97	0.0	19.97	0.00154	0.00815	19.69	473.90	0.9283
15.0	5.97	0.77	20.39	0.0	20.39	-0.00154	0.00833	18.98	456.77	0.8948
20.0	4.67	0.61	20.39	0.0	20.39	0.00051	0.00833	19.17	461.54	0.9041
25.0	3.00	0.39	20.52	0.0	20.52	0.00085	0.00839	19.07	459.10	0.8993
30.0	1.73	0.22	20.89	0.0	20.89	-0.00188	0.00855	18.47	444.50	0.8707
35.0	-0.13	-0.02	20.75	0.0	20.75	0.00034	0.00849	18.80	452.64	0.8867
40.0	-2.13	-0.28	20.71	0.0	20.71	0.0	0.00847	18.81	452.91	0.8872
45.0	-3.99	-0.52	20.66	0.0	20.66	0.00051	0.00845	18.91	455.13	0.8915
50.0	-5.74	-0.74	20.75	0.0	20.75	0.00017	0.00849	18.79	452.25	0.8859
55.0	-7.19	-0.93	20.89	0.0	20.89	0.00290	0.00855	18.92	455.35	0.8920
60.0	-8.25	-1.07	21.80	0.0	21.80	-0.00222	0.00890	17.63	424.33	0.8312
65.0	-8.64	-1.12	22.12	0.0	22.12	-0.00119	0.00908	17.45	419.99	0.8227
70.0	-7.24	-0.94	22.12	0.0	22.12	0.00051	0.00908	17.60	423.65	0.8299
75.0	-6.58	-0.85	22.26	0.0	22.26	0.00068	0.00914	17.50	421.28	0.8252
80.0	-6.45	-0.84	22.58	0.0	22.58	-0.00290	0.00928	16.93	407.48	0.7982
82.5	-6.48	-0.84	22.58	0.0	22.58	-0.00341	0.00464	16.59	399.24	0.7821
85.0	-6.48	-0.84	22.12	0.0	22.12	-0.00410	0.00908	17.19	413.78	0.8105
90.0	-6.55	-0.85	20.57	0.0	20.57	-0.00580	0.00839	18.39	442.72	0.8672
95.0	-6.38	-0.83	17.46	0.0	17.46	0.00597	0.00708	23.15	557.19	1.0915
100.0	-6.22	-0.81	15.95	0.0	15.95	0.00051	0.00644	24.74	595.60	1.1667
105.0	-6.17	-0.80	14.58	0.0	14.58	0.01383	0.00586	28.95	696.87	1.3651
110.0	-6.15	-0.80	16.91	0.0	16.91	0.00529	0.00684	23.85	574.02	1.1244
115.0	-6.15	-0.80	20.66	0.0	20.66	-0.00956	0.00845	17.95	432.02	0.8463
120.0	-6.22	-0.81	21.85	0.0	21.85	0.00648	0.00896	18.37	442.17	0.8662
125.0	-6.38	-0.83	24.77	0.0	24.77	-0.01142	0.01024	14.68	353.27	0.6920
130.0	-6.48	-0.84	24.64	0.0	24.64	-0.00513	0.01019	15.26	367.43	0.7197
135.0	-6.50	-0.84	23.13	0.0	23.13	0.00017	0.00952	16.77	403.61	0.7906
140.0	-6.50	-0.84	21.67	0.0	21.67	0.00137	0.00888	18.07	434.90	0.8519
145.0	-6.68	-0.87	20.57	0.0	20.57	0.01417	0.00841	20.30	488.72	0.9573
150.0	-6.68	-0.87	23.27	0.0	23.27	-0.01588	0.00954	15.31	368.51	0.7219
155.0	-6.65	-0.86	21.71	0.0	21.71	0.00410	0.00890	18.27	439.91	0.8617
160.0	-6.65	-0.86	21.25	0.0	21.25	0.00239	0.00870	18.53	446.01	0.8737
165.0	-6.53	-0.85	21.44	0.0	21.44	-0.00137	0.00878	18.02	433.72	0.8496
170.0	-6.50	-0.84	21.25	0.0	21.25	-0.00034	0.00870	18.27	439.92	0.8617
175.0	-6.50	-0.84	20.98	0.0	20.98	0.00137	0.00859	18.69	449.80	0.8811
180.0	-6.50	-0.84	21.07	0.0	21.07	-0.00051	0.00861	18.43	443.58	0.8689

FORCED CONVECTION HEAT TRANSFER FROM A UNIFORMLY

HEATED CYLINDER IN A CROSSFLOW OF AIR

FREE STREAM DYN. HEAD EQUALS 11.14 CM OF WATER
FREE STREAM VELOCITY EQUALS 143.7 FT.PER SEC.(UNCORRECTED)
FREE STREAM VELOCITY EQUALS 148.3 FT.PER SEC.(CORRECTED)
THE REYNOLDS NUMBER EQUALS 298958. (UNCORRECTED)
THE REYNOLDS NUMBER EQUALS 308514. (CORRECTED)
DELTAX EQUALS 0.01625 FEET
ASURF EQUALS 0.000508 SQUARE FEET
QGEN EQUALS 0.20629 BTU PER HOUR
TU EQUALS 0.45 PER CENT

THETA (DEG)	DELTA-P (CM)	CP	DELTA-T (DEG F)	DELTA-T CORRECTION	DELTA-T CORRECTED	QCOND (BTU/HR)	QRAD (BTU/HR)	HT TRANS COEFF	NUSSELT NR	FROESSLING NR
0.0	11.25	1.01	18.60	-0.12	18.72	-0.00034	0.00788	20.84	497.16	0.8951
5.0	11.02	0.99	18.56	-0.16	18.72	0.00068	0.00786	20.95	499.76	0.8998
10.0	10.08	0.91	18.69	-0.23	18.93	-0.00085	0.00792	20.55	490.33	0.8828
15.0	8.69	0.78	18.60	-0.33	18.93	0.00137	0.00788	20.79	495.90	0.8928
20.0	6.60	0.59	18.88	-0.37	19.25	-0.00085	0.00800	20.20	481.93	0.8677
25.0	4.67	0.42	18.92	-0.43	19.35	0.00085	0.00801	20.26	483.39	0.8703
30.0	2.34	0.21	19.20	-0.51	19.71	-0.00154	0.00813	19.65	468.73	0.8439
35.0	-0.03	-0.00	19.06	-0.57	19.63	0.00017	0.00806	19.90	474.82	0.8548
40.0	-3.43	-0.31	18.97	-0.61	19.58	0.00017	0.00802	19.96	476.12	0.8572
45.0	-6.22	-0.56	18.92	-0.65	19.57	0.00051	0.00800	20.00	477.19	0.8591
50.0	-8.74	-0.78	19.01	-0.69	19.70	0.00000	0.00804	19.82	472.76	0.8511
55.0	-11.30	-1.01	19.10	-0.72	19.83	0.00154	0.00808	19.84	473.34	0.8522
60.0	-13.72	-1.23	19.61	-0.74	20.35	-0.00068	0.00823	19.10	455.63	0.8203
65.0	-14.86	-1.33	19.93	-0.76	20.69	-0.00068	0.00838	18.77	447.83	0.8063
70.0	-13.08	-1.17	20.07	-0.78	20.84	-0.00000	0.00848	18.69	445.89	0.8028
75.0	-10.06	-0.90	20.20	-0.78	20.98	0.00051	0.00857	18.60	443.83	0.7991
80.0	-10.03	-0.90	20.48	-0.79	21.27	-0.00256	0.00870	18.06	430.82	0.7756
82.5	-9.91	-0.89	20.29	-0.79	21.08	-0.00034	0.00431	18.40	438.92	0.7902
85.0	-10.16	-0.91	20.07	-0.79	20.86	-0.00444	0.00852	18.26	435.51	0.7841
90.0	-9.88	-0.89	18.46	-0.79	19.25	-0.00529	0.00782	19.76	471.36	0.8486
95.0	-9.30	-0.83	15.44	-0.79	16.24	0.00615	0.00649	24.98	595.98	1.0730
100.0	-8.94	-0.80	14.07	-0.79	14.86	0.00444	0.00589	27.14	647.51	1.1658
102.5	-8.89	-0.80	13.69	-0.79	14.68	0.00137	0.00290	27.26	650.38	1.1709
105.0	-8.79	-0.79	13.89	-0.80	14.69	0.00529	0.00581	27.58	657.95	1.1846
110.0	-8.76	-0.79	15.12	-0.82	15.94	0.00768	0.00634	25.65	611.87	1.1016
115.0	-8.81	-0.79	18.42	-0.84	19.26	-0.00580	0.00779	19.71	470.17	0.8465
120.0	-8.86	-0.80	20.16	-0.85	21.01	0.00068	0.00856	18.60	443.72	0.7989
125.0	-8.97	-0.80	22.08	-0.87	22.94	-0.01075	0.00942	15.98	381.11	0.6861
130.0	-9.17	-0.82	21.12	-0.88	22.00	-0.00085	0.00898	17.58	419.50	0.7553
135.0	-9.68	-0.87	19.93	-0.90	20.83	-0.00154	0.00845	18.56	442.75	0.7971
140.0	-9.30	-0.83	18.33	-0.92	19.25	0.00205	0.00774	20.52	489.65	0.8815
145.0	-9.42	-0.85	17.27	-0.94	18.22	0.00973	0.00727	22.56	538.31	0.9692
150.0	-9.52	-0.86	18.83	-0.98	19.81	-0.00871	0.00789	18.86	449.95	0.8101
155.0	-9.52	-0.86	18.05	-0.99	19.04	0.00085	0.00755	20.64	492.41	0.8865
160.0	-9.47	-0.85	17.50	-1.00	18.51	0.00358	0.00735	21.55	514.11	0.9256
165.0	-9.32	-0.84	17.92	-1.01	18.93	-0.00119	0.00755	20.55	490.31	0.8827
170.0	-9.32	-0.84	18.01	-1.02	19.03	0.00017	0.00760	20.58	490.95	0.8839
175.0	-9.17	-0.82	18.14	-1.02	19.17	0.00051	0.00766	20.46	488.12	0.8788
180.0	-9.09	-0.82	18.42	-1.02	19.44	-0.00051	0.00780	20.05	478.43	0.8614

FORCED CONVECTION HEAT TRANSFER FROM A UNIFORMLY

HEATED CYLINDER IN A CROSSFLOW OF AIR

FREE STREAM DYN. HEAD EQUALS 15.40 CM OF WATER
FREE STREAM VELOCITY EQUALS 171.1 FT.PER SEC.(UNCORRECTED)
FREE STREAM VELOCITY EQUALS 176.2 FT.PER SEC.(CORRECTED)
THE REYNOLDS NUMBER EQUALS 340095. (UNCORRECTED)
THE REYNOLDS NUMBER EQUALS 350116. (CORRECTED)
DELTAX EQUALS 0.01625 FEET
ASURF EQUALS 0.000508 SQUARE FEET
QGEN EQUALS 0.20628 BTU PER HOUR
TU EQUALS 0.43 PER CENT

THETA (DEG)	DELTA-P (CM)	CP	DELTA-T (DEG F)	DELTA-T CORRECTION	DELTA-T CORRECTED	QCOND (BTU/HR)	QRAD (BTU/HR)	HT TRANS COEFF	NUSSELT NR	FROESSLING NR
0.0	0.0	0.0	18.14	0.0	18.14	-0.00051	0.00825	21.44	499.95	0.8449
5.0	0.0	0.0	18.01	0.0	18.01	0.00102	0.00810	21.79	508.04	0.8586
10.0	0.0	0.0	18.14	0.0	18.14	-0.00051	0.00830	21.43	499.80	0.8447
15.0	0.0	0.0	18.14	0.0	18.14	0.0	0.00819	21.50	501.38	0.8473
20.0	0.0	0.0	18.14	0.0	18.14	0.00034	0.00820	21.54	502.22	0.8488
25.0	0.0	0.0	18.24	0.0	18.24	0.00034	0.00826	21.42	499.55	0.8443
30.0	0.0	0.0	18.42	0.0	18.42	0.00017	0.00834	21.18	493.96	0.8348
35.0	0.0	0.0	18.65	0.0	18.65	0.00034	0.00849	20.93	487.96	0.8247
40.0	0.0	0.0	18.97	0.0	18.97	-0.00341	0.00864	20.17	470.26	0.7948
45.0	0.0	0.0	18.37	0.0	18.37	0.00700	0.00835	21.97	512.24	0.8657
50.0	0.0	0.0	19.65	0.0	19.65	-0.00358	0.00897	19.41	452.67	0.7650
55.0	0.0	0.0	19.97	0.0	19.97	-0.00017	0.00912	19.42	452.91	0.7654
60.0	0.0	0.0	20.25	0.0	20.25	0.0	0.00927	19.16	446.82	0.7551
65.0	0.0	0.0	20.52	0.0	20.52	0.00085	0.00940	18.97	442.46	0.7478
70.0	0.0	0.0	21.03	0.0	21.03	-0.00205	0.00964	18.23	425.00	0.7183
75.0	0.0	0.0	20.98	0.0	20.98	0.00102	0.00962	18.56	432.70	0.7313
80.0	0.0	0.0	21.21	0.0	21.21	0.00222	0.00973	18.46	430.38	0.7274
85.0	0.0	0.0	22.03	0.0	22.03	-0.00102	0.01013	17.44	406.70	0.6873
87.5	0.0	0.0	22.35	0.0	22.35	-0.00068	0.00514	17.15	399.85	0.6758
90.0	0.0	0.0	22.58	0.0	22.58	-0.00290	0.01038	16.83	392.48	0.6633
92.5	0.0	0.0	21.71	0.0	21.71	0.01127	0.00499	19.85	462.86	0.7822
95.0	0.0	0.0	22.35	0.0	22.35	-0.01946	0.01034	15.55	362.57	0.6128
100.0	0.0	0.0	16.91	0.0	16.91	0.00990	0.00771	24.28	566.20	0.9569
105.0	0.0	0.0	14.12	0.0	14.12	0.01280	0.00631	29.68	692.15	1.1697
110.0	0.0	0.0	14.76	0.0	14.76	0.00102	0.00661	26.78	624.50	1.0554
115.0	0.0	0.0	15.67	0.0	15.67	0.00068	0.00705	25.12	585.76	0.9899
120.0	0.0	0.0	16.77	0.0	16.77	0.00119	0.00756	23.48	547.41	0.9251
125.0	0.0	0.0	18.19	0.0	18.19	0.00034	0.00827	21.48	500.79	0.8463
130.0	0.0	0.0	19.70	0.0	19.70	-0.00119	0.00899	19.60	457.14	0.7726
135.0	0.0	0.0	20.89	0.0	20.89	-0.00324	0.00955	18.24	425.37	0.7189
140.0	0.0	0.0	21.21	0.0	21.21	-0.00137	0.00971	18.13	422.66	0.7143
145.0	0.0	0.0	21.16	0.0	21.16	-0.00034	0.00969	18.26	425.84	0.7197
150.0	0.0	0.0	21.03	0.0	21.03	-0.00051	0.00964	18.37	428.36	0.7239
155.0	0.0	0.0	20.75	0.0	20.75	0.00017	0.00950	18.69	435.86	0.7366
160.0	0.0	0.0	20.52	0.0	20.52	-0.00171	0.00939	18.73	436.77	0.7381
165.0	0.0	0.0	19.84	0.0	19.84	0.00324	0.00907	19.90	464.07	0.7843
170.0	0.0	0.0	20.02	0.0	20.02	-0.00188	0.00916	19.21	447.88	0.7569
175.0	0.0	0.0	19.70	0.0	19.70	-0.00051	0.00900	19.67	458.70	0.7752
180.0	0.0	0.0	19.24	0.0	19.24	-0.00222	0.00877	19.99	466.09	0.7877

FORCED CONVECTION HEAT TRANSFER FROM A UNIFORMLY

HEATED CYLINDER IN A CROSSFLOW OF AIR

FREE STREAM DYN. HEAD EQUALS 21.32 CM OF WATER
FREE STREAM VELOCITY EQUALS 202.2 FT.PER SEC.(UNCORRECTED)
FREE STREAM VELOCITY EQUALS 207.4 FT.PER SEC.(CORRECTED)
THE REYNOLDS NUMBER EQUALS 395887. (UNCORRECTED)
THE REYNOLDS NUMBER EQUALS 406067. (CORRECTED)
DELTAX EQUALS 0.01625 FEET
ASURF EQUALS 0.000508 SQUARE FEET
QGEN EQUALS 0.20629 BTU PER HOUR
TU EQUALS 0.43 PER CENT

THETA (DEG)	DELTA-P (CM)	CP	DELTA-T (DEG F)	DELTA-T CORRECTION	DELTA-T CORRECTED	QCOND (BTU/HR)	QRAD (BTU/HR)	HT TRANS COEFF	NUSSELT NR	FROESSLING NR
0.0	21.44	1.01	17.37	0.51	16.85	0.00068	0.00812	23.23	537.76	0.8439
5.0	20.85	0.98	17.55	0.47	17.08	-0.00102	0.00821	22.72	525.74	0.8250
10.0	18.97	0.89	17.46	0.40	17.06	0.00051	0.00817	22.93	530.64	0.8327
15.0	15.75	0.74	17.50	0.30	17.20	-0.00068	0.00819	22.60	523.13	0.8209
20.0	12.55	0.59	17.37	0.23	17.13	0.00085	0.00813	22.88	529.44	0.8308
25.0	6.48	0.30	17.46	0.12	17.34	0.00017	0.00818	22.52	521.17	0.8179
30.0	0.51	0.02	17.59	0.0	17.59	-0.00119	0.00825	22.03	509.95	0.8003
35.0	-5.92	-0.28	17.41	-0.14	17.55	0.00171	0.00816	22.42	518.97	0.8144
40.0	-12.50	-0.59	17.69	-0.28	17.97	-0.00154	0.00830	21.54	498.44	0.7822
45.0	-19.56	-0.92	17.55	-0.42	17.97	0.00119	0.00823	21.84	505.47	0.7932
50.0	-27.05	-1.27	17.73	-0.56	18.29	0.0	0.00832	21.32	493.36	0.7742
55.0	-34.54	-1.62	17.92	-0.67	18.59	0.00119	0.00841	21.09	488.12	0.7660
60.0	-40.64	-1.91	18.42	-0.79	19.21	-0.00051	0.00858	20.22	467.92	0.7343
65.0	-45.85	-2.15	18.78	-0.86	19.64	-0.00068	0.00882	19.73	456.59	0.7165
70.0	-50.67	-2.38	18.97	-0.88	19.85	0.0	0.00898	19.57	453.04	0.7110
75.0	-53.37	-2.50	19.15	-0.81	19.96	0.00102	0.00897	19.57	452.83	0.7106
80.0	-54.28	-2.55	19.61	-0.70	20.31	0.00085	0.00920	19.20	444.34	0.6973
85.0	-53.59	-2.51	20.29	-0.65	20.95	-0.00495	0.00955	18.03	417.36	0.6550
90.0	-50.04	-2.35	19.65	-0.60	20.26	-0.01314	0.00925	17.88	413.76	0.6493
95.0	-44.32	-2.08	15.49	-0.47	15.96	0.00700	0.00721	25.44	588.71	0.9239
97.5	-41.91	-1.97	14.25	-0.42	14.67	0.00137	0.00331	27.17	628.74	0.9867
100.0	-44.32	-2.08	13.20	-0.37	13.57	0.00990	0.00611	30.48	705.40	1.1070
102.5	-35.05	-1.64	13.43	-0.33	13.76	-0.00068	0.00311	28.45	658.36	1.0332
105.0	-35.81	-1.68	13.57	-0.33	13.89	0.00324	0.00628	28.81	666.76	1.0463
110.0	-23.11	-1.08	14.80	-0.47	15.27	0.00222	0.00688	26.01	601.88	0.9445
115.0	-17.68	-0.83	16.63	-0.65	17.29	-0.00137	0.00778	22.46	519.87	0.8158
120.0	-15.49	-0.73	18.10	-0.79	18.89	0.00239	0.00849	20.87	483.07	0.7581
125.0	-15.24	-0.71	20.20	-0.88	21.09	-0.00734	0.00954	17.69	409.43	0.6425
130.0	-14.86	-0.70	20.34	-0.93	21.27	-0.00273	0.00961	17.96	415.62	0.6522
135.0	-15.60	-0.73	19.75	-0.98	20.72	0.00205	0.00931	18.92	437.78	0.6870
140.0	-17.27	-0.81	19.70	-1.02	20.72	0.00188	0.00929	18.90	437.44	0.6865
145.0	-16.87	-0.79	20.16	-1.05	21.20	-0.00888	0.00952	17.45	403.91	0.6339
150.0	-18.29	-0.86	18.24	-1.07	19.31	0.00341	0.00849	20.53	475.07	0.7455
155.0	-17.65	-0.83	17.23	-1.07	18.30	0.00273	0.00806	21.63	500.58	0.7856
160.0	-16.89	-0.79	16.95	-1.07	18.02	0.00205	0.00799	21.89	506.66	0.7951
165.0	-17.02	-0.80	17.23	-1.07	18.30	0.0	0.00803	21.34	493.85	0.7750
170.0	-15.62	-0.73	17.50	-1.07	18.57	-0.00427	0.00816	20.56	475.75	0.7466
175.0	-15.37	-0.72	16.63	-1.07	17.70	0.00068	0.00775	22.16	512.91	0.8049
180.0	-15.24	-0.71	15.95	-1.02	16.97	0.00205	0.00743	23.31	539.59	0.8468

FORCED CONVECTION HEAT TRANSFER FROM A UNIFORMLY

HEATED CYLINDER IN A CROSSFLOW OF AIR

FREE STREAM DYN. HEAD EQUALS 36.95 CM OF WATER
FREE STREAM VELOCITY EQUALS 273.5 FT.PER SEC.(UNCORRECTED)
FREE STREAM VELOCITY EQUALS 277.8 FT.PER SEC.(CORRECTED)
THE REYNOLDS NUMBER EQUALS 487288. (UNCORRECTED)
THE REYNOLDS NUMBER EQUALS 494945. (CORRECTED)
DELTAX EQUALS 0.01625 FEET
ASURF EQUALS 0.000508 SQUARE FEET
QGEN EQUALS 0.20867 BTU PER HOUR
TU EQUALS 0.43 PER CENT

THETA (DEG)	DELTA-P (CM)	CP	DELTA-T (DEG F)	DELTA-T CORRECTION	DELTA-T CORRECTED	QCOND (BTU/HR)	QRAD (BTU/HR)	HT TRANS COEFF	NUSSELT NR	FROESSLING NR
0.0	36.80	1.00	16.08	0.0	16.08	-0.00102	0.00894	24.33	537.06	0.7634
5.0	35.92	0.97	15.95	-0.04	15.98	0.00034	0.00884	24.66	544.39	0.7738
10.0	32.18	0.87	15.90	-0.10	16.00	-0.00034	0.00882	24.56	542.10	0.7706
15.0	26.59	0.72	15.76	-0.18	15.95	0.00034	0.00873	24.74	546.01	0.7761
20.0	21.34	0.58	15.72	-0.28	16.00	-0.00068	0.00870	24.53	541.56	0.7698
25.0	11.30	0.31	15.49	-0.45	15.94	0.00239	0.00855	25.02	552.26	0.7850
30.0	2.03	0.05	15.90	-0.65	16.55	-0.00427	0.00878	23.27	513.76	0.7303
35.0	-9.02	-0.24	15.17	-0.93	16.10	0.00205	0.00831	24.75	546.39	0.7766
40.0	-21.59	-0.58	14.99	-1.22	16.21	0.00051	0.00819	24.42	539.02	0.7662
45.0	-33.91	-0.92	14.94	-1.48	16.42	-0.00051	0.00817	23.99	529.48	0.7526
50.0	-46.23	-1.25	14.76	-1.72	16.48	-0.00085	0.00806	23.87	526.96	0.7490
55.0	-59.56	-1.61	14.35	-1.94	16.29	0.00700	0.00783	25.13	554.64	0.7884
60.0	-70.48	-1.91	15.81	-2.09	17.90	-0.00563	0.00877	21.37	471.73	0.6705
65.0	-80.26	-2.17	15.76	-2.37	18.14	0.00171	0.00876	21.89	483.26	0.6869
70.0	-87.25	-2.36	16.18	-2.47	18.64	0.00017	0.00901	21.11	466.01	0.6624
75.0	-92.33	-2.50	16.63	-2.41	19.04	0.00154	0.00928	20.78	458.68	0.6520
80.0	-93.47	-2.53	17.50	-2.33	19.83	-0.00034	0.00979	19.72	435.28	0.6187
82.5	-92.71	-2.51	18.01	-2.28	20.29	-0.00171	0.00504	18.95	418.27	0.5945
85.0	-91.19	-2.47	18.28	-2.22	20.50	-0.01212	0.01024	17.89	395.02	0.5615
90.0	-84.58	-2.29	15.81	-2.09	17.90	-0.00563	0.00878	21.37	471.70	0.6705
95.0	-80.01	-2.17	11.83	-1.86	13.69	0.01280	0.00649	30.93	682.66	0.9703
100.0	-78.36	-2.12	11.28	-1.63	12.91	0.00512	0.00618	31.67	699.16	0.9938
105.0	-60.71	-1.64	12.10	-1.53	13.64	0.00307	0.00664	29.61	653.71	0.9292
110.0	-40.39	-1.09	13.75	-1.72	15.47	0.00171	0.00757	25.81	569.82	0.8100
115.0	-31.50	-0.85	15.86	-2.05	17.90	-0.00666	0.00876	21.26	469.28	0.6670
120.0	-29.21	-0.79	16.18	-2.33	18.50	0.00273	0.00894	21.55	475.72	0.6762
125.0	-30.73	-0.83	17.23	-2.42	19.65	-0.00307	0.00948	19.66	433.93	0.6168
130.0	-29.08	-0.79	17.46	-2.47	19.92	-0.00085	0.00960	19.59	432.52	0.6148
135.0	-29.34	-0.79	17.46	-2.50	19.96	-0.00205	0.00960	19.44	429.11	0.6099
140.0	-30.23	-0.82	16.91	-2.56	19.47	-0.00154	0.00929	20.02	441.83	0.6280
145.0	-30.86	-0.84	15.95	-2.63	18.58	-0.00239	0.00874	20.94	462.31	0.6571
150.0	-31.75	-0.86	14.35	-2.70	17.04	0.00427	0.00792	23.69	522.91	0.7433
155.0	-31.50	-0.85	13.89	-2.80	16.69	0.00085	0.00768	23.81	525.63	0.7471
160.0	-31.37	-0.85	13.66	-2.93	16.59	0.00017	0.00756	23.89	527.42	0.7497
165.0	-30.10	-0.81	13.48	-2.93	16.41	-0.00137	0.00746	23.99	529.50	0.7526
170.0	-29.24	-0.79	12.93	-2.93	15.86	0.00171	0.00715	25.24	557.11	0.7919
175.0	-27.94	-0.76	12.84	-2.93	15.77	0.00085	0.00709	25.29	558.15	0.7934
180.0	-25.76	-0.70	12.97	-2.93	15.90	-0.00000	0.00715	24.95	550.84	0.7830

of Nichrome ribbon. "TU" is the turbulence intensity level at the given free stream velocity. "DELTA-T CORRECTION" is the correction for the resultant effect of viscous heating of the cylinder and heating of the ambient air during high speed runs (Appendix C).

B. DISCUSSION

To illustrate the discussion, the Nusselt number and the pressure coefficient have been plotted as a function of their angular location in Figures 9 through 14.

The results in general only confirmed the trend of those published by Giedt [15] with regard to approximate locations of minimum and maximum points and the angular pattern of heat transfer characteristics around the cylinder. The magnitudes of the heat transfer rates are somewhat less than those of Giedt. This is most probably explained by the lower turbulence level of the wind tunnel employed in this experiment (~0.5%). Also, the alignment of the cylinder was about one deg in error, as it leaned toward the rear of the test section. This discrepancy probably decreased the normal component of the wind striking the cylinder, and may have consistently decreased the heat transfer rates.

At the lower Reynolds numbers of 57,000 and 82,000, the heat transfer results were in close agreement with the resulting pressure coefficient distribution around the cylinder. The boundary layer remained laminar and

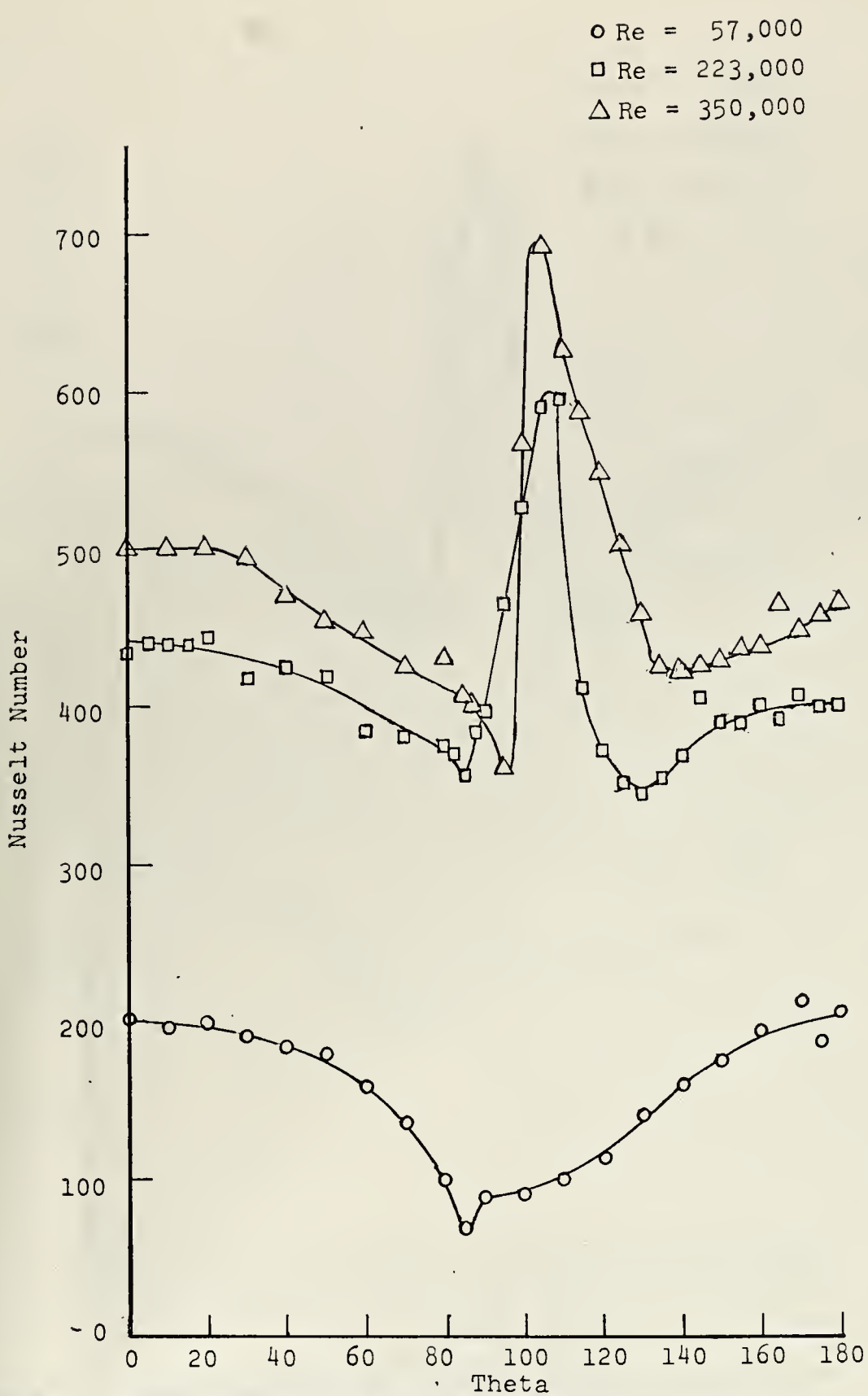

Figure 9. Heat Transfer Results at Reynolds Numbers of 57,000, 223,000 and 350,000

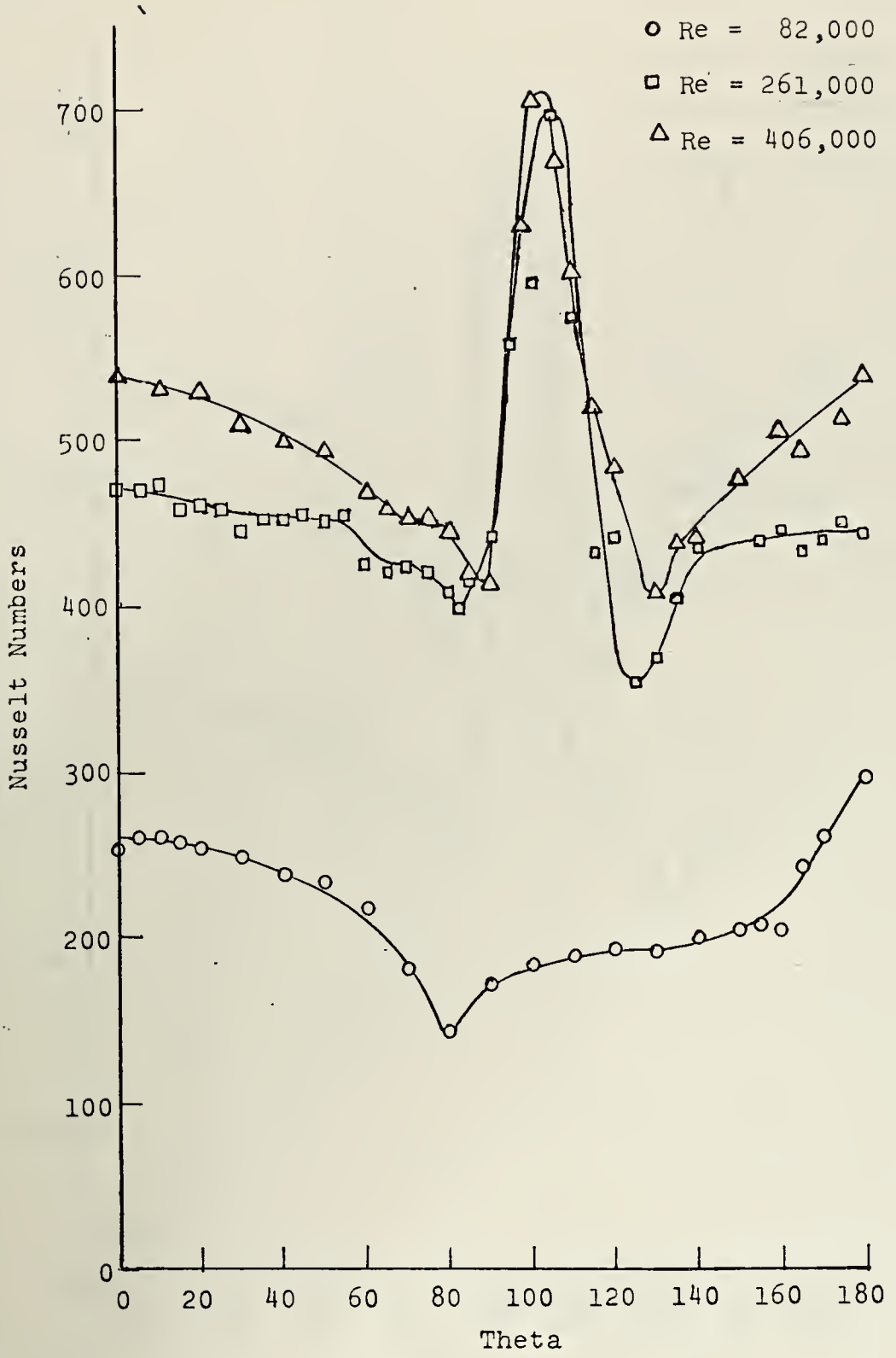

Figure 10. Heat Transfer Results at Reynolds Numbers of 82,000, 261,000 and 406,000

Figure 11. Heat Transfer Results at Reynolds Numbers of 153,000, 309,000 and 495,000

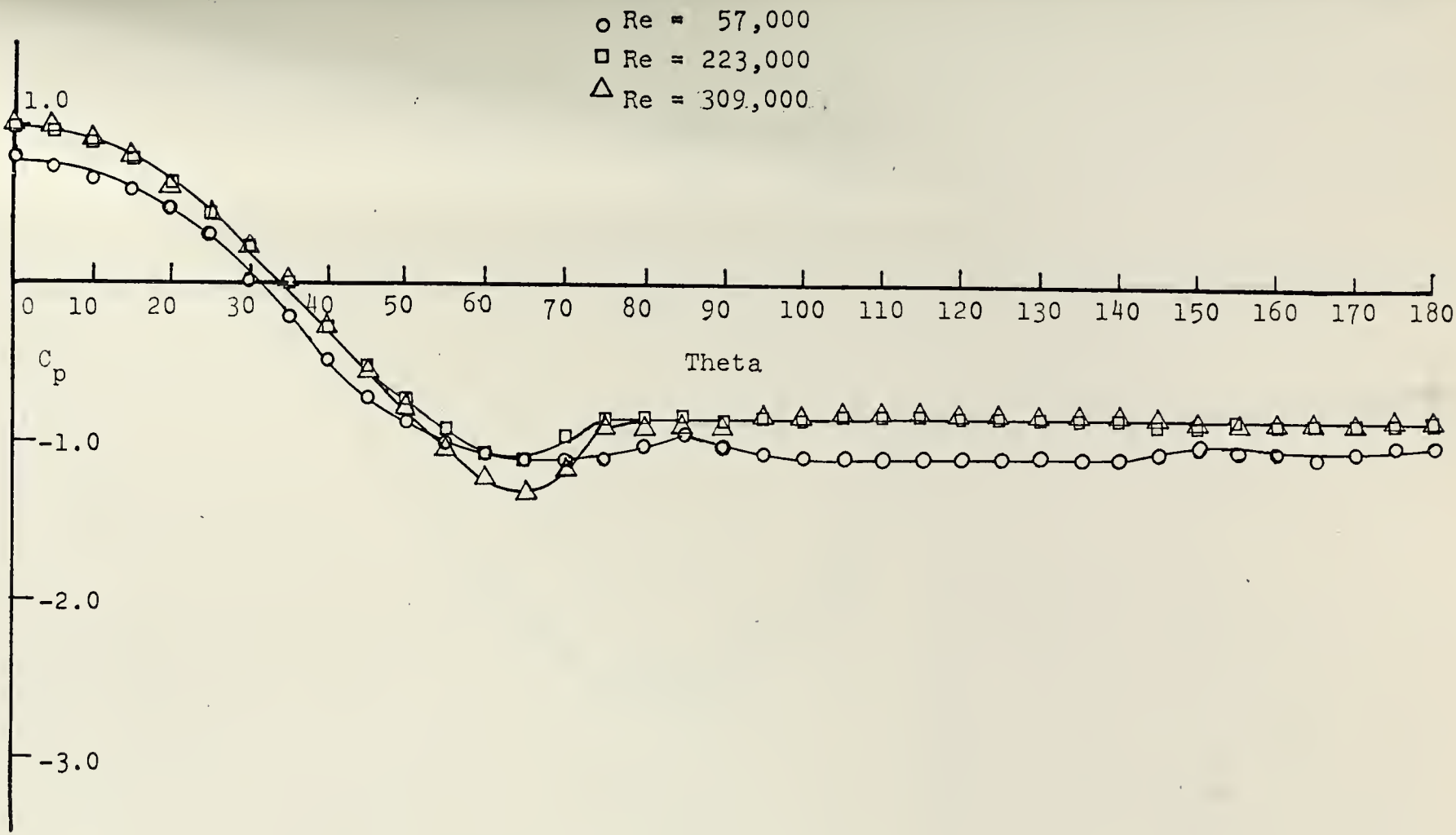

Figure 12. Surface Pressure Distribution at Reynolds Numbers of 57,000, 223,000 and 309,000

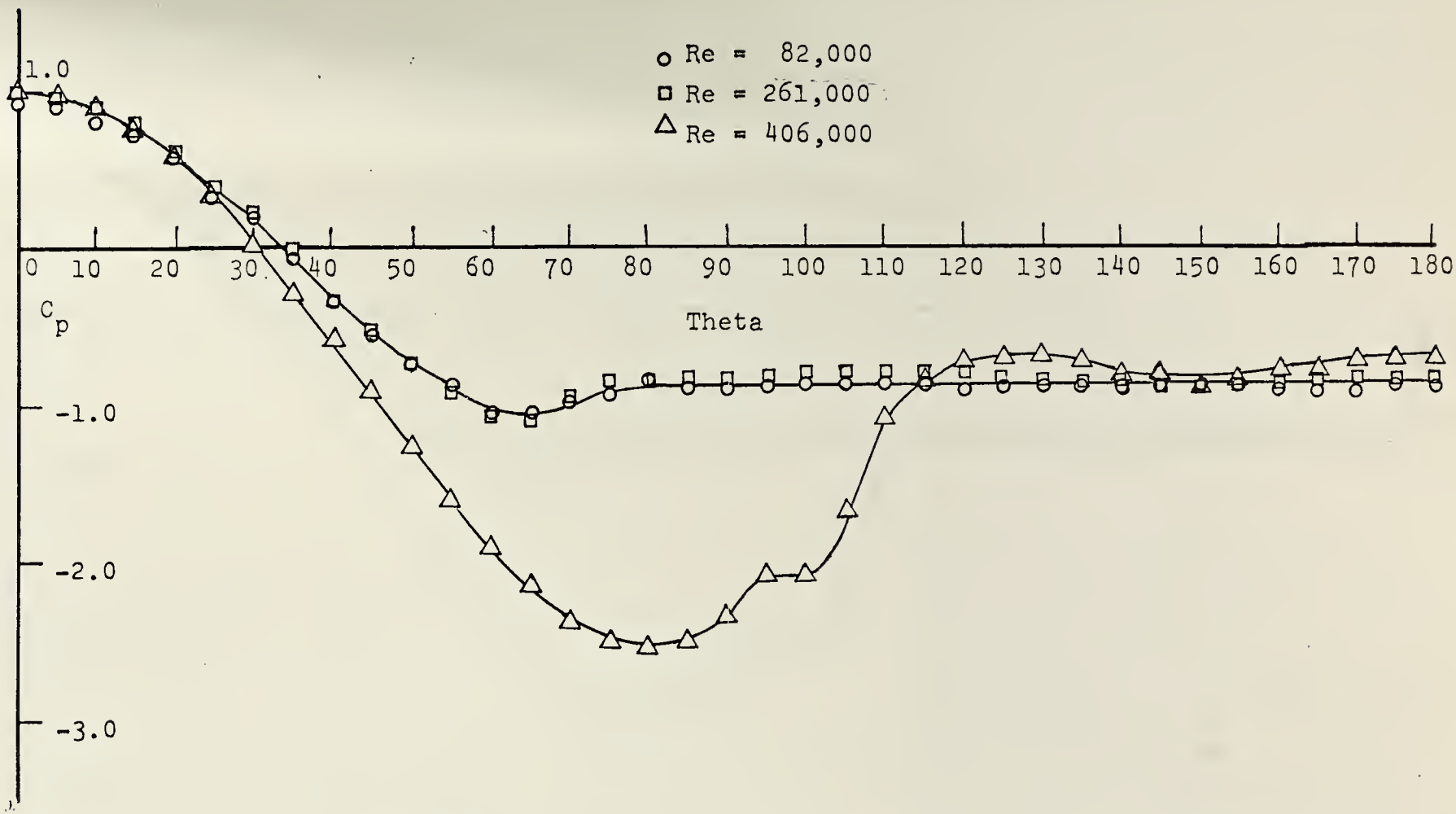

Figure 13. Surface Pressure Distribution at Reynolds Numbers of 82,000, 261,000 and 406,000

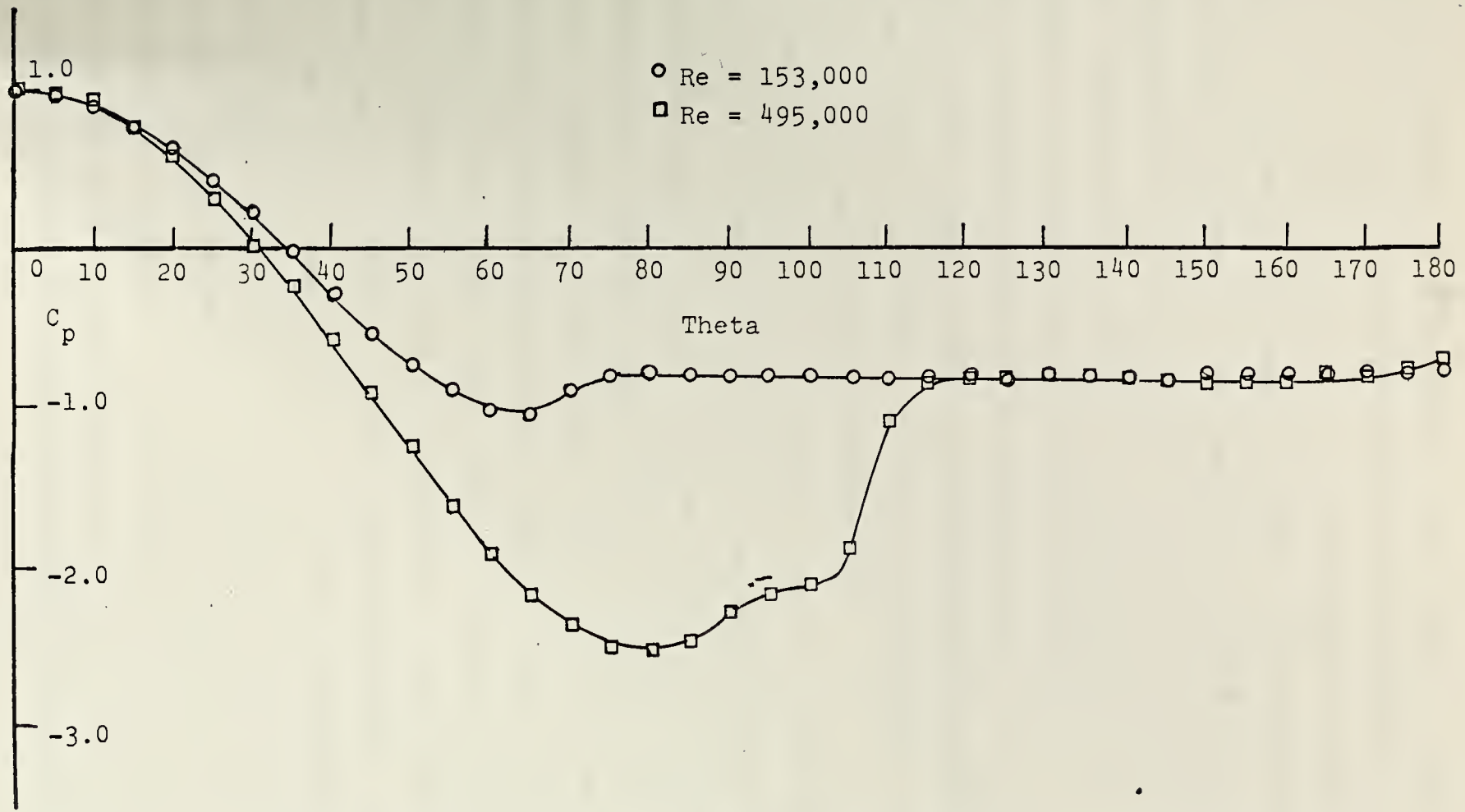

Figure 14. Surface Pressure Distribution at Reynolds Numbers of 153,000 and 495,000

separated at about 82.5 and 80 deg, respectively. This laminar flow regime was reflected in the heat transfer results by a single minimum value of the Nusselt number, which was located at the separation point. Also, maximum heat transfer occurred at the stagnation points. The corresponding pressure distributions also depicted laminar flow. These were characterized by a minimum at 65 deg followed by a fairly small recovery in the form of a smooth, continuous rise, and a flattening out at the separation points. Additionally, there were distinct peaks in the two pressure coefficient curves at 85 and 80 deg, respectively, just as the curve flattened out.

Unfortunately, at the intermediate range of Reynolds numbers studied ($82{,}000<Re<300{,}000$), the surface pressure distribution did not reflect the same conditions of flow inferred by the heat transfer results. As before, the pressure coefficient distributions were representative of subcritical flow, and indicated a laminar boundary layer separation at about 80-85 deg. The heat transfer results, however, depicted a region of transitional flow in the boundary layer, and therefore were representative of critical flow. There were, for example, two minimum values of Nusselt number. The first minimum occurred at an angular location of about 85 deg, and marked the beginning of transition to a turbulent boundary layer. At this point the boundary layer may have separated, become turbulent, and then reattached at a subsequent point, having become

fully turbulent. This transition region, known as the "separation bubble", is exhibited by the angular distribution of the local Nusselt number, at this range of Reynolds numbers. The second heat transfer minimum occurred at about 130 deg, and represented the separation of the turbulent boundary layer. At this range of Reynolds numbers, and between the two minima described, maximum heat transfer occurred at an angular position corresponding to the reattachment of a fully turbulent boundary layer.

The lack of agreement of the pressure information can most probably be attributed to the location of the pressure pickups on the smooth acrylic tube and not in the region of the test section.

At the higher Reynolds numbers of 406,000 and 495,000 there was close agreement between the heat transfer and surface pressure results. Both indicated critical flow conditions. For each run the heat transfer results exhibited two minimum values of the Nusselt number. The first minimum values where transitional flow began were located at 90 and 82.5 deg, respectively. The second minimum values where the boundary layer separated were located at 130 and 135 deg, respectively for the two runs. The points of maximum heat transfer where the boundary layers reattached and became fully turbulent were located at 100 and 95 deg, respectively.

For these same two Reynolds numbers the surface pressure distributions had minimum values at 80 deg, which

differed from all other experimental runs which had pressure minimums at 65 deg. Also, the rise of the pressure curve, from the minimum, was not smooth, but was characterized by a double inflection, which depicted the "separation bubble." The first inflection point represented the initial detachment of the laminar boundary layer. Its angular locations of 90 deg and 85 deg for the two runs corresponded identically with the locations of the first minimum values of the Nusselt number. The second inflection point indicates reattachment and complete transition to a turbulent boundary layer. Its angular location of 100 deg in both runs, corresponded closely with the location of the maximum values of the Nusselt number. Also the pressure distributions for these Reynolds numbers flattened out at angular locations of about 130 and 120 deg, respectively, corresponding reasonably well with the second minimum values of the Nusselt number.

In contrast to Giedt's findings [15] for Reynolds numbers above 153,000, the value of h_θ at the rear stagnation point was not always greater than its value at the forward stagnation point.

It was not found that the angular location of minimum values of h_θ invariably increased as the Reynolds number increased. Instead, there were variations in the flow conditions from one run to the next. A higher velocity run at times produced an apparently smoother flow than one of the lower velocity runs. For example, the initial minimum

values of h_θ for Reynolds numbers of 153,000; 173,000; and 223,000 were 90,100 and 100 deg, respectively. However, at a Reynolds number of 260,000, the first heat transfer minimum occurred at 82.5 deg. In the same way, the initial minimum value of h_θ for Reynolds numbers of 309,000; 350,000 and 406,000 were 85, 95 and 90 deg respectively. But apparently a very smooth flow existed at a Reynolds number of 495,000, since the first heat transfer minimum then occurred at 85 deg. This inconsistancy was probably caused by the surface defects of the test cylinder. These defects were less pronounced during the two high speed runs because of the higher surface temperatures involved.

It is thought that the large thermal capacity of the foam rubber and acrylic in the interior of the tube fostered complicated internal flows of heat. These heat flows depended upon the magnitude and direction of the angular rotation of the cylinder from a previous steady state position to the present position. Also, the magnitudes of the steady state surface temperature differences varied, depending upon whether the cylinder was rotated to a position from a previous steady state position, or was initially warmed up there and heated to a steady state condition. Specifically, and for example, rotating a test thermocouple at five deg intervals gradually around a distance of 20 deg to a critical location seemed to amplify these temperature differences than if the cylinder had initially been warmed up with a test thermocouple in that critical

location. This was especially true when approaching and arriving at the first minimum value of the Nusselt number. Variations near the front of the cylinder were only about 0.5°F or less, but were on the order of five °F at the critical position, and about one °F at the rear stagnation point.

An uncertainty analysis was performed and is described in Appendix F. In this analysis the uncertainty of the Nusselt number was found to be about three per cent at the forward stagnation point, about six per cent at the rear stagnation point, and on the order of 25% at the critical point where the boundary layer either begins its transition to turbulent flow or separates.

C. COMPARISON OF EXPERIMENTAL RESULTS WITH EXISTING THEORY

The heat transfer at the forward stagnation point can be conveniently compared to Squire's solution, which generates a Froessling number ($F = Nu/\sqrt{Re}$) of 0.995 for this application. The Froessling number calculated from the present set of experimental results was about 0.93-.92 at Reynolds numbers from 153,000 to 261,000. At Reynolds numbers below and above this range, the Froessling number decreased to as low as .84, excluding the run at a Reynolds number of 495,000. This latter run had a surprising, low Froessling number of 0.76 at the forward stagnation point, which could not be explained. For this run the power source for the main circuit and the wind tunnel were both

in their maximum positions, which possibly placed an unacceptable strain on the experiment. It is also curious to note that the Nusselt number at the forward and rear stagnation points are identical for the two experimental runs of 406,000 and 495,000.

For an evaluation of the data beyond the forward stagnation point an appropriate theoretical solution was required. All existing theoretical solutions only predict the heat transfer from the forward half of a cylinder, prior to the point of laminar boundary layer separation at about 80 deg. Spalding and Pun [12] have summarized fifteen approximate solution methods. However, since all fifteen are applicable to isothermal cylinders, none would provide a meaningful comparison for the data collected in this experiment with a constant heat flux cylinder. Spalding and Pun compared the various methods with that of Froessling who used an "exact", series method of solution limited by the number of terms employed. It was shown that Schuh's method of solution for an isothermal cylinder ranked in the highest class of accuracy and within 1-3 per cent of Froessling's solution. Schuh also published [26] one of the few approximate methods of solution for a constant heat flux cylinder.

In Fig. 15 the two theoretical solutions of Schuh are plotted to illustrate the significant difference in the heat transfer profile between the two types of cylinders usually employed. As one would expect, the two solutions

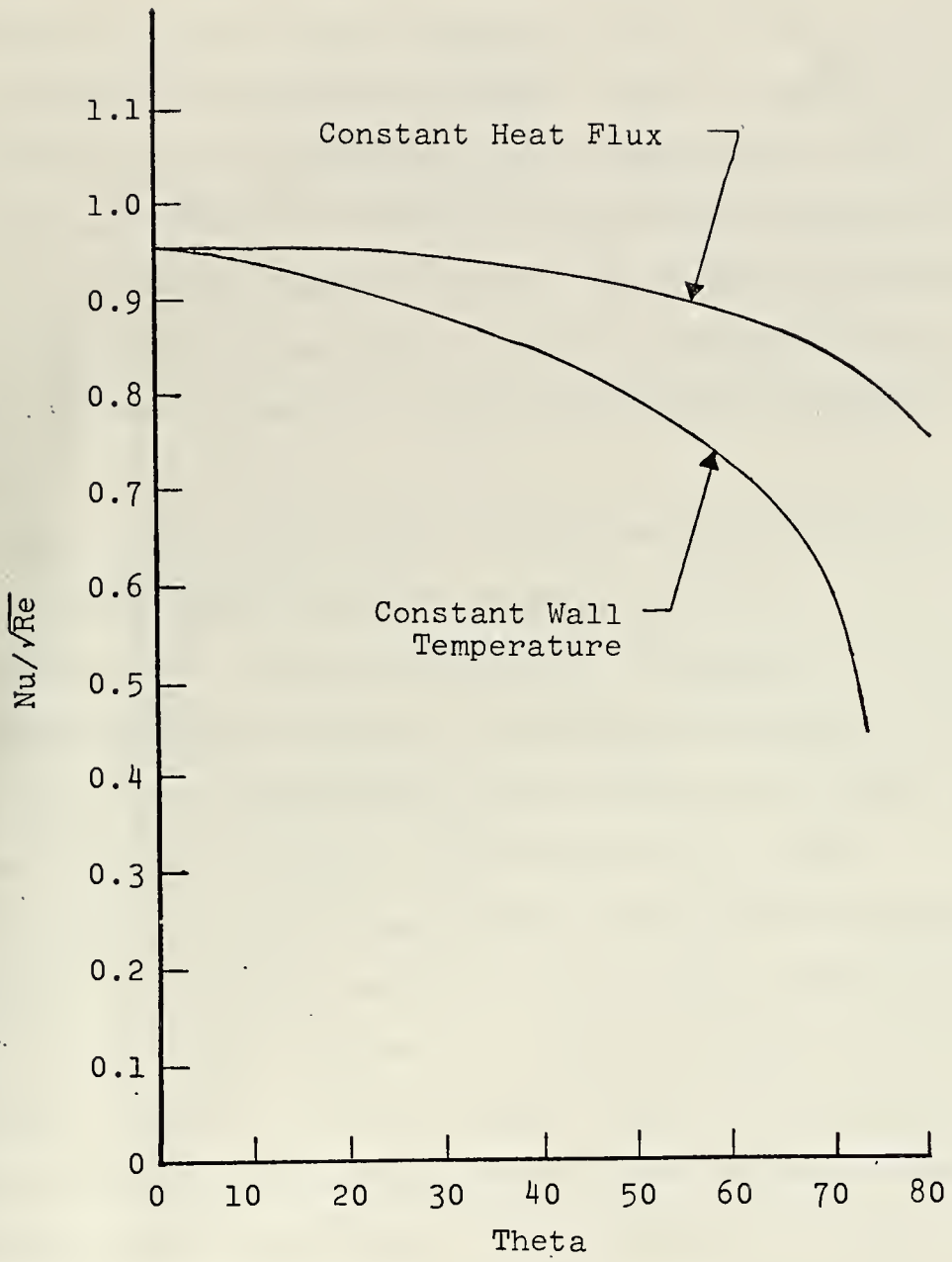

Figure 15. Theoretical Solutions of H. Schuh for Both Isothermal and Constant Heat Flux Cylinders

converge at the forward stagnation point, for in that vicinity the constant heat flux cylinder also has a constant wall temperature. Moving farther around the cylinder the ratio of relatively greater heat transfer from the constant heat flux cylinder continually increases. This is physically represented by an increasing surface temperature, which is required to provide an increasing temperature difference across the thermal boundary layer. The increased temperature difference is required to drive a constant flux of thermal energy through the thickening thermal boundary layer.

Some of the experimental results of Giedt [15] for heat transfer from a constant heat flux cylinder are compared to Schuh's solution in Fig. 16. The nature of the divergence of Giedt's results from the theoretical curve is most probably explained by the significantly higher level of free stream turbulence (2.25% compared to 0.5%).

In Fig. 17 some of the present results are compared with Schuh's solution, and most of them agree within about six per cent. This agreement is largely due to the low turbulence level of the wind tunnel used (0.5%). These results indicate that slightly less heat transfer occurs than that predicted by Schuh. The results are closely grouped, implying that any experimental errors are fairly consistent.

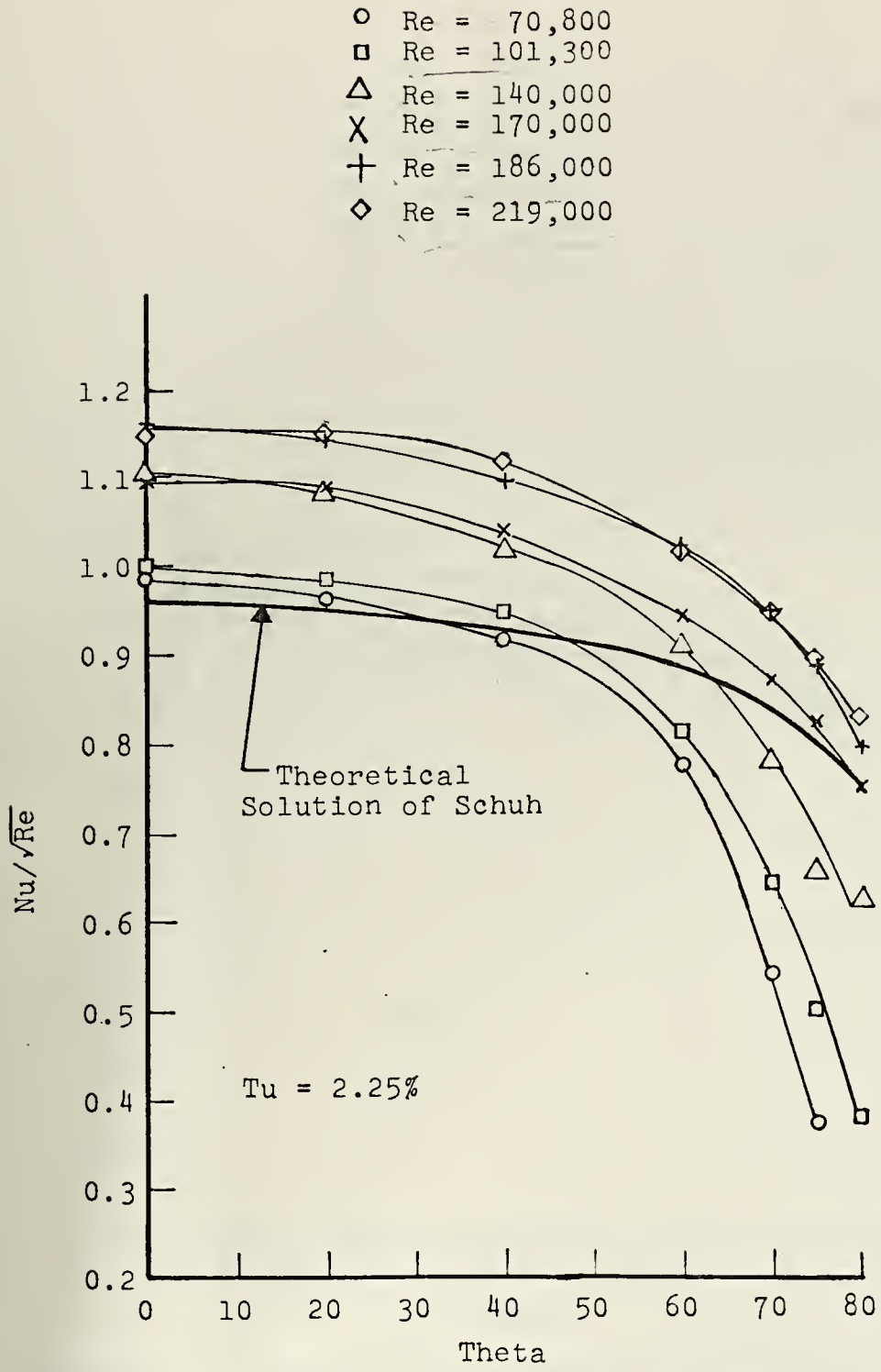

Figure 16. Comparison of Giedt's Experimental Results to the Theoretical Solution of Schuh

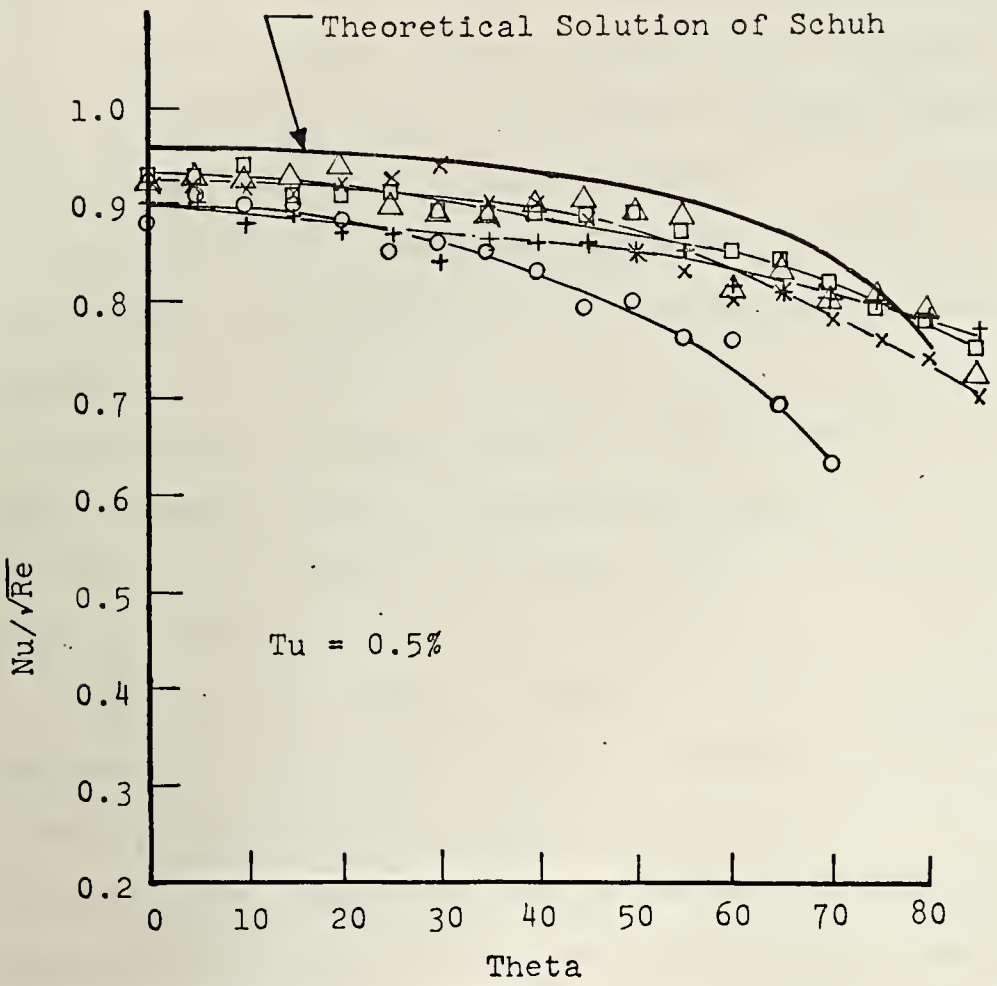

Figure 17. Comparison of Experimental Results of the Present Investigation to the Theoretical Solution of Schuh

VII. CONCLUSIONS AND RECOMMENDATIONS

Heat transfer and pressure coefficients were determined around a heated, right circular cylinder placed in a cross flow of air. The heat transfer results were generally in agreement with the pattern of heat transfer found previously for subcritical and critical flow.

The heat transfer results were compared with the classic results of Giedt [15], and indicated relatively lower heat transfer rates. This is most probably explained by the considerably lower free stream turbulence level of the wind tunnel employed in this experiment. It has been previously shown by other researchers that higher free stream turbulence levels markedly increase the heat transfer rates.

The heat transfer results were also compared and showed good agreement with the approximate analytical solution of Schuh for the laminar flow region on the front portion of the cylinder.

The surface pressure distribution did not in all experimental runs support the heat transfer results. Specifically, in several runs the pressure information failed to indicate the "separation bubble" which represents the transition in the boundary layer to turbulent flow, and depicted subcritical flow instead. In these instances the heat transfer results clearly represented critical flow effects.

It is possible that the pressure measuring system was not adequately sensitive to detect all of the surface pressure variations. However, it is more probable that the location of the surface pressure pickup was too distant from the test section. It is recommended that on the next cylinder constructed, the pressure taps be located in the test region.

An uncertainty analysis was performed and showed that the uncertainty in the heat transfer results was about three per cent at the forward stagnation point, six per cent at the rear stagnation point and on the order of 25% at the peaks in the heat transfer curves, where fluctuations seemed to be amplified.

The heat transfer results were possible adversely affected by some defects in the test cylinder, which can be avoided in a second cylinder being constructed.

The easily deformable acrylic tube and its large thermal expansion coefficient as compared to Nichrome ribbon, and the curing properties of the sealant used to bond the Nichrome to the surface resulted in a number of surface irregularities. A plan for avoiding this defect is being implemented in the construction of the second cylinder. In the "Discussion" by B.H. Sage appended to Ref. 32, small surface irregularities are reported to have caused unusually large variations in the heat transfer, especially in the rear portion of a cylinder. Seban [32] stated that

similar surface defects "disturbed the flow near the separation line."

It is recommended that the TRUMP computer program [43] be utilized to evaluate various insulating materials as a suitable replacement for the foam rubber. It should be possible to eliminate the complicated thermal flows and rotational behaviour, long transient warm-up period, and possible internal free convection as the acrylic tube usually expanded clear of the foam rubber filler.

It is recommended that the cylinder vertical alignment be carefully checked before all experimental runs. The base plate moving parts and metal interfaces should be overhauled, sanded smooth and lubricated. The rotating disc should be marked to indicate every one deg; it is the author's opinion that in a tunnel with a low turbulence level, a sufficiently accurate study is possible that warrants this refinement. The wooden floor has become warped from heat and should be renewed.

A major source of concern with regard to accurately measuring the free stream velocity was the air speed manometer. It is recommended that a hot wire anemometer be installed near the cylinder in such a manner as not to disturb the flow. This also precludes the problem of involving corrections for wind tunnel boundary constraints.

It is also recommended that a separate study of the same cylinder be made using cholesteric liquid crystals as a temperature sensor on the surface of the cylinder.

These crystals indicate temperature through a change in color, and offer the possibility of providing a highly desirable visual display of the temperature field much as smoke streaks provide a visual display of various flow phenomena.

APPENDIX A

Wind Tunnel Blockage Corrections

The test section velocity obtained from the air speed manometer and its associated pressure pickups refers to a clear test section. In Ref. 42, Pope discusses the effects of the tunnel boundary restrictions in combination with a two-dimensional model mounted in the test section. The flow area is reduced by the physical presence of the model and its relatively slower moving wake. Both of these disturbances cause the air to accelerate as it flows past the model in order to preserve continuity. Hence the measured velocity must be corrected for solid blocking and wake blocking, respectively.

Calculation of the solid blockage correction:

This boundary correction was calculated using the equation of Pope [42].

$$\epsilon_{SB} = \left(\frac{\pi^2}{3}\right)\left(\frac{r}{H}\right)^2 \qquad (44)$$

$$\epsilon_{SB} = \frac{9.86}{3}\left[\left(\frac{1}{2}\right)\left(\frac{4.5}{45}\right)\right]^2$$

$$\epsilon_{SB} = 0.008215$$

Calculation of the wake blockage correction:

This boundary correction is a function of the drag coefficient, and had to be evaluated for each run. The

equation used is from Pope [42], and the drag coefficients were were taken from Fig. 1.4 of Ref. 5.

$$\varepsilon_{WB} = \left(\frac{1}{4}\right)\left(\frac{D}{H}\right) C_D \qquad (45)$$

$$\varepsilon_{WB} = \frac{C_D}{40}$$

Run	Uncorrected Reynolds Nr.	C_D	ε_{WB}	$\varepsilon_t = \varepsilon_{SB}+\varepsilon_{WB}$
1	54,785	1.20	0.03	0.038
2	79,296	1.20	0.03	0.038
3	97,522	1.20	0.03	0.038
4	147,675	1.20	0.03	0.038
5	166,381	1.20	0.03	0.038
6	215,044	1.20	0.03	0.038
7	215,185	1.20	0.03	0.038
8	250,655	1.05	0.026	0.034
9	251,928	1.05	0.026	0.034
10	298,958	0.95	0.023	0.031
11	340,095	0.85	0.021	0.029
12	395,887	0.70	0.017	0.025
13	487,288	0.30	0.007	0.015

Application of the total blockage correction

The right column of the table provides the total blockage correction required for this experiment. Only the free stream velocity and the Reynolds number were corrected for boundary effects. The boundary corrections did not enter

into calculation of the pressure coefficients.

Specifically,

$$U_{corrected} = U_{uncorrected}\,(1+\varepsilon_t)$$

$$Re_{corrected} = Re_{uncorrected}\,(1+\varepsilon_t)$$

APPENDIX B

Computer Program for Data Reduction

```
C
C
C
C
C
C
C
C
C
C     THIS PROGRAM INCORPORATES A FINITE DIFFERENCE SCHEME
C     TO COMPUTE THE THERMAL ENERGY BALANCE AT EACH ELEMENT
C     ASSOCIATED WITH A NODE OR DATA POINT. A NODE/DATA
C     POINT LIES IN THE CENTER OF AN ELEMENT. AN INTERFACE
C     BETWEEN ELEMENTS IS HALFWAY BETWEEN ANY TWO NODES.
C     EACH ELEMENT IS 0.375 INCHES WIDE AND 0.0031 INCHES
C     THICK. THE ARC LENGTH OF AN ELEMENT IS EQUAL TO THE
C     DISTANCE BETWEEN INTERFACES WITH ADJACENT ELEMENTS.
C
C
C     UNITS EMPLOYED IN THE PROGRAM ARE:
C        LENGTH-FEET
C        AREA-SQUARE FEET
C        TEMPERATURE-DEGREES FAHRENHEIT
C        ENERGY-BTU PER HOUR
C
      IMPLICIT REAL*8(A-H,O-Z)
C     THE NUMBER OF DATA POINTS, N, IS ENTERED.
      READ(5,5)N
    5 FORMAT(I5)
C     EPS=THE TOTAL WIND TUNNEL BOUNDARY CORRECTION FOR
C     SURFACE BLOCKAGE AND WAKE BLOCKAGE.
      EPS=0.038215
      GSUBC=32.174
      RANKN=459.67
      PY=3.14159265358 98
C     STEFAN=THE STEFAN-BOLTZMANN CONSTANT.
      STEFAN=0.000000001714
C     D=DIAMETER OF THE CYLINDER IN FEET.
      D=4.46875/12.0
C     ALTO=THE TOTAL LENGTH OF NICHROME RIBBON IN THE MAIN
C     CIRCUIT.
      ALTO=39.0*PY*D+1.0/12.0
C     R=RESISTANCE OF THE MAIN HEAT GEN. CIRCUIT (OHMS).
      R=20.527
C     CONDNI=THE THERMAL CONDUCTIVITY OF NICHROME.
      CONDNI=7.51
C     EMISS=THE THERMAL EMISSIVITY OF NICHROME.
      EMISS=0.7
C     ACOND=THE AREA PERMITTING CIRCUMFERENTIAL CONDUCTION.
      ACOND=0.0031*0.375/144.0
C
C     THE VOLTAGE LEVEL, V, IS READ TO DETERMINE THE POWER.
C     THE DYNAMIC PRESSURE, U,IS READ IN CM. OF WATER.
C     DTHETA=THE ARC LENGTH OF AN ELEMENT ASSOCIATED WITH
C     ANY NODE/DATA POINT IN ANGULAR DEGREES.
C     TU=THE TURBULENCE LEVEL OF THE WIND TUNNEL AT THIS
C     FREE STREAM VELOCITY.
      READ(5,10)V,U,DTHETA,TU
   10 FORMAT(F10.6,10X,F10.3,10X,F10.3,10X,F10.6)
C
C     THE KINEMATIC VISCOSITY, CONDUCTIVITY & DENSITY OF AIR
C     (VISC, COND, AND RO) ARE THE FILM TEMPERATURE VALUES.
      READ(5,20)VISC,COND,RO
   20 FORMAT( 1X,3(F15.8,5X))
C
C     TTCF=THE TOTAL WIND TUNNEL CORRECTION/CONVERSION
C     FACTOR,AND IS DEFINED AS THE RATIO OF THE TUNNEL
C     CORRECTION FACTOR,X, TO THE AREA CONTRACTION
C     CONVERSION FACTOR,WHICH IS A FUNCTION OF A2/A1.
      TTCF=1.0
C     DELTAX=THE ARC LENGTH OF AN ELEMENT ASSOCIATED WITH A
C            PARTICULAR NODE/DATA POINT IN FEET.
      DELTAX=D/2.0*DTHETA*PY/180.0
```

```
C       ASURF=THE SURFACE AREA OF AN ELEMENT ASSOCIATED WITH A
C             PARTICULAR NODE/DATA POINT.
        ASURF=0.375*DELTAX/12.0
        ASURF1=ASURF
        ALFA=CONDNI*ACOND/DELTAX
C       QGEN=THE HEAT GENERATION RATE WITHIN A PARTICULAR
C       ELEMENT,(BTU/HR).
        QGEN=((V**2/R)/ALTO)*DELTAX*3600.0/1054.35026449
        QGEN1=QGEN
C       THE VELOCITY IS EVALUATED IN FEET PER SECOND.
        VELU=DSQRT(U*2.0*GSUBC*TTCF/(RO*0.488256196))
C       THE VELOCITY IS CORRECTED FOR SURFACE,WAKE BLOCKAGES.
        VEL=DSQRT(U*2.0*GSUBC*TTCF/(RO*0.488256196))*(1.0+EPS)
        DYNHD=U*TTCF
C       THE REYNOLDS NUMBER IS COMPUTED.
        REYNU=VELU*D*3600.0/VISC
C       THE REYNOLDS NUMBER IS COMPUTED USING CORRECTED VEL.
        REYN=VEL*D*3600.0/VISC
C
        WRITE(6,22)
   22 FORMAT('1',/////////,45X,'FORCED CONVECTION HEAT TR',
     1'ANSFER FROM A UNIFORMLY',//,51X,'HEATED CYLINDER IN',
     2' A CROSSFLOW OF AIR',///)
        WRITE(6,23) DYNHD,VELU,VEL,REYNU,REYN,DELTAX,ASURF,
     1QGEN,TU
   23 FORMAT(44X,'FREE STREAM DYN. HEAD EQUALS',F6.2,1X,
     1'CM OF WATER',/ ,45X,'FREE STREAM VELOCITY EQUALS',F6.
     21,1X,'FT.PER SEC.(UNCORRECTED)',/ ,45X,'FREE STREAM ',
     3'VELOCITY EQUALS',F6.1,1X,'FT.PER SEC.(CORRECTED)',/ ,
     446X,'THE REYNOLDS NUMBER EQUALS',F8.0,1X,'(UNCORRECT',
     5'ED)',/ ,46X,'THE REYNOLDS NUMBER EQUALS',F8.0,1X,
     6'(CORRECTED)',/ ,59X,'DELTAX EQUALS',F8.5,1X,'FEET',
     7/ ,60X,'ASURF EQUALS',F9.6,1X,'SQUARE FEET',/ ,61X,
     8'QGEN EQUALS',F8.5,1X,'BTU PER HOUR',/ ,63X,'TU EQUAL'
     9,'S',F5.2,1X,'PER CENT',///)
        WRITE(6,24)
   24 FORMAT(21X,'THETA',2X,'DELTA-P',2X,'CP',2X,'DELTA-T',3
     1X,'DELTA-T',3X,'DELTA-T',4X,'QCOND',4X,'QRAD',3X,'HT '
     2,'TRANS',2X,'NUSSELT',2X,'FROESSLING',/ ,21X,'(DEG)',
     33X,'(CM)',8X,'(DEG F)',1X,'CORRECTION',1X,'CORRECTED',
     41X,'(BTU/HR)',1X,'(BTU/HR)',2X,'COEFF',7X,'NR',8X,'NR'
     5,/)
C
        DO 50 I=1,N
C       TDELM=THE LOCAL TEMPERATURE DIFFERENCE BETWEEN THE
C       NICHROME RIBBON AND THE AMBIENT TEMPERATURE IN MV.
C       TDELT=TDELM CONVERTED TO DEGREES F.
C       TAMM=THE AMBIENT TEMPERATURE IN MILLIVOLTS.
C       TAMB=TAMM CONVERTED TO DEGREES F.
C       TFWM=THE TEMPERATURE DIFFERENCE AT THE NEXT SUCCESSIVE
C       NODE/DATA POINT IN MILLIVOLTS.
C       TFWD=TFWM CONVERTED TO DEGREES F.
C       TBACM=THE TEMPERATURE DIFFERENCE AT THE PREVIOUS
C       NODE/DATA POINT IN MILLIVOLTS.
C       TBACK=TBACM CONVERTED TO DEGREES F.
C       TCORM=THE HEATED AIR AND VISCOUS HEATING CORRECTION TO
C       DELTA T, IN MILLIVOLTS.
C       TCORF=TCORM CONVERTED TO DEGREES F.
C       THETA=THE ANGLE MEASURED FROM THE FWD STAGNATION POINT
        READ(5,25) TDELM,TAMM,TFWM,TBACM,TCORM,THETA
   25 FORMAT(2X,6(F10.5,2X))
C
C       THE FOLLOWING EQUATIONS REPRESENT A COPPER-CONSTANTAN
C       THERMOCOUPLE CONVERSION TABLE.
        IF(TDELM.GT.(0.521))GO TO 26
        TDELT=45.75163398*(TDELM-0.215)+10.0
        GO TO 28
   26 IF(TDELM.GT.(0.854))GO TO 27
        TDELT=45.01607717*(TDELM-0.543)+25.0
        GO TO 28
   27 TDELT=44.16403785*(TDELM-0.877)+40.0
   28 IF(TFWM.GT.(0.521))GO TO 29
```

```
      TFWD=45.75163398*(TFWM-0.215)+10.0
      GO TO 31
   29 IF(TFWM.GT.(0.854))GO TO 30
      TFWD=45.01607717*(TFWM-0.543)+25.0
      GO TO 31
   30 TFWD=44.16403785*(TFWM-0.877)+40.0
   31 IF(TBACM.GT.(0.521))GO TO 32
      TBACK=45.75163398*(TBACM-0.215)+10.0
      GO TO 34
   32 IF(TBACM.GT.0.854) GO TO 33
      TBACK=45.01607717*(TBACM-0.543)+25.0
      GO TO 34
   33 TBACK=44.16403785*(TBACM-0.877)+40.0
   34 TAMB=43.219076*(TAMM-0.765)+67.0
      TCORF=46.5116279*TCORM
C
C     T=THE LOCAL TEMPERATURE AT A NODE/DATA POINT.
      T=TAMB+TDELT
      ASURF=ASURF1
      QGEN=QGEN1
C     QCOND=THE NET HEAT FLOW INTO AN ELEMENT BY CONDUCTION.
      QCOND=ALFA*(TFWD+TBACK-(2.0*TDELT))
C     QRAD=THE HEAT FLOW RATE FROM AN ELEMENT BY RADIATION.
      QRAD=STEFAN*EMISS*ASURF*((T+RANKN)**4-(TAMB+RANKN)**4)
C     TDELCO=THE LOCAL TEMPERATURE DIFFERENCE CORRECTED FOR
C     THE NET EFFECT OF HEATED AIR AND VISCOUS HEATING.
      TDELCO=TDELT-TCORF
C     HCONV=THE LOCAL FORCED CONVECTION HEAT TRANSFER COEFF.
      HCONV=(QCOND+QGEN-QRAD)/(ASURF*TDELCO)
C     GNU=THE LOCAL NUSSELT NUMBER.
      GNU=HCONV*D/COND
C     THE FROESSLING NUMBER IS CALCULATED.
      F=GNU/DSQRT(REYN)
C     THE LOCAL DELTA P IS READ IN INCHES OF WATER.
      READ(5,43) DELTAP
   43 FORMAT(F10.3)
C     THE PRESSURE COEFFICIENT IS CALCULATED.
      DELTAP=2.54*DELTAP
      CP=DELTAP/DYNHD
C
      WRITE(6,49)THETA,DELTAP,CP,TDELT,TCORF,TDELCO,QCOND,
     1QRAD,HCONV,GNU,F
   49 FORMAT(19X,F7.1,2X,F6.2,2X,F5.2,1X,F6.2,2X,F7.2,3X,F7.
     12,3X,F8.5,1X,F8.5,2X,F6.2,3X,F7.2,2X,F8.4)
   50 CONTINUE
      STOP
      END
```

APPENDIX C

Wind Tunnel Calibration for the Combined Effect of Ambient Air Temperature Rise and Viscous Heating of the Cylinder

In general the free stream air temperature steadily increased during the operation of the wind tunnel. This temperature rise was attributed to the viscous heating in the boundary layer of the wind tunnel walls and the energy added by the rotating impeller. At low speeds ($Re \leq 260,000$) this temperature rise was very gradual and did not affect the accurate measurement of ΔT. The measured ΔT represented the temperature rise solely due to the applied power. Although the surface of the cylinder became warmer due to the heated air this extraneous heating of both the cylinder and the air were at the same rate, and ΔT remained a true measurement. During high speed runs, however, the rate of temperature rise of the tunnel air was rapid and exceeded the corresponding cylinder surface temperature rise. This effect caused the measured ΔT to be smaller than it should have been.

At the same time, and also for the high speed runs, the viscous heating of the cylinder surface provided a counter effect, tending to increase the measured ΔT. In all of the high speed runs this latter effect was dominated by the ambient air temperature rise.

Rather than attempting to uncouple these two effects, a scheme was devised to calibrate their combined effect out of the data for the high speed runs. The Nichrome ribbon was not energized and the cylinder was heated only by the extraneous effects discussed in the preceding paragraphs. After several hours steady state conditions were determined using the same technique as described in Section V. EXPERIMENTAL PROCEDURE for an ordinary run. The temperature difference ($T_\theta - T_{air}$) was then measured at various angular locations around the cylinder, and treated as a correction factor for the data collected during an actual run with applied power at that Reynolds number.

Calibration runs were performed at Reynolds numbers of 309,000, 406,000, and 495,000, and the ΔT correction factors are provided in Section VI-A TABULAR RESULTS. In the data reduction computer program (Appendix B) the ΔT correction factors are subtracted from the measured ΔT just prior to the calculation of the local heat transfer coefficient. The radiation and conduction losses are based upon the uncorrected, measured ΔT. The ΔT correction factors are most often negative because the heated air effect was dominant.

APPENDIX D

Wind Tunnel Turbulence Level Measurement

The turbulence level of the Aerolab wind tunnel test section was measured with a Thermo-Systems hot wire anemometer at eleven different free stream velocities ranging from 10 to 110 mph.

Initially, a Thermo-Systems calibrator model 1125 was used to calibrate the probe. The cold wire (room temperature) resistance was 7.77 ohms. With zero air flow through the calibrator the initial probe voltage was 1.667 volts. The probe voltage was then recorded for various controlled values of air flow velocity through the calibrator. The results of this calibration are presented in Fig. 18, as a plot of the probe voltage squared, V^2, versus the square root of the air flow velocity through the calibrator, $\sqrt{U}$. The intercept of the linear calibration curve which resulted, was the square of the actual value of initial probe voltage, V_0, to be used in the turbulence level calculations.

The probe was then mounted in the center of the test section on a vertical rod whose height could be adjusted in one inch increments. At each air speed for which turbulence level measurements were taken, the rod was used to traverse the vertical height of the test section. The probe voltage, V, and the rms voltage, e, were recorded at

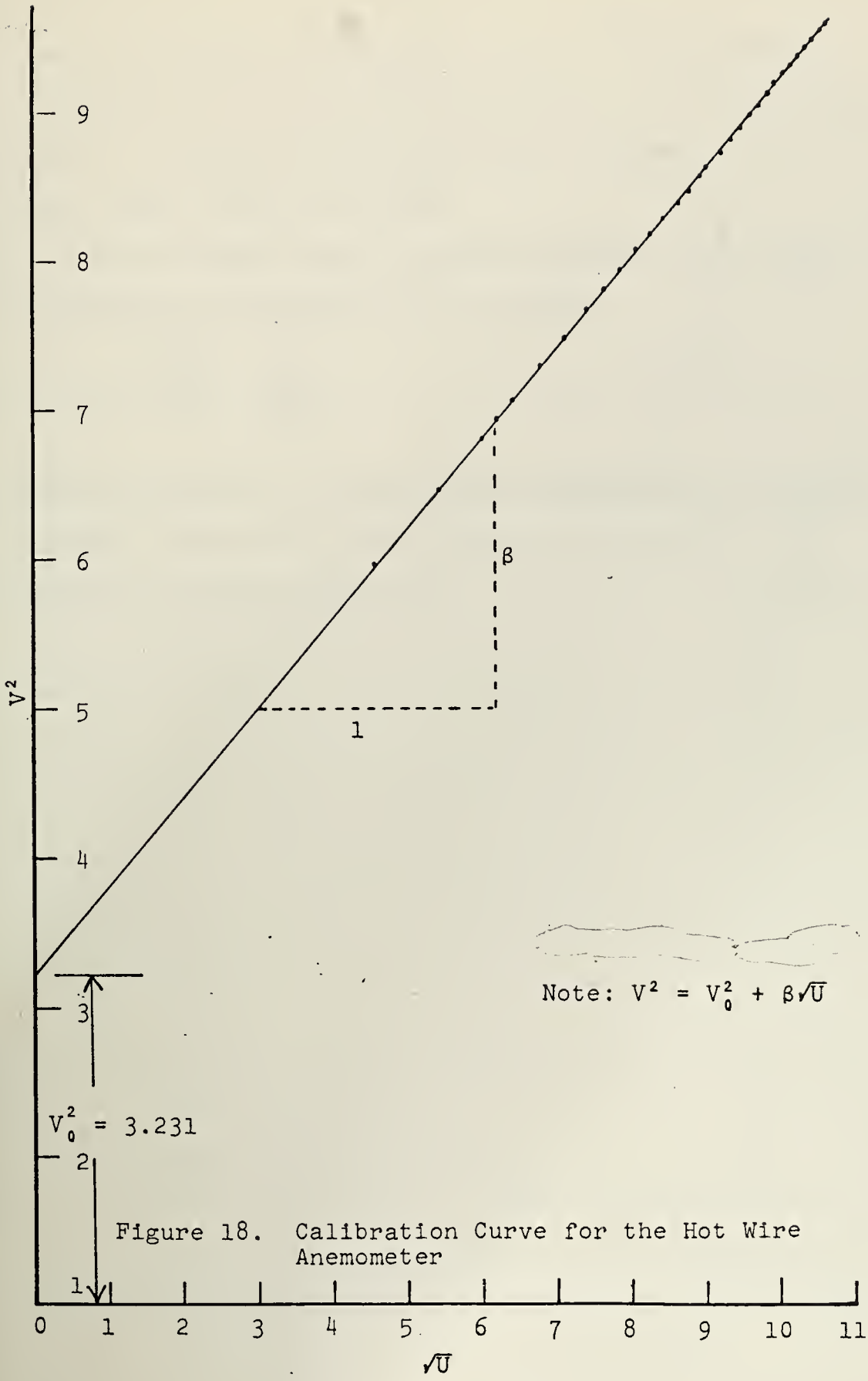

Figure 18. Calibration Curve for the Hot Wire Anemometer

five inch intervals along the vertical. These readings were observed to be constant for any given air speed except near the floor and ceiling where wall boundary layer effects caused some fluctuation.

The turbulence level, Tu, was calculated at the various air speeds by making use of the relation

$$Tu = \frac{\sqrt{\overline{U'^2}}}{\overline{U}} = \frac{4\ e\ V}{V^2 - V_0^2} \quad ,$$

where $\overline{U}$ represents the mean free stream velocity, and $\sqrt{\overline{U'^2}}$ is the mean fluctuation in the free stream velocity. The results are shown in Fig. 19.

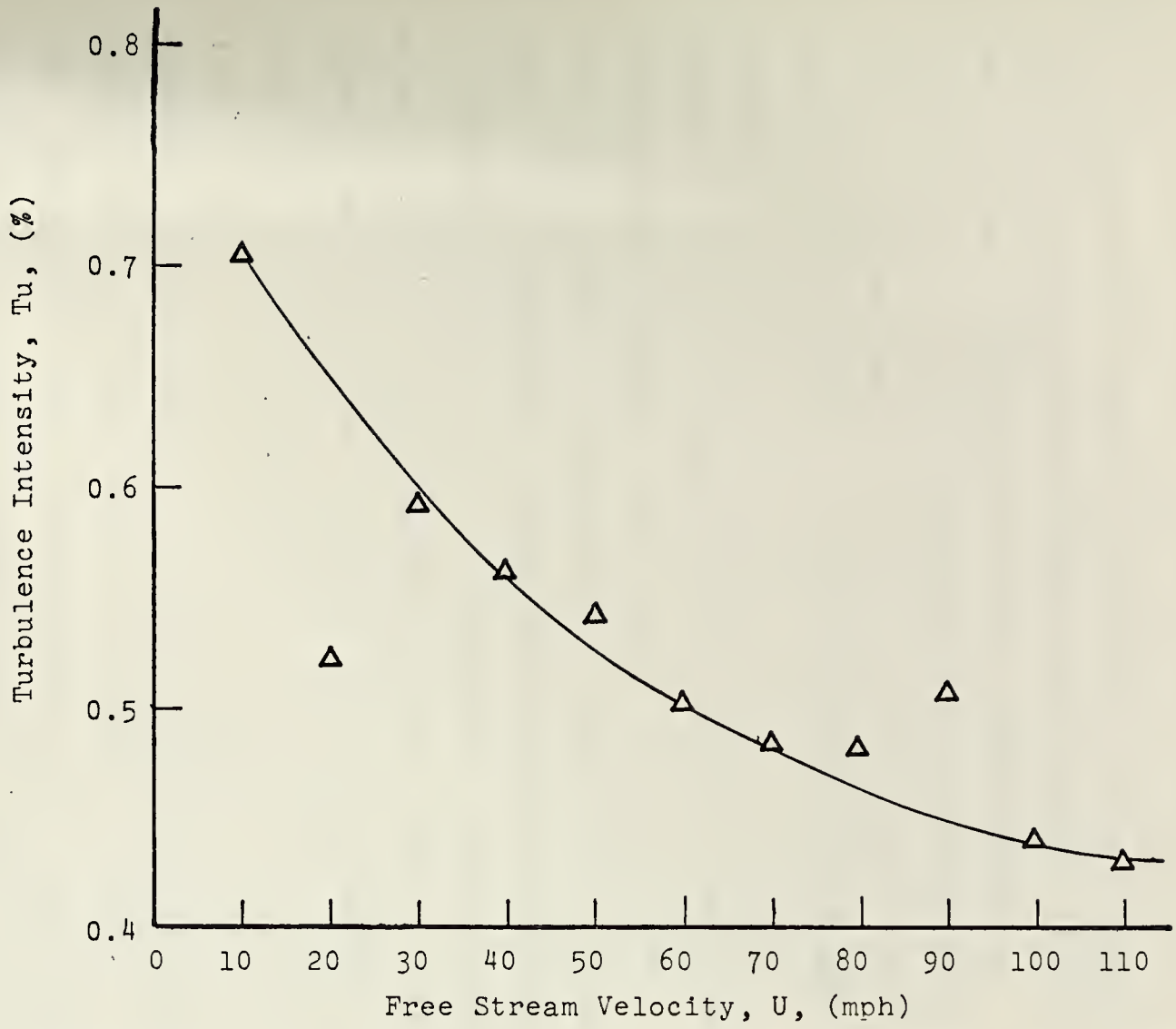

Figure 19. Turbulence Intensity Level of the Wind Tunnel Determined at Various Air Speeds

APPENDIX E

Endurance Test for the Acrylic Tube

An eighteen in section of the 4.5 in o.d. cast acrylic tubing was wrapped with six turns of the Nichrome ribbon. The ribbon was instrumented with one copper-constantan thermocouple. The surface temperature was then measured using a Leeds and Northrup millivolt potentiometer and an ice bath for a reference. A Lambda 60 volt power supply was used to provide a 2.0-2.5 amp current through the ribbon. The tube was thereby heated, uniformly and slowly, to temperature levels of 100°F, 110°F, 120°F and 150°F, and cooled slowly to room temperature after each heating cycle. The heating and cooling rates were only about one to two degrees F per min., to minimize the relative differences between the acrylic and the Nichrome during the expansion and contraction. In all of the heating cycles except the final one the cylinder did not physically deform, as there was not a noticeable expansion of the acrylic. In the final test, between 130-135°F the acrylic began to visibly expand causing the ribbon to tighten. This immediately caused a hoop stress on the surface which deformed the cylinder by constraining its expansion in the area where the ribbon was wrapped. The cylinder expanded further in the unwrapped areas. When the cylinder cooled

it contracted uniformly leaving a smaller, deformed diameter in the region of the ribbon.

From this test it was concluded that to avoid the risk of deformation the actual test cylinder should not be heated above 120°F.

In a second test the surface temperature was heated to 180°F, severely deforming the cylinder. However, the R.T.V. sealant was unaffected and held solidly.

APPENDIX F

Uncertainty Analysis

As in all experimental studies, there existed some degree of uncertainty with regard to the accuracy of various results, which stemmed from the data collected. To evaluate the levels of uncertainty involved, the method of Kline and McClintock described in Ref. 44 was employed.

The measured variables which were the origins of the uncertainty were ΔP_{1-2}, $\Delta P_{cylinder}$, ΔT, V, and R (see nomenclature for the definitions of these terms). The fluid properties of air were extracted from table A-7 of Ref. 45, and their uncertainty is neglected in the analysis.

The magnitude of the uncertainty associated with the pressure measurements depended upon the flow velocity of the run, and the angular location on the cylinder. Similarly, the magnitude of the uncertainty associated with the temperature measurements depended upon the angular location.

In this appendix the calculations of uncertainty are shown in detail for a representative Reynolds number of 260,600, and at the forward stagnation point of the cylinder. Uncertainties for other flow velocities and locations are discussed.

The Pressure Coefficient

The pressure coefficient was calculated from equation 28,

$$C_P = \frac{\Delta P_{cylinder}}{\Delta P_{1-2}}$$

Applying the technique referenced above, one has

$$\frac{\omega_{C_P}}{C_P} = \sqrt{\left(\frac{\omega_{\Delta P_{cylinder}}}{\Delta P_{cylinder}}\right)^2 + \left(\frac{\omega_{\Delta P_{1-2}}}{\Delta P_{1-2}}\right)^2} \quad ,$$

where ω is the uncertainty interval, or precision range. At the forward stagnation point,

$$\Delta P_{cylinder} = 7.5 \pm 0.1 \text{ cm water (10 to 1)}$$

$$\Delta P_{1-2} = 7.7 \pm 0.1 \text{ cm water (10 to 1)}$$

Substituting, one has

$$\frac{\omega_{C_P}}{C_P} = \sqrt{\left(\frac{0.10}{7.52}\right)^2 + \left(\frac{0.10}{7.71}\right)^2} \simeq 0.02 \quad .$$

Therefore, the uncertainty in the pressure coefficient was about two per cent. In the wake, the uncertainty was about four per cent because the unsteady motion of the air lessened the readability of the manometer.

At the higher Reynolds numbers the uncertainty in the pressure coefficient was about three per cent at the forward stagnation point and about six per cent in the wake. The higher speed flows produced larger fluctuations on the manometer.

At the lower Reynolds numbers the measured pressures were small and the uncertainty intervals were a significant fraction of these pressures. As a result the uncertainty

in the pressure coefficient was large, reaching as high as 49% for the lowest run. (Re = 57,000)

The Heat Transfer Coefficient

The heat transfer coefficient was calculated from the equation,

$$h_\theta = \frac{\frac{V^2}{R}}{A_s \Delta T}$$

where A_s is a constant (see nomenclature for definition of terms). Continuing,

$$\frac{\omega_h}{h} = \sqrt{\left(\frac{2\omega_v}{v}\right)^2 + \left(\frac{\omega_R}{R}\right)^2 + \left(\frac{\omega_{\Delta T}}{\Delta T}\right)^2}$$

For the experimental run at a Reynolds number of 260,600,

$V = 59.1 \pm 0.3$ volts (10 to 1)

$R = 20.5 \pm 0.2$ ohms (10 to 1)

$\Delta T = 20.0 \pm 0.5°F$ (10 to 1), at the forward stagnation point.

Substituting, one has,

$$\frac{\omega_h}{h} = \sqrt{\left(2 \circ \frac{0.3}{59.1}\right)^2 + \left(\frac{0.2}{20.5}\right)^2 + \left(\frac{0.5}{20.0}\right)^2} \simeq 0.03.$$

The uncertainty in the heat transfer coefficient was about three per cent at the forward stagnation point for all the experimental runs.

At the transition point where the boundary layer becomes turbulent, or at the separation point in laminar

flow, the temperature difference had an uncertainty interval of about five°F, and the uncertainty in the heat transfer coefficient was on the order of 25%.

The uncertainty of the heat transfer coefficient in the wake was about six per cent.

The Nusselt Number

The Nusselt number was calculated from equation 3,

$$Nu = \frac{hD}{k} .$$

Continuing,

$$\frac{\omega_{Nu}}{Nu} = \sqrt{\left(\frac{\omega_h}{h}\right)^2 + \left(\frac{\omega_D}{D}\right)^2}$$

and

$$D = 4.47 \pm .05 \text{ in (10 to 1)}.$$

The uncertainty of the measurement of the diameter was negligible. Therefore, the uncertainty in the Nusselt number was the same as the uncertainty in the heat transfer coefficient.

The Reynolds Number

The Reynolds number was calculated from equation 1,

$$Re = \frac{UD}{\nu} ,$$

and its uncertainty is the same as that of the free stream velocity, U, which was calculated from equation 29,

$$U = \sqrt{\frac{2(\Delta P_{1-2})}{\rho}}$$

Continuing,

$$\frac{\omega_{Re}}{Re} = \frac{\omega_U}{U} = 0.5\,\frac{\omega_{\Delta P_{1-2}}}{\Delta P_{1-2}} = 0.5\left[\frac{0.1}{7.71}\right] \simeq 0.007.$$

Therefore, the uncertainty in the Reynolds number is approximately half the uncertainty in the dynamic pressure, and equals about 0.7%. At the high Reynolds numbers this uncertainty doubles.

The Froessling Number

The Froessling number was calculated from equation 4,

$$F = \frac{Nu}{\sqrt{Re}}\ .$$

Continuing,

$$\frac{\omega_F}{F} = \sqrt{\left(\frac{\omega_{Nu}}{Nu}\right)^2 + \left(\frac{\omega_{Re}}{2Re}\right)^2}\ .$$

Substituting from previous results, one has

$$\frac{\omega_F}{F} = \sqrt{(0.03)^2 + (0.0035)^2} \simeq 0.03\ .$$

The uncertainty of the Froessling number was generally about the same as that of the Nusselt number. At the forward stagnation point the uncertainty of the Froessling number was about 3-4% in most cases.

LIST OF REFERENCES

1. Wood, B.D., Applications of Thermodynamics, p. 357, Addison-Wesley, 1969.

2. Kreith, F., Principles of Heat Transfer, 2d ed., p. 262, 401-410, International Textbook Co., 1965.

3. Grober, H., Erk, S., and Grigull, V., Fundamentals of Heat Transfer, 3d ed., p. 273-280, McGraw-Hill, 1961.

4. Eckert, E.R.G. and Drake, R.M., Jr., Analysis of Heat and Mass Transfer, p. 403, McGraw-Hill, 1972.

5. Schlichting, H., Boundary-Layer Theory, 6th ed., p. 29-42, 162,290,408-410, McGraw-Hill, 1968.

6. Great Britain Aeronautical Research Committee, R and M 1179, The Airflow Around a Circular Cylinder in the Region Where the Boundary Layer Separates from the Surface, by Fage, A., 1928.

7. Great Britain Aeronautical Research Committee, R and M 1369, Further Experiments on the Flow Around a Cylinder, by A. Fage and V.M. Falkner, 1931.

8. National Advisory Committee for Aeronautics, Technical Note 3169, On the Drag and Shedding Frequency of Two-Dimensional Bluff Bodies, by A. Roshko, p. 1-29, July 1954.

9. Roshko, A., "Experiments on the Flow Past a Circular Cylinder at Very High Reynolds Number," Journal of Fluid Mechanics, v. 10, May 1961.

10. Achenbach, E., "Distribution of Local Pressure and Skin Friction Around a Circular Cylinder in Cross-Flow up to Re = 5×10^6, Journal of Fluid Mechanics, v. 34, part 4, p. 625-639, 1968.

11. Naval Ship Research and Development Center Report 3647, Location of Separation on a Circular Cylinder as a Function of Reynolds Number, by D.W. Coder, November 1971.

12. Spalding, D.B. and Pun, W.M., "A Review of Methods for Predicting Heat-Transfer Coefficients for Laminar Uniform-Property Boundary Layer Flows," International Journal of Heat and Mass Transfer, v. 5, p. 239-249, 1962.

13. National Advisory Committee for Aeronautics, Technical Memorandum 1050, Heat Transfer Over the Circumference of a Heated Cylinder in Transverse Flow, by Ernst Schmidt and Karl Wenner, p. 1-20, October 1943.

14. Squire, Modern Developments in Fluid Dynamics, Goldstein, S. editor, v. 2, p. 631, Oxford-Clarendon, 1938.

15. Giedt, W.H., "Investigation of Variation of Point Unit Heat-Transfer Coefficient Around a Cylinder Normal to an Air Stream," Transactions of the ASME, p. 375-381, May 1949.

16. Fand, R.M., "Heat Transfer by Forced Convection From a Cylinder to Water in Crossflow," International Journal of Heat and Mass Transfer, v. 8, p. 995-1010, 1965.

17. Douglas, W.J.M. and Churchill, S.W., "Recorrelation of Data for Convective Heat Transfer Between Gases and Single Cylinders with Large Temperature Differences," Chem. Engng. Prog. Symp. Series 52, p. 23-28, 1956.

18. Van der Hegge Zijnen, B.G., "Modified Correlation Formulae for the Heat Transfers by Natural and by Forced Convection from Horizontal Cylinders," Applied Science Resume, v. 6, section A, p. 129-140, 1957.

19. Armed Services Technical Information Agency, ASTIA AD 290-339, Estimation of the Heat Transfer from the Rear of an Immersed Body to the Region of Separated Flow, P.D. Richardson, September 1962.

20. Perkins, H.C., Jr. and Leppert, G., "Forced Convection Heat Transfer from a Uniformly Heated Cylinder," Journal of Heat Transfer, v. 84, p. 257-261, August 1962.

21. Perkins, H.C., Jr. and Leppert, G., "Local Heat-Transfer Coefficients on a Uniformly Heated Cylinder," International Journal of Heat and Mass Transfer, v. 7, p. 143-158, 1964.

22. Jarcy, J.R., Flow Field, Drag, and Heat Transfer of a Heated Cylinder in a Subsonic Crossflow of Air, Master's Thesis, Air Force Institute of Technology, June 1967.

23. Richardson, P.D., "Heat and Mass Transfer in Turbulent Separated Flows," Chemical Engineering Science, v. 18, p. 149-155, 1963.

24. Sogin, H.H. and Subramanian, V.S., "Local Mass Transfer from Circular Cylinders in Cross Flow," Journal of Heat Transfer, p. 483-493, November 1961.

25. Armed Services Technical Information Agency, AD 118075, "Heat Transfer to Boundary Layers with Pressure Gradients," R.A. Seban and H.W. Chan, May 1958.

26. Armed Services Technical Information Agency AD 66184, "A New Method for Calculating Laminar Heat Transfer on Cylinders of Arbitrary Cross-Section and on Bodies of Revolution at Constant and Variable Wall Temperature," H. Schuh, 1953.

27. Howarth, L., Squire, H.B., and Lock, C.W.H., Modern Developments in Fluid Dynamics, High Speed Flow, v. 2, p. 791-793, Clarendon Press, Oxford, 1953.

28. Kestin, J., "The Effect of Free-Stream Turbulence on Heat Transfer Rates," Advances in Heat Transfer, v. 3, p. 1-32, 1966.

29. National Advisory Committee for Aeronautics Technical Note 4018, Influence of Turbulence on Transfer of Heat From Cylinders, by J. Kestin and P.F. Maeder, p. 1-78, October 1957.

30. Kestin, J., "Discussion," Journal of Heat Transfer, p. 175, May 1967.

31. Kestin, J. and Wood, R.T., "The Mechanism which Causes Free Stream Turbulence to Enhance Stagnation-Line Heat and Mass Transfer," Heat Transfer 1970, v. 2, p. 2-7, 1970.

32. Seban, R.A., "The Influence of Free Stream Turbulence on the Local Heat Transfer From Cylinders," Journal of Heat Transfer, p. 101-107, May 1960.

33. Armed Services Technical Information Agency, "The Effect of Free Stream Turbulence on the Heat Transfer from Cylinders," Seban, R.A., p. 1-32, September 1957.

34. Giedt, W.H., "Effect of Turbulence Level of Incident Air Stream on Local Heat Transfer and Skin Friction on a Cylinder," Journal of the Aeronautical Sciences, p. 725-730, November 1961.

35. Hilpert, R., "Warmeabgabe von Geheizten Drahten und Rohren im Luftstrom," Forsch, Gebiete Ingenieurwesen, v. 4, p. 215, 1933.

36. Richardson, P.D., "On Hilpert's Measurements of Heat Transfer from Cylinders Transverse to an Airstream," Journal of Heat Transfer, p. 283, August 1963.

37. McAdams, W.H., Heat Transmission, 3d. ed., New York, 1954.

38. Oosthuizen, P.H., and Madan, S., "The Effect of Flow Direction on Combined Convective Heat Transfer from Cylinders to Air," Journal of Heat Transfer, p. 240-242, May 1971.

39. Jackson, T.W. and Yen, H.H., "Combining Forced and Free Convective Equations to Represent Combined Heat-Transfer Coefficients for a Horizontal Cylinder," Journal of Heat Transfer, p. 247-248, May 1971.

40. Oosthuizen, P.H. and Madan, S., "Combined Convective Heat Transfer from Horizontal Cylinders in Air," Journal of Heat Transfer, p. 194-196, February 1970.

41. Davenport, M.E., Magee, P.M. and Leppert,G., "Thermocouple Attachment to a Direct Current Heater," Journal of Heat Transfer, p. 187-188, May 1962.

42. Pope, A., Wind-Tunnel Testing, 2d. ed., p. 268-286, Wiley and Sons, 1954.

43. Edwards, A.L., TRUMP: A Computer Program for Transient and Steady-State Temperature Distributions in Multidimensional Systems, Lawrence Radiation Laboratory UCRL-14754, Rev II, University of California, Livermore.

44. Kline, S.J. and McClintock, F.A., "Describing Uncertainties in Single-Sample Experiments," Mech. Engr., v. 75, January 1953.

45. Chapman, A.J., Heat Transfer, 2d ed., New York, 1967.

INITIAL DISTRIBUTION LIST

		No. Copies
1.	Library, Code 0212 Naval Postgraduate School Monterey, California 93940	2
2.	Chairman, Code 59 Department of Mechanical Engineering Naval Postgraduate School Monterey, California 93940	1
3.	T.E. Cooper, Code 59g Department of Mechanical Engineering Naval Postgraduate School Monterey, California 93940	3
4.	Defense Documentation Center Cameron Station Alexandria, Virginia 22314	2
5.	W.H. Giedt Department of Mechanical Engineering University of California Davis, California	1
6.	LCDR John F. Meyer Charleston Naval Shipyard Charleston, South Carolina	1

Security Classification

DOCUMENT CONTROL DATA - R & D

(Security classification of title, body of abstract and indexing annotation must be entered when the overall report is classified)

1. ORIGINATING ACTIVITY (Corporate author)	2a. REPORT SECURITY CLASSIFICATION
Naval Postgraduate School Monterey, California 93940	2b. GROUP

3. REPORT TITLE

An Experimental Investigation of the Heat Transfer Characteristics of a Heated Cylinder Placed in a Cross Flow of Air

4. DESCRIPTIVE NOTES (Type of report and, inclusive dates)

Master's and Mechanical Engineer's Thesis; June 1973

5. AUTHOR(S) (First name, middle initial, last name)

John Ferrandello Meyer

6. REPORT DATE	7a. TOTAL NO. OF PAGES	7b. NO. OF REFS
June 1973	131	45

8a. CONTRACT OR GRANT NO.	9a. ORIGINATOR'S REPORT NUMBER(S)
b. PROJECT NO.	
c.	9b. OTHER REPORT NO(S) (Any other numbers that may be assigned this report)
d.	

10. DISTRIBUTION STATEMENT

Approved for public release; distribution unlimited.

11. SUPPLEMENTARY NOTES	12. SPONSORING MILITARY ACTIVITY
	Naval Postgraduate School Monterey, California 93940

13. ABSTRACT

Local heat transfer and pressure coefficients around a right circular cylinder were experimentally determined at Reynolds numbers ranging from 57,000 to 495,000. The turbulence intensity of the free stream was approximately 0.5%. The cylinder was heated externally with a constant heat flux and simultaneously cooled in a cross flow of air. A uniform heat source was provided by energizing Nichrome ribbon with a constant, measured current. The steady state surface temperature increase above the air temperature was indicated by thermocouple information. Employing Newton's law of cooling, heat transfer coefficients were determined as a function of the angular location from the forward stagnation line. The free stream dynamic pressure and surface pressure distribution around the cylinder were obtained using static pressure pick-ups and their associated manometers. A comparison is made between the heat transfer and pressure data collected. Experimental results compared within about six per cent of the theoretical solution of Schuh.

DD FORM 1 NOV 68 1473 (PAGE 1)

S/N 0101-807-6811

Security Classification

A-31408

KEY WORDS	LINK A		LINK B		LINK C	
	ROLE	WT	ROLE	WT	ROLE	WT
)rced convection heat transfer						
/linder heat transfer						
lght circular cylinder heat transfer						
)nstant heat flux cylinder heat transfer						
luff body heat transfer						
ncompressible flow around a cylinder						
ree stream turbulence						
)cal heat transfer coefficients around a cylinder						
)undary layer around a cylinder						
ubcritical flow around a cylinder						
ransition region in boundary layer						
aminar boundary layer heat transfer						
urbulent boundary layer heat transfer						
ransition region heat transfer						
ritical flow around a cylinder						

Thesis
M567 Meyer
c.1

145044

An experimental investigation of the heat transfer characteristics of a heated cylinder placed in a cross flow of air.